

1-1-2008

**Synthesis and characterization of novel thermoplastic elastomers employing polyhedral oligomeric silsesquioxane physical crosslinks.**

Bradley Seurer  
*University of Massachusetts Amherst*

Follow this and additional works at: [https://scholarworks.umass.edu/dissertations\\_1](https://scholarworks.umass.edu/dissertations_1)

---

**Recommended Citation**

Seurer, Bradley, "Synthesis and characterization of novel thermoplastic elastomers employing polyhedral oligomeric silsesquioxane physical crosslinks." (2008). *Doctoral Dissertations 1896 - February 2014*. 1115.

<https://doi.org/10.7275/16ef-mb55> [https://scholarworks.umass.edu/dissertations\\_1/1115](https://scholarworks.umass.edu/dissertations_1/1115)

This Open Access Dissertation is brought to you for free and open access by ScholarWorks@UMass Amherst. It has been accepted for inclusion in Doctoral Dissertations 1896 - February 2014 by an authorized administrator of ScholarWorks@UMass Amherst. For more information, please contact [scholarworks@library.umass.edu](mailto:scholarworks@library.umass.edu).

★ UMASS/AMHERST ★



312066 0310 5100 3



University of  
Massachusetts  
Amherst

L I B R A R Y





Digitized by the Internet Archive  
in 2015

<https://archive.org/details/synthesischaract00seur>



This is an authorized facsimile, made from the microfilm master copy of the original dissertation or master thesis published by UMI.

The bibliographic information for this thesis is contained in UMI's Dissertation Abstracts database, the only central source for accessing almost every doctoral dissertation accepted in North America since 1861.

**UMI**<sup>®</sup> Dissertation  
Services

From: ProQuest  
COMPANY

300 North Zeeb Road  
P.O. Box 1346  
Ann Arbor, Michigan 48106-1346 USA  
800.521.0600 734.761.4700  
web [www.umi.proquest.com](http://www.umi.proquest.com)



**SYNTHESIS AND CHARACTERIZATION OF NOVEL THERMOPLASTIC  
ELASTOMERS EMPLOYING POLYHEDRAL OLIGOMERIC  
SILSESQUOXANE PHYSICAL CROSSLINKS**

A Dissertation Presented

By

BRADLEY SEURER

Submitted to the Graduate School of the  
University of Massachusetts Amherst in partial fulfillment  
Of the requirements for the degree of

DOCTOR OF PHILOSOPHY

February 2008

Polymer Science and Engineering



UMI Number: 3315482

#### INFORMATION TO USERS

The quality of this reproduction is dependent upon the quality of the copy submitted. Broken or indistinct print, colored or poor quality illustrations and photographs, print bleed-through, substandard margins, and improper alignment can adversely affect reproduction.

In the unlikely event that the author did not send a complete manuscript and there are missing pages, these will be noted. Also, if unauthorized copyright material had to be removed, a note will indicate the deletion.



---

UMI Microform 3315482  
Copyright 2008 by ProQuest LLC  
All rights reserved. This microform edition is protected against  
unauthorized copying under Title 17, United States Code.

---

ProQuest LLC  
789 East Eisenhower Parkway  
P.O. Box 1346  
Ann Arbor, MI 48106-1346

© Copyright by Bradley Seurer 2008

All Rights Reserved

**SYNTHESIS AND CHARACTERIZATION OF NOVEL THERMOPLASTIC  
ELASTOMERS EMPLOYING POLYHEDRAL OLIGOMERIC  
SILSESQUIOXANE PHYSICAL CROSSLINKS**

A Dissertation Presented

by

BRADLEY SEURER

Approved as to style and content by:

---

E. Bryan Coughlin-Chairman

---

Alfred J. Crosby-Member

---

H. Henning Winter-Member

---

Shaw Ling Hsu, Department Head  
Polymer Science and Engineering

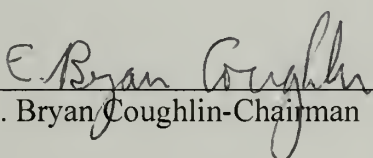
**SYNTHESIS AND CHARACTERIZATION OF NOVEL THERMOPLASTIC  
ELASTOMERS EMPLOYING POLYHEDRAL OLIGOMERIC  
SILSESQUIOXANE PHYSICAL CROSSLINKS**

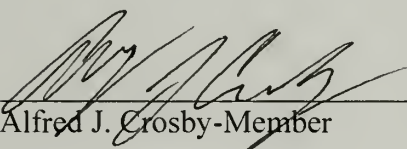
A Dissertation Presented

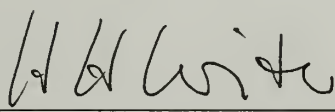
by

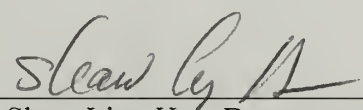
BRADLEY SEURER

Approved as to style and content by:

  
E. Bryan Coughlin-Chairman

  
Alfred J. Crosby-Member

  
H. Henning Winter-Member

  
Shaw Ling Hsu, Department Head  
Polymer Science and Engineering

THE UNIVERSITY OF CHICAGO  
DEPARTMENT OF CHEMISTRY  
RESEARCH REPORT

RESEARCH REPORT  
NO. 1000  
1950

RESEARCH REPORT

RESEARCH REPORT

RESEARCH REPORT

RESEARCH REPORT

RESEARCH REPORT

## DEDICATION

To my parents, Dennis and JoAnn Seurer,  
for their incessant love and support.

## ACKNOWLEDGMENTS

I want to thank Dr. Coughlin for being a great mentor and advisor. Thank you for the opportunity to work in your group. I became a better scientist not only because of the knowledge I have obtained over the past 5 years in your group, but also by the stronger ability to communicate in a scientific manner. I also appreciate all the support in my job search. I want to thank my committee, Dr. Crosby and Dr. Winter, for all the insightful research discussions and the helpful knowledge imparted in my thesis project, as well as the various defenses over my graduate career. Thanks to Dr. 'DV' Venkataraman for serving as a substitute committee member for my ORP. I also thank the chemistry department at Winona State University, especially Dr. Kopitzke, Dr. Miertschin, and Dr. Nalli, where I really learned the joys of science, especially chemistry.

I want to thank everyone in the polymer science and engineering department for all the support over the years. Specifically, I thank Dr. Lesser, who went out of his way to help with my research project, as well searching for a job. I also want to thank him for the use of his facilities, and for the mechanical research discussions. Thanks to Peter Walsh and Hossein Baghdadi for helpful discussions on DMA and rheology studies for my project. I am also grateful for all the help from Jack Hirsh and Greg Dabkowski, especially all the science and non-science related discussions. I also thank other staff members, Erin, Eileen, and Vivien, in whom PSE would not run without.

I am very grateful to have worked in the Coughlin group; I'm thankful for all the helpful research discussions, as well as non-science related conversations. Thanks specifically to Gregoire, Gunjan, Yoan, and Sergio for taking an expanded interest in my research project, and suggesting and helping in different studies. I also want to thank the

rest of the research group, Raji, Greg, Ramon, Firat, Pat, Push, Jen, Bernabe, Nui, Ying, Chris, Shilpi, Justin, Bon-Cheol, Ranga, and Makoto. I have really enjoyed working with all of you over my graduate career.

I want to thank all my friends and housemates over my years at UMass. We have enjoyed many great times together. I will never forget the Sundays we have spent watching our favorite less-than-stellar football teams. I will also have fond memories of all the intramural and summer sports teams I've played on. We had some good teams and bad teams, but it was always fun, and a great distraction from school. I want to thank specifically those who have been great friends to be over the years, including Kevin W., Kevin S., Bryan, Hossein, Andrew, Chris, Janet, Katie, and Derek. A special thanks to Mark Callahan, who was always there for me, and helped keep me sane with those ritual Rafters nights. Thank you for being there when I needed you, and thanks for all the fun over the years.

I want to thank all my friends back in Minnesota for all the love and support over my years here. I always enjoyed my trips back to Minnesota to see everyone. Thanks for all the fun and conversations over the years, and keeping me sane during my graduate career. I want to thank specifically my dear friends Chris, Pat, Brad, Jim, Brett, and Will.

Last, but most importantly, I wish to thank my family, especially mom and dad. They have given me every opportunity to succeed in life, from financial support to all the love and care one could ever need. Thank you, also, for putting up with me for the past 5 years. Thank you all so much!



## ABSTRACT

### SYNTHESIS AND CHARACTERIZATION OF NOVEL THERMOPLASTIC ELASTOMERS EMPLOYING POLYHEDRAL OLIGOMERIC SILSESQUIOXANE PHYSICAL CROSSLINKS

FEBRUARY 2008

BRADLEY SEURER, B.S., WINONA STATE UNIVERSITY

M.Sc., UNIVERSITY OF MASSACHUSETTS AMHERST

Ph.D., UNIVERSITY OF MASSACHUSETTS AMHERST

Directed by: Prof. E. Bryan Coughlin

Polyhedral oligomeric silsesquioxanes (POSS) are molecularly precise isotropic particles with average diameters of 1-2 nm. A typical  $T_8$  POSS nanoparticle has an inorganic  $Si_8O_{12}$  core surrounded by eight aliphatic or aromatic groups attached to the silicon vertices of the polyhedron promoting solubility in conventional solvents. Previously, efficient synthetic methods have been developed whereby one of the aliphatic groups on the periphery is substituted by a functional group capable of undergoing either homo- or copolymerization. In the current investigations, preparative methods for the chemical incorporation of POSS macromonomers in a series elastomers have been developed.

Analysis of the copolymers using WAXD reveals that pendant POSS groups off the polymer backbones aggregate, and can crystallize as nanocrystals. From both line-broadening of the diffraction maxima, and also the oriented diffraction in a drawn material, the individual POSS sub-units are crystallizing as anisotropically shaped crystallites. The formation of POSS particle aggregation is strongly dependent on the

nature of the polymeric matrix and the POSS peripheral group. X-ray studies show aggregation of POSS in ethylene-propylene elastomers occurred only with a phenyl periphery, whereas POSS particles with isobutyl and ethyl peripheries disperse within the polymer matrix. By altering the polymer matrix to one containing chain repulsive fluorine units, aggregation is observed with both the phenyl and isobutyl peripheries. Altering the polymer chain to poly(dimethylcyclooctadiene), POSS aggregates with isobutyl, ethyl, cyclopentyl, and phenyl peripheries.

The formation of POSS nanocrystals increases the mechanical properties of these novel thermoplastic elastomers. The storage modulus increases significantly with the addition of POSS, as does the length and magnitude of the rubbery plateau region. Tensile tests of these elastomers show an increase in elastic modulus with increasing POSS loading, with values in the range of commercial elastomers. The elongation at break was as high as 720%. Cyclic tensile test show some hysteresis of the elastomers. However, the curves show Mullins effect behavior, commonly seen in elastomers. Elastomers with POSS dispersion, however, show poor mechanical properties. These results demonstrate the novel material property gains by the incorporation and aggregation of POSS in thermoplastic elastomers, as well as the influence of the POSS periphery.

## TABLE OF CONTENTS

	Page
ACKNOWLEDGMENTS.....	v
ABSTRACT.....	vii
LIST OF TABLES.....	xii
LIST OF FIGURES.....	xiii
LIST OF SCHEMES.....	xvi
LIST OF ABBREVIATIONS.....	xvii
CHAPTERS	
1 INTRODUCTION.....	1
1.1 Composites.....	1
1.2 Nanocomposites.....	2
1.3 Polyhedral Oligomeric Silsesquioxane.....	2
1.4 Polymers containing POSS.....	6
1.5 Elastomers.....	11
1.5.1 Background.....	11
1.5.2 Naturally occurring elastomers.....	12
1.5.3 Synthetic elastomers.....	13
1.5.4 Halogen based elastomers.....	14
1.5.5 Silicon based elastomers.....	15
1.5.6 Hydrocarbon based elastomers.....	15
1.6 Elastomers containing POSS.....	17
1.7 Summary.....	22
1.8 References.....	23
2 SYNTHESIS AND CHARACTERIZATION OF ETHYLENE- PROPYLENE-POSS THERMOPLASTIC ELASTOMERS.....	27
2.1 EPDM background.....	27
2.2 Synthesis of EPDM elastomers.....	28
2.3 POSS elastomer background.....	30
2.4 Project goals.....	31

2.5	Experimental Section.....	32
2.5.1	Materials.....	32
2.5.2	Synthesis of PhPOSSnorbornene.....	32
2.5.3	Polymerization of ethylene-propylene-POSS terpolymers...	33
2.5.4	Polymer characterization.....	34
2.6	Results and discussion.....	36
2.6.1	Reaction results.....	36
2.6.2	WAXD studies.....	38
2.6.3	Thermal characterization.....	43
2.6.4	Dynamic mechanical analysis studies.....	45
2.6.5	Rheology.....	50
2.6.6	Tensile tests.....	57
2.6.7	TEM.....	61
2.7	Conclusions.....	63
2.8	References.....	64
3	SYNTHESIS AND CHARACTERIZATION OF POLY(OCTAFLUOROPENTYL ACRYLATE)-POSS ELASTOMERS.....	67
3.1	Fluoroelastomer background.....	67
3.2	Project goals.....	69
3.3	Synthetic methods.....	69
3.3.1	Materials.....	69
3.3.2	Polymerization of POSSmethacrylate and octafluoropentyl acrylate.....	70
3.3.3	Polymer characterization.....	70
3.4	Results and discussion.....	72
3.4.1	Polymerization.....	72
3.4.2	WAXD.....	75
3.4.3	Thermal characterization.....	78
3.4.4	Rheology.....	80
3.4.5	TEM.....	85
3.5	Conclusions.....	86
3.6	References.....	87
4	PERIPHERAL EFFECT ON POSS AGGREGATION IN POLY(DIMETHYLCYCLOOCTADIENE)- POSS COPOLYMERS.....	89

4.1	Background.....	89
4.2	Project goals.....	91
4.3	Experimental.....	92
4.3.1	Materials.....	92
4.3.2	Synthesis of PhPOSSnorbornene macromonomer.....	92
4.3.3	Polymerization.....	93
4.3.4	Polymer characterization.....	93
4.4	Results and characterization.....	94
4.4.1	Polymerization.....	94
4.4.2	Thermal characterization.....	97
4.4.3	Wide angle X-ray studies.....	99
4.5	Conclusions.....	102
4.6	References.....	103
5	SUMMARY AND FUTURE WORK.....	104
5.1	Dissertation summary.....	104
5.2	POSS peripheral effect on aggregation in copolymers.....	105
5.3	Mechanical studies.....	106
5.4	Future Work.....	108
5.4.1	WAXD studies.....	108
5.4.2	Mechanical properties.....	109
5.4.3	Synthesis of novel POSS containing polymers.....	110
5.4.4	POSS triblock copolymers.....	111
5.5	References.....	113
	APPENDICES.....	115
	BIBLIOGRAPHY.....	129



## LIST OF TABLES

Table	Page
2.1. Ethylene-propylene-ethylidene norbornene terpolymers synthesized using varying metallocene catalysts activated by MAO <sup>23</sup> .....	30
2.2. Summary of molecular weight data of EP-POSS polymers.....	36
2.3. Estimation of POSS domain sizes using Scherer's equation.....	42
2.4. Thermal characterization of EPPOSS terpolymers.....	43
2.5. Dynamic mechanical analysis data.....	47
2.6. Tensile properties of EP and EPPOSS polymers.....	59
3.1. Octafluoropentyl acrylate-POSS copolymerization results.....	73
3.2. POSS domain sizes estimated using Scherer's equation.....	77
3.3. Thermal characterization of POSS-octafluoropentyl acrylate copolymers.....	79
4.1. Reaction results of DMCOD-POSS copolymers.....	95
4.2. Thermal characterization DMCOD-POSS copolymers.....	97
4.3. POSS domain sizes in DMCOD-POSS copolymers.....	102

## LIST OF FIGURES

Figure	Page
1.1. POSS .....	2
1.2. Composite materials .....	3
1.3. Synthesis of POSS molecules. ....	4
1.4. Melting points of T <sub>8</sub> POSS with varying carbon chain lengths <sup>7</sup> and TGA of T <sub>8</sub> POSS with varying carbon chain lengths. <sup>7</sup> .....	5
1.5. TGA of polyethylene-POSS copolymers in air. Films in (a) were cast from xylenes and (b) were cooled from the melt. <sup>32</sup> .....	8
1.6. Sturcture of POSS-polyimide polymer <sup>34</sup> .....	9
1.7. Profilometry measurements on Kapton-POSS and Kapton film <sup>34</sup> .....	10
1.8. Global consumption or rubber. <sup>41</sup> .....	13
1.9. Structure of epichlorhydrin based elastomer.....	14
1.10. Configurations of polybutadiene. From left to right, trans 1,4, cis-1,4 and cis-1,2.....	16
1.11. Structure of styrene-butadiene-styrene-POSS thermoplastic elastomer <sup>45</sup> ...	18
1.12. Structure of polyurethane-POSS thermoplastic elastomer <sup>48</sup> .....	19
1.13. Synthesis of POSS-(n-butyl acrylate)-POSS triblock thermoplastic elasotmers <sup>47</sup> .....	20
1.14. Characterization of Poly(1,4-butadiene)-POSS copolymers. <div style="margin-left: 40px;"> <b>Top left:</b> Wide angle X-ray diffraction pattern of copolymers, with increasing POSS incorporation from bottom top <b>Bottom Left:</b> TEM image of butadiene-POSS copolymers with 52 wt% POSS incorporation. <b>Top right:</b> Cartoon of POSS raft-like structure in polybutadiene-POSS copolymers with high POSS </div>	

	incorporations(>30 weight %). <b>Bottom right:</b> Cartoon of POSS raft-like structure with low POSS incorporations. <sup>50</sup> .....	21
2.1.	(L) Structure of EPDM, with ethylidene norbornene as the diene (M) Car seal made from EPDM <sup>4</sup> (R) Roofing material made from EPDM <sup>5</sup> ..	27
2.2.	Structures of metallocene catalysts used in EPDM synthesis.....	30
2.3.	DEPT135 NMR of EPIbuPOSS copolymers. Peak assignments based upon literature <sup>31</sup> show ethylene(E) and propylene(P) sequences.....	37
2.4.	Wide angle X-ray diffraction pattern of EPIbuPOSS polymers.....	39
2.5.	Wide angle X-ray diffraction data of (left) EPEtPOSS polymers and (right) EPPhPOSS polymers.....	40
2.6.	WAXD patterns for EPPhPOSS copolymers by different preparation methods.....	41
2.7.	Dynamic mechanical analysis of EPPhPOSS polymer samples. Plot shows the storage modulus as a function of temperature. Samples were heated from -100 to 200°C at 5 K per minute.....	46
2.8.	Dynamic mechanical study of EPPh36 polymers, varying polymer film preparation techniques, including a slow evaporation method (7 days), fast evaporation (2 hours), and by pressing the sample at 5000 psi at 150°C. Each sample was heated from -100°C to 200°C twice, at a rate of 5°C/minute, using a frequency of 1 Hz and with an initial force of 0.05 N. This plot measures the storage modulus as a function of temperature.....	49
2.9.	Rheology data of EP and EPPOSS polymer samples. Each test measures the storage modulus( $G'$ ) and loss modulus( $G''$ ) as a function of percent strain of each sample at varying temperatures. Each sample was in the linear viscoelastic regime.....	51
2.10.	Rheology data of EPPOSS polymer samples. Each test measures the storage modulus( $G'$ ) and loss modulus( $G''$ ) as a function of percent strain of each sample at varying temperatures. Each sample was in the linear viscoelastic regime. The Ph10 and 30-E'/3 samples are from DMA data, and comparing to rheology data by dividing values by 3, as $E'=3G'$ .....	53
2.11.	Frequency sweeps of EPPh30 at varying temperatures, from 25°C to 200°C..	54
2.12.	Frequency sweep of EPIbu30, at 50°C and 100°C.....	55



2.13.	Molecular weight between crosslinks for EPPh10 (top curve), EPPh30 samples (middle curve), and EPPh30 on second heating, assuming a polymer density of 1 g/mL.....	56
2.14.	Tensile tests of EP and EPPhPOSS polymers, pulled at a rate of 20 mm/min. Each sample was tested 4 times, and the graph values represent an average of the combined tests.....	58
2.15.	Cyclic tensile tests on a EPPh21 dog bone sample. During the test, a sample Stretched to 100% elongation and allowed to relax back to zero displacement five consecutive times at a rate of 20 mm/min. Next, the sample was stretched to 200% elongation, where the same 5 cycles were run. This was followed by 5 cycles at 300% elongation.....	60
2.16.	TEM images of EPPh30 polymers, viewed with natural contrast.....	62
3.1.	Common monomers used in the synthesis of fluoroelastomers.....	68
3.2.	<sup>1</sup> H NMR of poly(octafluoropentylacrylate-IbuPOSS) copolymer.....	74
3.3.	WAXD patterns of POFPA-IbuPOSS copolymers.....	76
3.4.	WAXD patterns of POFPA-IoPOSS copolymers.....	76
3.5.	WAXD patterns of POFPA-PhPOSS copolymers.....	77
3.6.	Modulus as a function of temperature in POFPA and POFPA copolymers..	81
3.7.	Frequency sweep of POFPA homopolymer sample.....	83
3.8.	Frequency sweep of POFPA-Ph14 sample.....	83
3.9.	Frequency sweep of POFPA-Ibu10 sample.....	84
3.10.	TEM images of POFPA-Ibu36 sample.....	86
4.1.	<sup>1</sup> H NMR of DMCOD-EtPOSS copolymer.....	96
4.2.	WAXD patterns for DMCOD-IbuPOSS copolymers.....	99
4.3.	WAXD patterns for DMCOD-PhPOSS copolymers.....	100
4.4.	WAXD patterns for DMCOD-CpPOSS copolymers.....	100
4.5.	WAXD patterns for DMCOD-EtPOSS copolymers.....	101

## LIST OF SCHEMES

Scheme	Page
2.1. EP-POSS Polymerization. ....	36
3.1. Polymerization of octafluoropentylacrylate-POSS copolymers.....	72
4.1. Polymerization of polyisoprene-like POSS copolymers.....	91
5.1 Synthesis of poly(epichlorohydrin)-POSS elastomers.....	110
5.2 Synthesis of POSS-hBD-POSS triblock copolymers.....	111
5.3 Synthesis of POSS-PDMS-POSS block copolymers.....	112

## LIST OF ABBREVIATIONS AND SYMBOLS

AIBN	2,2'-azobis(2-methylpropionitrile)
CGC	Constrained geometry catalyst
CpPOSS	Cyclopentyl-POSS
Cyl	Cyclohexyl
DMA	Dynamic mechanical analysis
DSC	Differential scanning calorimetry
E'	Tensile storage modulus
E''	Tensile loss modulus
EP	Poly(ethylene- <i>co</i> -propylene)
EPPOSS	Ethylene-propylene-POSS
EPDM	Ethylene-propylene-diene monomer
Et	Ethylene
EtPOSS	Ethyl-POSS
DMCOD	1,5-Dimethyl-1,5-cyclooctadiene
Flu	Fluorenyl
G'	Shear storage modulus
G''	Shear loss modulus
GPC	Gel permeation chromatography
HFP	Hexafluoropropylene
IbuPOSS	Isobutyl-POSS
Ind	Indenyl
IoPOSS	Isooctyl-POSS
MAO	Methaluminoxane
M <sub>n</sub>	Number average molecular weight
M <sub>w</sub>	Weight average molecular weight
NMR	Nuclear magnetic resonance
PDI	Polydispersity index
Ph	Phenyl
PhPOSS	Phenyl-POSS
POFPA	Polyoctafluoropentyl acrylate
POSS	Polyhedral Oligomeric Silsesquioxane
ROMP	Ring-opening metathesis polymerization
SBS	Poly(styrene- <i>b</i> -butadiene- <i>b</i> -styrene)
T <sub>7</sub>	Incompletely condensed POSS, Si <sub>7</sub> O <sub>12</sub> R <sub>7</sub> H <sub>3</sub>
T <sub>8</sub>	Completely condensed POSS, Si <sub>8</sub> O <sub>12</sub> R <sub>7</sub> R'
TEM	Transmission electron microscopy
TFE	Tetrafluoroethylene
TGA	Thermal gravimetric analysis
THF	Tetrahydrofuran
VDF	Vinylidene fluoride
WAXD	Wide angle X-ray diffraction

## CHAPTER 1

### INTRODUCTION

#### 1.1. Composites

Composites are the combination of two or more materials with varying physical and mechanical properties, used in order to obtain a material with properties of both constituent parent materials.<sup>1</sup> Composites are fabricated both synthetically and naturally. Wood and bones are two examples of naturally occurring composites. Wood is mostly comprised of three different materials, cellulose, hemicellulose, and lignin. Lignin is a highly crosslinked aromatic polymer, which acts as the matrix to hold cellulose and hemicellulose reinforcement material together. Synthetic composites are commonly used in many applications, including automotive, aircraft, and structural materials. Bricks are one common, synthetic composite, which have traditionally been fabricated from straw and mud, but currently with clay and sand.<sup>1,2</sup> Other synthetic composites include automotive components, aircraft components, structural materials, sporting goods, dental materials, amongst many others.

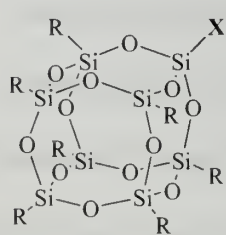
The two main components found in composites are a matrix and a reinforcement material. In polymer composites, the matrix is often a resin, such as a polyester, epoxy, or phenolic. In general, the matrix serves several purposes, including keeping the reinforcement material in place, to distribute or transfer the load, for processibility, and for dimensional stability.<sup>1</sup> The reinforcement materials can be a number of materials with different physical properties, such as mechanical, electrical, or thermal. Examples are fibers, carbon nanotubes, buckeyballs, and inorganic materials. In combination, the matrix and reinforcement material can provide for a strong, lightweight material.

## 1.2. Nanocomposites

Polymer nanocomposites are polymers reinforced with another material, which disperses in the polymer matrix, and has at least one dimension on the nanometer scale.<sup>2</sup> These include nano-scaled materials either blended in with, or chemically attached to, the polymer chain. Reinforcement materials, or fillers, are typically inorganic in nature, and are usually more dense than the organic polymers. In traditional macro- or micro-composites, material properties are determined by the sum of each of the components, weighted by their respective volume fraction. This simple approach often underestimates the material properties, as interfacial interactions also contribute. As the size of the individual components decrease, the contributions from the interfacial interactions increase. When one of the components has dimensions at the nanometer level, this interaction becomes a very important component of material properties. At the same filler loading, a composite with nanometer sized filler will have stronger properties than one with larger dimensions. This leads to lighter materials, as less of the filler is needed to obtain the same material properties.<sup>2</sup>

## 1.3. Polyhedral Oligomeric Silsesquioxane

One class of materials that can be used in nanocomposites are polyhedral



oligomeric silsesquioxanes (POSS). POSS molecules, as shown in Figure 1.1, are cage structured molecules with organic peripheral groups, incorporated for solubility in common organic solvents and compatibility with polymers and surfaces.<sup>3</sup> The cage consists entirely

**Figure 1.1.** POSS of silicon and oxygen atoms, with a 1 to 1.5 ratio of silicon to oxygen. POSS macromonomers and fillers have a diameter of 1 to 3 nanometers. POSS



incorporation into polymers increase the use temperature, surface hardening, oxidative resistance and mechanical properties of the homopolymer analog, as well as decreases the polymer flammability, heat evolution and viscosity.<sup>3</sup> POSS comprises a subset of a larger group of silsesquioxanes, which are materials with the empirical formula  $\text{RSiO}_{1.5}$ , where R can be an alkyl, alkylene, aryl, or arylene group. Silsesquioxane polymer or oligomer structures include cage, ladder, and random. Ladder type polymer silsesquioxanes have oxidative resistance at temperatures over  $500^{\circ}\text{C}$ , have good insulating properties and good gas permeability.

POSS comprises an important group of organic-inorganic hybrid materials.<sup>4-5</sup>

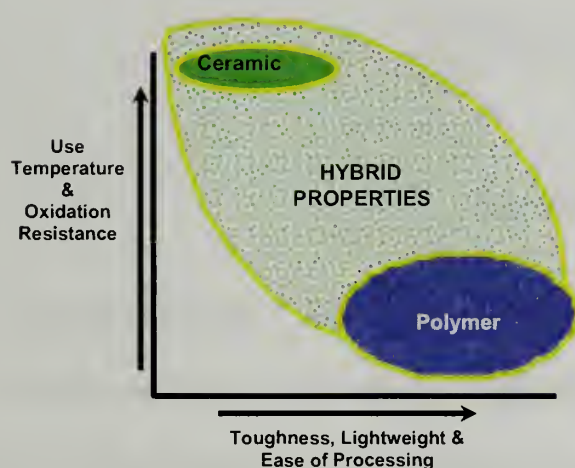


**Figure 1.2. Composite materials**

Organic materials, such as polymers, are strong, lightweight materials (Figure 1.2). Inorganic materials are generally brittle, but have good high temperature resistance. When the two are combined, a composite material with the strengths of both is made, which cannot otherwise be obtained with a single material.

POSS is synthesized by the hydrolysis of organotrichlorosilanes or trialkoxysilanes (Figure 1.3).<sup>3</sup> Products of these reactions include cage structures of varying sizes, ladder like silsesquioxane structures, random structures, and partially-condensed cage structures. Two important structures formed are the fully condensed  $\text{T}_8$  caged structure and the partially condensed  $\text{T}_7$  structure. The  $\text{T}_8$  POSS molecule has 8 silicon atoms, twelve oxygen atoms, and eight organic peripheral groups. This can be

thought of as the smallest possible particle of silica. These molecules are commonly blended into polymer matrices. POSS can also be chemically attached to other small molecules, polymers, or inorganic materials.

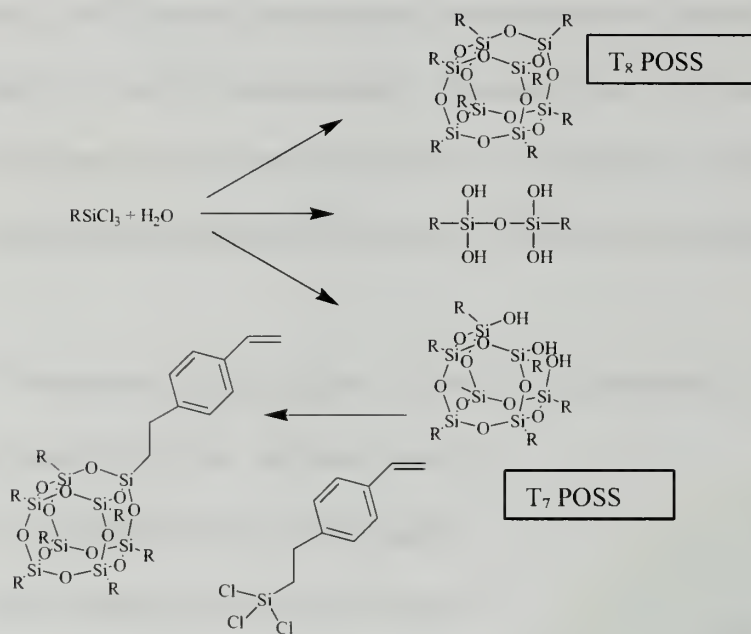


**Figure 1.3.** Synthesis of POSS molecules

This is accomplished using the T<sub>7</sub> POSS cage structure. The T<sub>7</sub> structure contains 7 silicon atoms, 12 oxygen atoms, and 7 peripheral groups, which leaves three silanol groups to be used for further modification by reactions with an organotrichlorosilane and allows for the addition of one unique, reactive functionality. Alcohols, chlorosilanes, epoxides, halides, isocyanates, methacrylates, nitriles, norbornenyls, olefins, silanes, silanols, and styrenes are typical groups added to T<sub>7</sub> POSS molecules.<sup>6</sup>

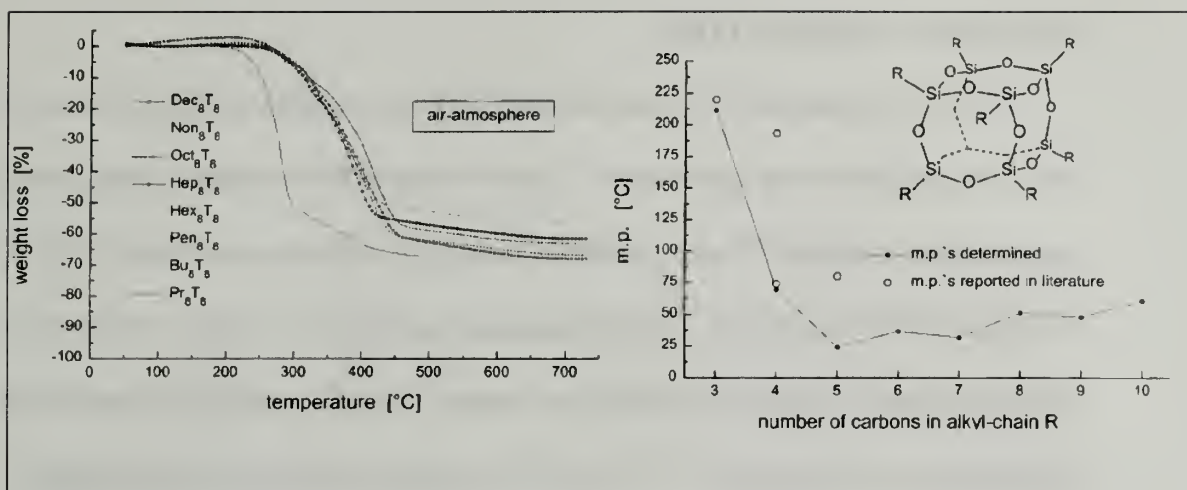


**Figure 1.4.** (R) Melting points of  $T_8$  POSS with varying carbon chain lengths.<sup>7</sup> (L) TGA of  $T_8$  POSS with varying carbon chain lengths.<sup>7</sup>

An important aspect in POSS molecules are the non-reactive peripheral groups. The peripheral group will effect the interaction of POSS with polymer chains in copolymers or blends. Physical properties of POSS monomers change with different peripheral groups. Octa-substituted POSS molecules with different carbon chain lengths were found to have varying melting points, as shown in Figure 1.4.<sup>7</sup> Melting points show an initial decrease with increasing chain length up to a pentyl chain, which then increases, with an odd-even effect observed with increasing chain length. TGA data obtained under nitrogen show an increase in decomposition temperature with an increase in alkyl chain length.<sup>7</sup> These physical changes should have an effect when POSS monomers are incorporated into polymers. Much of the research on POSS containing copolymers makes use of a single peripheral group in their studies, and there is little extensive work on the effect of these peripheries on the properties of a given POSS containing copolymers.



#### 1.4. Polymers containing POSS

POSS is commonly incorporated into polymers, creating novel copolymers with interesting properties and applications. These include POSSnorbornene copolymers for shape memory materials,<sup>8,9</sup> epoxy polymer and epoxy networks containing POSS,<sup>10-17</sup> polyamide POSS copolymers,<sup>18</sup> polybenzoxazine copolymers,<sup>19</sup> poly(vinylphenol-co-vinylpyrrolidone-co-isobutylstyrylPOSS) polymers,<sup>20</sup> polyfluorene-POSS copolymers for blue luminescent applications,<sup>21-22</sup> and POSS containing polymers for lithography.<sup>23</sup>

Polystyrene-POSS and polymethyl methacrylate(PMMA)-POSS copolymers were some of the first POSS copolymers synthesized. Styryl-POSS is synthesized by the addition of styrylethyltrichlorosilane or styryltrichlorosilane to a T<sub>7</sub> POSS molecule. This monomer can then be copolymerized with styrene<sup>24-25</sup> or p-methylstyrene.<sup>26-27</sup> Free radical polymerization using 2,2'-azobis(2-methylpropionitrile) (AIBN) produced random, atactic copolymers with high molecular weights and random POSS distributions. The addition of POSS enhanced the thermal properties, increasing the glass transition temperature, thermal decomposition temperature, and char yield. Syndiotactic polystyrene-POSS copolymers were also synthesized using the piano stool catalyst CpTiCl<sub>3</sub>.<sup>25</sup> Catalyst activity decreased when POSS was used in the feed. Up to 24 wt% of POSS was incorporated, with <sup>13</sup>C NMR studies showing a copolymer with a high syndiotactic microstructure.

The first methacrylate substituted POSS homopolymer was synthesized by Lichtenhan et al. in 1995.<sup>27</sup> The authors used AIBN initiated free radical polymerization with a POSS-methacrylate (MA) to make both homopolymers of POSS with cyclopentyl (Cp) and cyclohexyl (Cy) peripheries and a copolymer with both peripheries.

Homopolymers of CpPOSSmethacrylate and CyPOSSmethacrylate show a 10% decomposition temperature of 388 °C, while PMMA decomposes below 200 °C. The change in POSS peripheries had an effect on the homopolymers and monomers. Both monomers show a broad, two-step transition where the monomer melts, polymerizes and then decomposes, but the cyclopentyl substituted monomer's transition starts 5 °C higher. (192 vs 187 °C) The CpPOSS homopolymer was insoluble in common organic solvents, while the cyclohexyl and a 50/50 Cp/CyPOSS copolymer were both soluble. Expanded studies were performed on poly(methyl methacrylate) (PMMA) polymers with POSSmethacrylate, using tethered and blended POSS.<sup>27</sup> Wide angle x-ray diffraction (WAXD) studies show significant POSS crystallization diffraction peaks of the blend at POSS incorporations as low as 1 vol %. In the case of the copolymer, at least 5 vol % was required to observe significant crystallization. DSC data shows melting exotherms, suggesting that at low POSS filler loadings (less 0.05 vol %), POSS enters the amorphous regime of the PMMA homopolymer until a solubility limit is reached, after which the POSS filler forms crystallinities. Thermal and rheology data suggest the untethered-POSS distributes both as dispersed particles and crystallites.

Polyethylene-POSS copolymers were synthesized by two methods.<sup>29-31</sup> They were synthesized by a two-step process; copolymerization of cyclooctene and norbornenylPOSS using Grubbs' first generation catalyst, followed by hydrogenation of the copolymer. Polyethylene-POSS copolymers were also synthesized using metallocene catalysts, with methaluminoxane (MAO) as a cocatalyst and a vinyl, norbornenyl, or olefinic substituted POSS. High molecular weight copolymers were synthesized with as high as 56 weight % POSS incorporation. Thermal characterization studies show a 90 °C

increase in the thermal decomposition temperature of POSS copolymers from polyethylene homopolymers, under an air atmosphere. Further characterization studies show a dual crystalline nature of the copolymers, where there exist regions of polyethylene crystallization, POSS aggregation, and areas of POSS dispersion in amorphous polyethylene regimes.<sup>32</sup>

The degree of crystallinity of each of the components can be tuned by the method of processing the copolymer. When the copolymer is solution cast from xylenes, polyethylene crystalline domains dominate, and only small POSS domains are formed. However, when the copolymer is cooled from the melt, POSS crystallization is predominant. Figure 1.5 shows TGA decomposition data in air of the ethylene-POSS copolymer, where (a) is cast from xylenes and (b) is cooled from the melt. In (b), POSS crystallites protect the polyethylene domains, greatly increasing the decomposition temperature.

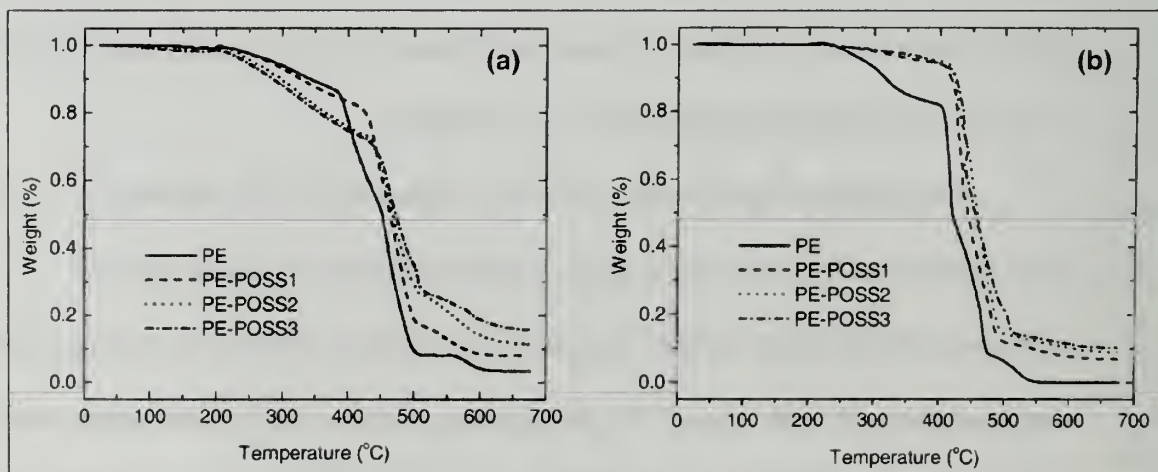


**Figure 1.5.** TGA of polyethylene-POSS copolymers in air. Films in (a) were cast from xylenes and (b) were cooled from the melt.<sup>32</sup>

Polystyrene-, polymethylmethacrylate- and polyethylene-POSS copolymers have shown an increase in thermal oxidative resistance of the copolymers versus the homopolymers, which could be advantageous in space applications. A region 500-2000 kilometers above the surface of the earth is known as low earth orbit (LEO). This is the altitude where satellites and the international space station orbit the earth, and most space missions take place. Resistant polymeric materials, such as Kapton (polyimides) and Teflon (polytetrafluoroethylene) are used in such space applications, but these materials slowly degrade due to their bombardment by atomic oxygen and ultraviolet radiation, which are common in LEO. POSS could be employed to protect satellites and the international space station, as it can protect materials from UV and atomic oxygen degradation. When POSS degrades, its peripheral groups decompose, and the  $\text{SiO}_{1.5}$  POSS cage oxidizes to form silica ( $\text{SiO}_2$ ). Silica is strongly oxidative resistant, with a melting point of  $1713^\circ\text{C}$ .<sup>32</sup> Formation of silica on the surface of material should protect the underlying material from further oxidation. Polyimide-POSS copolymers, Figure 1.6, were tested for space applications.<sup>33</sup>

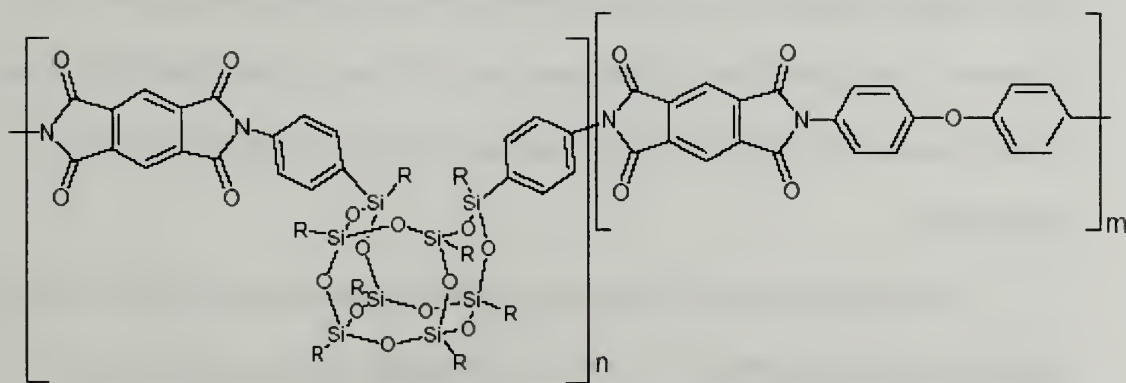


**Figure 1.6.** Structure of POSS-polyimide polymer<sup>34</sup>



The oxidative resistance of these copolymers were studied using depth profilometry and AFM imaging to determine atomic oxygen etching on the polymer surface. Figure 1.7 shows two samples that were exposed to a hyperthermal atomic oxygen beam, with a screen employed to protect selective parts of the material. The materials were exposed to an amount of atomic oxygen fluence equivalent to ten days in low earth orbit.

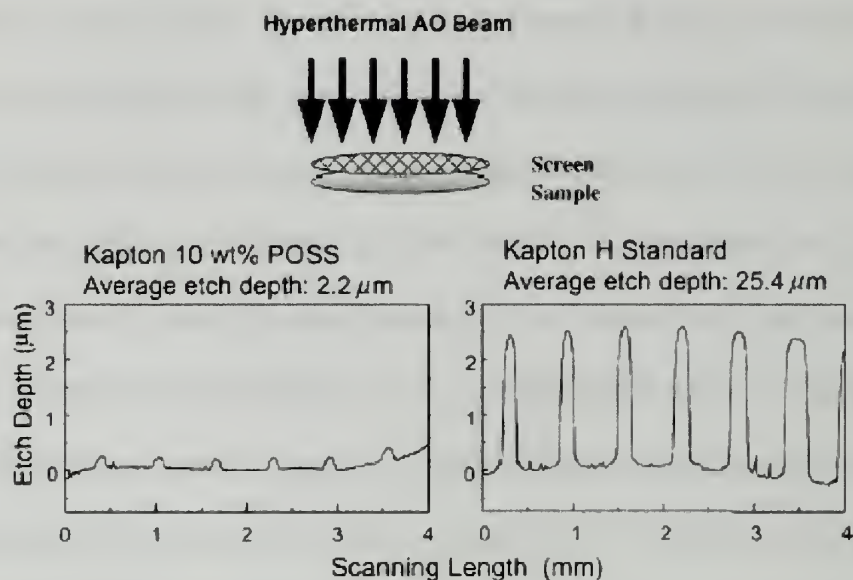


**Figure 1.7.** Profilometry measurements on Kapton-POSS and Kapton film<sup>34</sup>

In the Kapton homopolymer, material is etched away over time, while in the POSS copolymer, the degradation is significantly less. This study shows that POSS greatly protects Kapton from atomic oxygen, making it a potential material for space applications.

Novel architectures have also been employed incorporating POSS, including dendrimers containing POSS,<sup>35-37</sup> and a hemi-telechelic polymer of polystyrene endcapped with an individual POSS monomer.<sup>38</sup> There are a few examples of dendrimers with octa-substituted POSS as the core.<sup>36-37</sup> Hill *et al.* synthesized polyamidoamine (PAMAM) dendrimers with isocyanatePOSS as branch ends.<sup>35</sup> POSS

was attached to dendrimers with between two and five generations. Solubility studies of the dendrimers show that POSS like behavior dominates solubility at as little as 33% by weight of POSS substitution. DSC studies show 'PAMAM-like' glass transitions at 50 wt. % or less POSS substitution. At high POSS incorporation levels, there were no resolved glass transitions, but there were POSS-like melting temperatures, which are indicative of POSS crystalline domains.

## **1.5. Elastomers**

### **1.5.1. Background**

Elastomers, or rubbers, are amorphous materials that can undergo long, reversible deformations.<sup>39-41</sup> Polymers used in elastomers are materials that are nearly or completely amorphous, have a low glass transition temperature, and have low secondary forces. These polymers are subsequently crosslinked to give the material high strength and resilience during deformation. Two types of crosslinking in elastomers are chemical and physical. Chemical crosslinking, or curing, produces a thermoset, where the crosslink is irreversible. Unlike thermosets, thermoplastic elastomers contain physical crosslinks which are reversible by heat or dissolution. This type of crosslinking is a physical interaction between polymer chain segments, which is employed in styrene-butadiene-styrene (SBS) block copolymers and thermoplastic polyurethane elastomers (TPU).<sup>41</sup> Different classes of elastomers include halogen-based elastomers, polysiloxane elastomers, saturated and unsaturated hydrocarbon elastomers, and acrylonitrile-butadiene (NBR) and hydrogenated acrylonitrile-butadiene elastomers (HNBR). Each type of elastomer has unique properties that make them useful in specific applications.

### 1.5.2. Naturally occurring elastomers

Rubber is not only made synthetically, but is also formed naturally in plants and trees. Although synthetic rubber is used more in the world today, natural rubber still plays a huge role in the marketplace. Many different plants produce some amount of rubber, but only *Hevea Brasiliensis* and *Perthenium Argentatum* plants can be used commercially. The chemical structure of hevea rubber and guayule rubber consistent entirely of cis-1,4-polyisoprene. Molecular weights are comparable, although the molecular weight of guayule rubber is dependent upon the age of the plant. To be commercially viable, rubber plants must contain a large amount of rubber, allow for a simple method to remove the rubber and the purification of the rubber must be inexpensive. Guayule rubber is found in the plant tissue of the *Perthenium Argentatum* plant. Three components must be separated from guayule rubber: plant tissue, resin, and the rubber. Plant tissue is insoluble in simple organic solvents, which makes it easy to separate. The rubber is separated from the latex by solvent extraction. Unlike guayule rubber, hevea rubber can be obtaining from the tapping of *Hevea Brasiliensis* trees and its contents separated by solvent extractions. Currently, commercialization of guayule rubber is not commonly practiced amongst rubber companies, as guayule rubber requires extensive purification process and the rubber yields are relatively low compared to haveau rubber.<sup>40</sup>

### 1.5.3. Synthetic elastomers

Natural rubber was originally used for most applications, but its usage has been surpassed by synthetic rubber (Figure 1.8). World War II marked the beginning of extensive industrial interest in synthetic rubbers, as the availability of natural rubber decreased during the war. Styrene-butadiene rubber was one of the most important

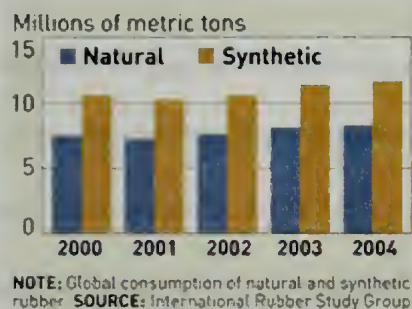


**Figure 1.8.** Global consumption of rubber.<sup>41</sup>

elastomers during this time, especially in the tire industry. Random copolymers were produced using an emulsion polymerization process. During the 1960s, a strong effort was put forth to produce block copolymers of styrene and butadiene.

Styrene and butadiene diblock copolymers and styrene-butadiene-styrene (SBS) triblocks are

unique elastomers. Although they are not vulcanized like natural rubber, styrene-butadiene random copolymers, or other thermosets, SBS elastomers have strong properties due to the presence of styrene aggregates in butadiene amorphous domains. Styrene aggregation acts as a physical crosslink, which can be disrupted by heat or dissolution. These polymers can be reprocessed by cooling the sample or evaporating the solvent to reform the styrene aggregates. These materials are known as thermoplastic elastomers. Other advantages of these SBS thermoplastics include a high tensile strength at moderate temperatures, good low-temperature properties, and the ability to be more easily recycled. Other thermoplastic elastomers include polyurethanes, polyesters, and polyamides.



#### 1.5.4. Halogen-based elastomers

Halogen-based elastomers are another subset of rubbers, characterized by the

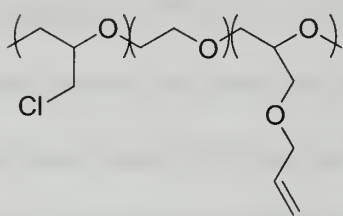


**Figure 1.9.** Structure of epichlorohydrin based elastomer

presence of fluorine, chlorine, or bromine on the polymer chain.<sup>39</sup> These are oil resistant elastomers, as the

electronegative halogens create dipoles which repel non-polar hydrocarbon solvents. Some chlorinated elastomers

include chlorinated polyethylene, polyepichlorohydrin, and

polychloroprene. Polyepichlorohydrin elastomers (Figure

1.9) are copolymers of epichlorohydrin and allyl glycidyl ether or terpolymers with ethylene oxide. Allyl glycidyl ether is a cure site monomer, which is used for subsequent peroxide or sulfur crosslinking. They can also be crosslinked by heating the elastomer in solution in the presence of a difunctional nucleophile. Epichlorohydrin elastomers have strong resistance to oil and gasoline, and have good low temperature flexibility. They are used commonly in the automotive industry as hoses, tubing, seals, gaskets, and coated fabrics.

Fluorine based elastomers have become increasingly popular, despite the high costs of fluoromonomers.<sup>43</sup> They are primarily used as shaft seals, gaskets, wire and cable coatings, along with many oil-field products. Fluoroelastomers are useful because of their high temperature resistance, fuel and oil resistance, low flammability, and high oxidation and weathering resistance. The industrial significance of fluoroelastomers started in the late 1950s, marked by the introduction of poly(vinylidene-fluoride-co-hexafluoropropylene), which were patented by DuPont(Viton) and 3M(Fluorel). Other

examples of fluoroelastomers include fluorosilicon elastomers, poly(propylene-co-tetrafluoroethylene), fluorovinylethers, and fluoroacrylates.

#### **1.5.5. Silicon based elastomers**

Silicon based elastomers are materials with excellent weather and thermal stability, ozone and oxidative resistance, low temperature flexibility and good solvent and oil resistance. The usage temperature of polysiloxanes range from -100 to 250 °C, and have  $T_g$  in the range of -127 °C.<sup>40</sup> The most commonly used silicon elastomer is polydimethylsiloxane (PDMS). PDMS can be synthesized by the ring-opening polymerization of octamethylcyclsiloxane using acids or bases. Octamethylcyclsiloxane is formed by the hydolysis of chloromethylsilanes, which also produce linear polysiloxanes. Polysiloxanes are usually copolymerized with a small amount of a vinyl-containing comonomer, which is used for subsequent crosslinking. Other monomers, containing phenyl and 3,3,3-trifluoropropyl groups, are copolymerized to give the elastomers better high temperature properties. Applications for these elastomers include fluids, greases, lubricants, seals, electrical insulation, coatings, caulks, implants, and prosthetics.

#### **1.5.6. Hydrocarbon based elastomers**

Hydrocarbon based elastomers are divided into two categories, saturated and unsaturated. Unsaturated hydrocarbon elastomers include polyisoprene, polybutadiene, and polyalkenylenes. Polybutadiene is synthesized by the polymerization of 1,3-butadiene. Three different configurations can be formed during polymerization: cis-1,4, trans-1,4 and vinyl, as shown in Figure 1.10. The configuration of the material determines its properties and uses.

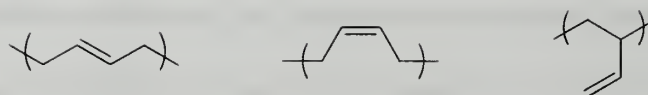


**Figure 1.10.** Configurations of polybutadiene. From left to right, trans 1,4, cis-1,4, and cis-1,2.

Polybutadienes that contain a high amount of cis-1,4 confirmations have low glass transition temperatures ( $-100$  to  $-109$  °C), high resilience, good tear strength, and high abrasion resistance. They are commonly used in tire manufacturing, high impact polystyrene and in golf balls. High-trans polybutadiene is not important industrially, due to its high crystallinity. Vinyl polybutadienes have much higher  $T_g$  values ( $-40$  °C for 70% vinyl), and can be used in post-polymerization functionalization. The relative amount of each of the configurations in polybutadiene is altered by the method of polymerization, reaction temperature, and other reaction condition modifications. The main drawbacks to these elastomers are their poor chemical and weatherability resistance. The high concentration of double bonds makes the rubber prone to degradation by oxidation. A large amount of anti-oxidants are commonly used to increase the shelf-life of these materials.

Saturated hydrocarbon elastomers are advantageous over their unsaturated counterparts, as their backbones are completely void of double bonds, making them much more oxidative and weather resistant. Saturated hydrocarbon elastomers include ethylene-propylene copolymers (EPM), ethylene-propylene-diene terpolymers (EPDM), crosslinked polyethylene elastomers, norbornene rubber and polyisobutylene elastomers.

These elastomers are commonly used for outdoor and high temperature applications, due to their good heat, oxidative, and water resistance. Polyisobutylene, butyl rubber, has very low gas permeability properties, making it good for many applications, including tire inner tubes and basketballs.<sup>40</sup>

EPDM elastomers are synthesized using ethylene and propylene, along with a diene, such as ethylidene norbornene, dicyclopentadiene, or 1,4-hexadiene. The remaining double bonds from the diene are used for peroxide or sulfur curing. Applications for these materials include seals for automotive trunks, doors, and seals, roofing membranes, hoses, tubing, wire and cable insulations, tire sidewalls, and footwear.

One drawback to hydrocarbon based elastomers is poor fuel and oil resistance. One method to improve oil resistance is to incorporate acrylonitrile into the hydrocarbon backbone. Acrylonitrile-butadiene copolymers (NBR) and hydrogenated acrylonitrile-butadiene rubbers (HNBR) are very fuel and oil resistant elastomers. NBR was initially developed in Germany in the 1930s using emulsion polymerization and named “Buna N”. Japan began the manufacturing of HNBR in 1959, which improved the heat and weathering resistance of the NBR. NBR and HNBR are used commonly today for fuel hoses, oil hoses, seals, printing rolls, blankets, adhesives, and brake shoes.<sup>40</sup>

### **1.6. Elastomers containing POSS**

Several thermoplastic elastomers containing POSS have been studied, as shown in Figure 1.11.<sup>45</sup> Haddad *et al.* grafted POSS onto styrene-butadiene-styrene block copolymers by hydrosilation reactions using Karstedt’s catalyst. By grafting POSS onto these elastomers rather than in a direct polymerization, the only changes from the parent



elastomer to the CpPOSS-modified elastomer are due to POSS incorporation. X-ray studies show aggregates of CpPOSS molecules in the butadiene domains. POSS aggregation in the butadiene domain causes a larger loss of long-range ordering of the SBS cylinders with an increase in the POSS loading. Mechanical data shows an increase in tensile modulus with the addition of POSS. This work was extended to the study of POSS peripheral effects on these SBS thermoplastic elastomers with a lamellar morphology.<sup>46</sup>

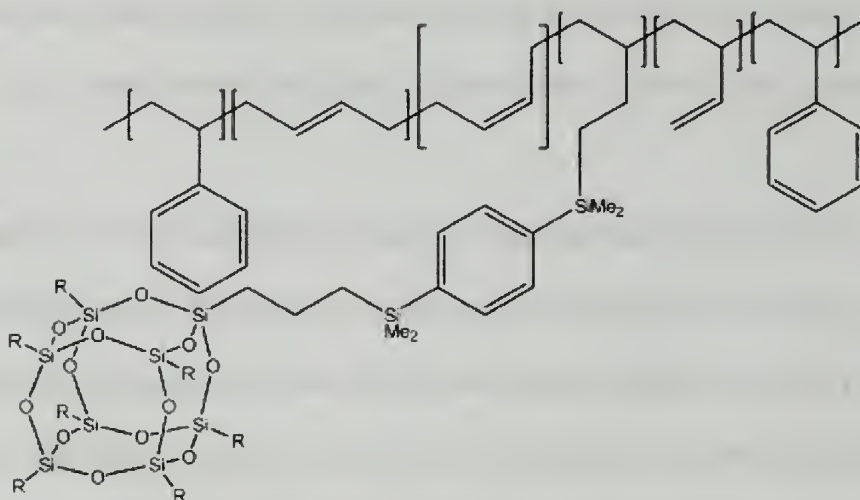


**Figure 1.11.** Structure of Styrene-Butadiene-Styrene-POSS thermoplastic elastomer<sup>45</sup>

The cyclic peripheries were changed to include cyclohexyl (Cy), cyclohexenyl (Cyl), phenyl(Ph), and cyclopentyl(Cp). The phenyl periphery shows the most notable changes in the morphology, as it interacts with the styrene phase. When compared to the parent copolymer, the PhPOSS-SBS polymer has a smaller lamellae d spacing, as well as a decrease in the order-to-disorder transition temperature( $T_{ODT}$ ), as PhPOSS acts as a plasticizer. CylPOSS also shows these effects, albeit to a smaller degree. CylPOSS and CpPOSS also see a smaller d spacing and decrease in  $T_{ODT}$ , but to a much smaller extent than with phenyl and cyclohexenyl peripheries. Increasing the amount of POSS to 20

weight % in the SBS triblocks cause a change in morphology, from a lamellar structure to a perforated layer morphology. Another study by this group looked at isobutylPOSS (IbuPOSS) SBS elastomers.<sup>47</sup> They found POSS was well-distributed in the butadiene domain, and did not interact with the styrene domains. Essentially, IbuPOSS swells the butadiene domain, shifting the phase diagram to a lower styrene content.

POSS was also polymerized into polyurethane thermoplastics, consisting of 4,4'-methylenebis(phenylisocyanate) hard segments and polytetramethylene glycol soft segments, as shown in Figure 1.12.<sup>48</sup> Hydrido-POSS was reacted with diallylbisphenol A to synthesize the POSS monomer. The monomers were randomly distributed in the polymer chain.

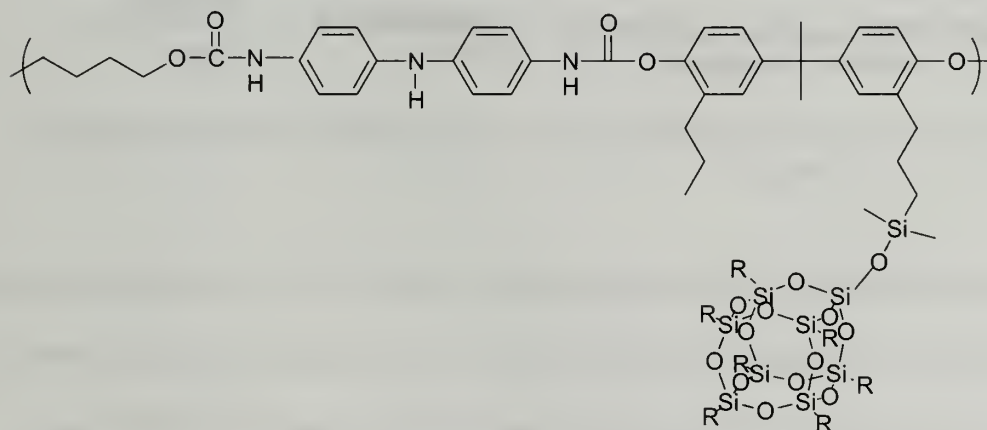


**Figure 1.12.** Structure of Polyurethane-POSS thermoplastic elastomer<sup>48</sup>

POSS increased the tensile modulus and strength of the polyurethane polymer. X-ray studies show a general structure disorientation of the polyurethane polymer when POSS was added. POSS did form aggregates within the hard polyurethane segments. As the polymer samples were stretched, both the POSS aggregates and polyurethane hard segments were destroyed.



Another thermoplastic polymer consisting of an ABA triblock copolymer, with a poly(n-butyl acrylate) inner block, and outer blocks of poly(methyl methacrylate-POSS), was synthesized using atom transfer radical polymerization, as shown in figure 1.13.<sup>47</sup>

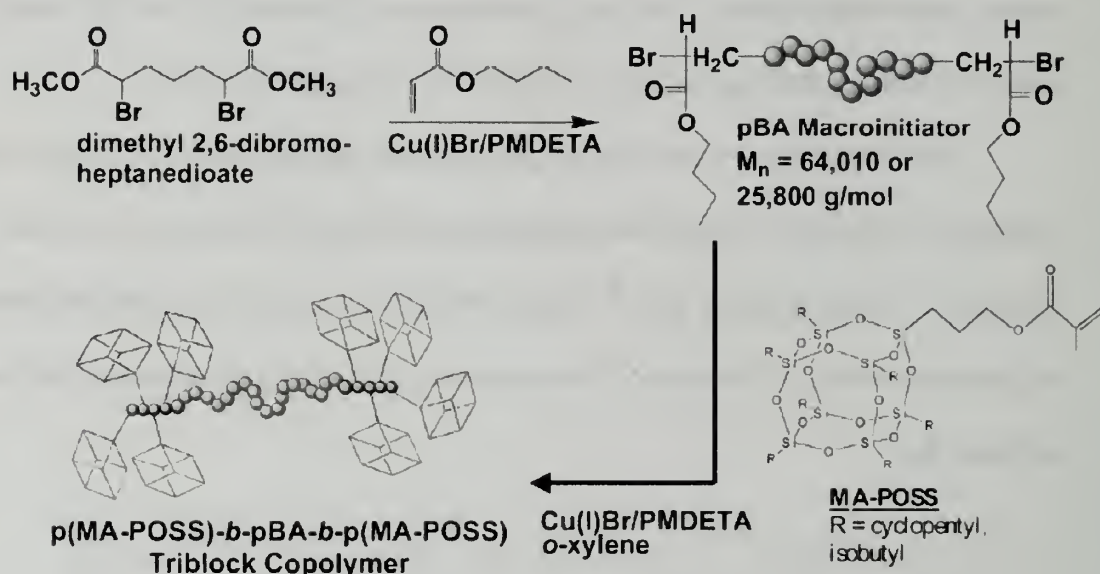


**Figure 1.13.** Synthesis of POSS-(n-butyl acrylate)-POSS triblock thermoplastic elastomers<sup>47</sup>

At small molar ratios of POSS:poly(n-butyl acrylate)(6/481/6), no microphase separation was observed. At higher ratios(10/201/10), a strong separation occurred, showing a morphology of poly(n-butyl acrylate) cylinders within a continuous POSS phase.

The two previous examples show POSS elastomers in block copolymers, in which there is phase segregation and POSS aggregation effects. In a different study, random copolymers of 1,4-butadiene and POSS were synthesized by ring-opening metathesis polymerization using Grubbs first generation catalyst with 1,5-cyclooctadiene and CpPOSSnorbornene monomers.<sup>49</sup> In this study, there are no competing domain segregation effects.

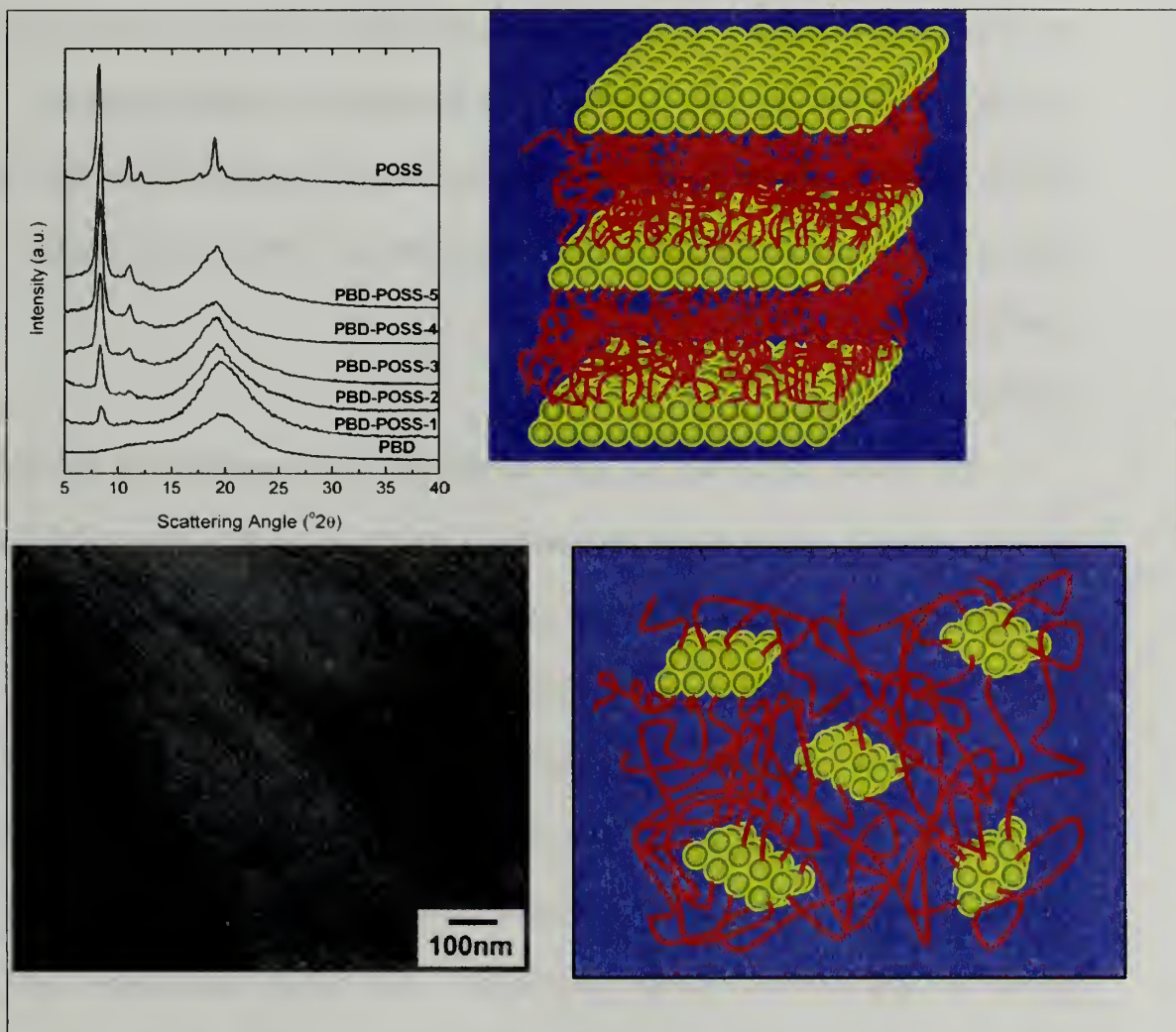


**Figure 1.14.** Characterization of Poly(1,4-butadiene)-POSS copolymers.

**Top left:** Wide angle X-ray diffraction pattern of copolymers, with increasing POSS incorporation from bottom top **Bottom Left:** TEM image of butadiene-POSS copolymers with 52 wt% POSS incorporation. **Top right:** Cartoon of POSS raft-like structure in polybutadiene-POSS copolymers with high POSS incorporations (>30 weight %). **Bottom right:** Cartoon of POSS raft-like structure with low POSS incorporations.<sup>50</sup>

POSS incorporations between 12 and 53 weight percent were obtained in these

copolymers. Wide-angle X-ray diffraction studies (Figure 1.14, top left) show an increase

in the POSS diffraction peaks with an increase in POSS content. The peaks remained relatively sharp, indicating relatively long POSS domain lengths. This data, combined with small angle x-ray scattering and transmission electron microscopy studies show a lamellar morphology in the copolymers with high POSS content, which allowed the authors to present a raft-like structure cartoon, with POSS crystallites forming between amorphous butadiene regimes. At lower POSS incorporations, smaller aggregates formed. (Figure 14, bottom right) These are more akin to a crosslinked elastomer, as a small amount of junction points between multiple polymer chain creates a physical crosslink domain.

### **1.7. Summary**

POSS molecules are unique hybrid organic-inorganic materials with excellent material properties, which enhance the oxidative resistance, mechanical properties, and decomposition temperatures of polymer when chemically incorporated into polymer chains. POSS molecules are also shown to aggregate in copolymers, which act as a physical crosslink. As shown in polybutadiene-POSS copolymers, POSS forms raft-like structures, which can protect the polymer from UV radiation, heat, and atomic oxygen. The smaller POSS domains are more like SBS physically crosslinked copolymer, as the styrene domains are either spherical or cylindrical. This presents great interest for future materials with novel properties. This includes elastomers, where POSS aggregation acts as a physical crosslink, giving novel thermoplastic elastomers, which will also have stronger mechanical and thermal properties. POSS polymers employing physical crosslinks are especially interesting, as random copolymers do not require the more intensive chemistries involved with synthesizing triblock copolymers.



Although there has been research on POSS copolymers with low  $T_g$  amorphous materials, there are still several fundamental questions to be answered. There has been little work done on how the polymer backbone and POSS periphery effects the aggregation of POSS in these amorphous polymers. It has been seen that POSS aggregates in these copolymer, but no research on how effective POSS acts as a physical crosslink for thermoplastic elastomers. To answer these fundamental questions, novel POSS containing copolymers must be synthesized with chemically different backbone to allow for the study of the POSS peripheral effect on aggregation, and have sufficient material strength to study the mechanical properties of these POSS containing copolymers.

#### 1.8. References

- (1) Harper, Charles. *Handbook of Plastics, Elastomers, and Composites*, 3<sup>rd</sup> Ed. McGraw-Hill, New York, 1996.
- (2) Joshi, M. and Butola, B. *Journal of Macromolecular Science Part C-Polymer Reviews* **2004**, 44, 389-410.
- (3) Li, G.; Wang, L.; Ni, H.; and Pittman Jr., C. *Journal of Inorganic and Organometallic Polymers* **2001**, 11, 123-154.
- (4) Sanchez, C.; Julián, B.; Belleville, P.; and Popall, M. *Journal of Materials Chemistry* **2005**, 15, 3559-3592.
- (5) Sanchez, C.; Soler-Illia, G.; Ribot, F.; Lalot, T.; Mayer, C.; and Cabuil V. *Chemistry of Materials* **2001**, 13, 3061-3083.
- (6) Hybrid Plastics <http://www.hybridplastics.com>
- (7) Bolln, C.; Tsuchida, A.; Frey, H.; and Mülhaupt, R. *Chemistry of Materials* **1997**, 2, 1475-1479.
- (8) Mather, P.; Jeon, H.; Romo-Uribe, A.; Haddad, T.; and Lichtenhan, J. *Macromolecules* **1999**, 32, 1194-1203.

- (9) Jeon, H.; Mather, P.; and Haddad, T. *Polymer International* **2000**, *49*, 453-457.
- (10) Liu, Y.; Zheng, S.; and Nie, K. *Polymer*, **2005**, *46*, 12016-12025.
- (11) Li, G.; Wang, L.; Toghiani, H.; Daulton, T.; Koyama, K.; Pittman Jr., C. *Macromolecules* **2001**, *34*, 8686-8693.
- (12) Li, G.; Wang, L.; Toghiani, H.; Daulton, T.; and Pittman Jr., C. *Polymer* **2002**, *43*, 4167-4176.
- (13) Lee, A. and Lichtenhan, J. *Macromolecules* **1998**, *31*, 4970-4974.
- (14) Abad, M.; Barral, L.; Fasce, D.; and Williams, J. *Macromolecules* **2003**, *36*, 3128-3135.
- (15) Matejka, L.; Strachota, A.; Plestil, J.; Whelan, P.; Steihhart, M.; and Slaof, M. *Macromolecules* **2004**, *37*, 9449-9456.
- (16) Strachota, A.; Kroutilova, I.; Kovarova, J.; and Matejka, L. *Macromolecules* **2004**, *37*, 9457-9464.
- (17) Laine, R.; Choi, J.; and Lee, I. *Advanced Materials* **2001**, *13*, 800.
- (18) Ricco L.; Russo S.; Monticelli O.; Bordo A.; and Bellucci F. *Polymer* **2005**, *46*, 6810-6819.
- (19) Lee, Y.; Kuo, S.; Su, Y.; Chen, J.; Tu, C.; and Chang, F. *Polymer* **2004**, *45*, 6321-6331.
- (20) Hongyao, X.; Kuo, S.; and Chang, F.; *Polymer Bulletin* **2002**, *48*, 469-474.
- (21) Lee, J.; Cho, H.; Jung, B.; Cho, N.; and Shim, H.; *Macromolecules* **2004**, *37*, 8523-8529.
- (22) Chou C.; Hsu S. ; Dinakaran K.; Chiu M.; and Wei K. *Macromolecules* **2005**, *38*, 745-751.
- (23) Tegou, E.; Bellas, V.; Gogolides, E.; Argitis, P.; Eon, D.; Cartry, G.; and Cardinaud, C. *Chemistry of Materials* **2004**, *16*, 2567-2577.
- (24) Haddad, T.; Viers, B.; and Phillips, S. *Journal of Inorganic and Organometallic Polymers* **2001**, *11*, 155-164.
- (25) Zheng, L.; Kasi, R.; Farris, R.; and Coughlin, E.B. *Journal of Polymer Science Part A: Polymer Chemistry* **2002**, *40*, 885-891.
- (26) Haddad, T. and Lichtenhan, J. *Macromolecules*, **1996**, *29*, 7302-7304.

- (27) Romo-Uribe, A.; Mather, P.; Haddad, T.; and Lichtenhan, J. *Journal of Polymer Science Part B: Polymer Physics* **1998**, *36*, 1857-1872.
- (28) Lichtenhan, Y.; Otonari, Y.; and Carr, M. *Macromolecules* **1995**, *28*, 8435-8437.
- (29) Kopesky, E.; Haddad, T.; Cohen, R.; and McKinley, G. *Macromolecules* **2004**, *37*, 8993-9004.
- (30) Zheng, L.; Farris, R.; and Coughlin, E.B. *Macromolecules* **2001**, *34*, 8034-8039.
- (31) Zheng, L.; Farris, R.; and Coughlin, E.B. *Journal of Polymer Science Part A: Polymer Chemistry* **2001**, *39*, 2920.
- (32) Lide, David. *CRC Handbook of Chemistry and Physics*, 81<sup>st</sup> Ed. CRC Press, New York, 2001.
- (33) Tsuchida, A.; Bolln, C.; Sernetz, F.; Frey, H.; and Mülhaupt, R.; *Macromolecules* **1997**, *30*, 2818-2824.
- (34) Waddon, A.; Zheng, L.; Farris, R.; and Coughlin, E.B. *Nano Letters* **2002**, *2*, 1149-1155.
- (35) Phillips, S.; Haddad, T.; and Tomczak, S. *Current Opinion in Solid State and Materials Science* **2004**, *8*, 21-29.
- (36) Dvornic, P.; Hartmann-Thompson, C.; Keinath, S.; and Hill, E. *Macromolecules*, **2004**, *37*, 7818-7831.
- (37) Ropartz L.; Morris R.; Schwartz G.; Foster D.; Cole-Hamilton, D.; *Inorganic Chemistry Communications* **2000**, *3*, 714-717.
- (38) Ropartz L.; Morris R.; Foster D.; Cole-Hamilton D. *Chemistry Communications* **2001**, *4*, 361-362.
- (39) Cardoen, G. and Coughlin, E.B. *Macromolecules* **2004**, *37*, 5123-5126.
- (40) Bhowmick, A. and Stephens, H. *Handbook of Elastomers*, 2<sup>nd</sup> Ed. Marcel Dekker, Inc., New York, 2001.
- (41) Sperling, L. *Physical Polymer Science*, 3<sup>rd</sup> Ed. Wiley Interscience & Sons, Inc. New York, 2001.
- (42) Odian, G. *Principles of Polymerization*, 3<sup>rd</sup> Ed. Wiley Interscience & Sons, Inc. New York, 1991.



- (43) Chemical and Engineering News  
<http://pubs.acs.org/cen/coverstory/83/8342elastomers.html>
- (44) Ameduri, B.; Boutevin, B.; and Kostov, G. *Progress in Polymer Science* **2001**, *26*, 105-187.
- (45) Fu, B.; Lee, A.; and Haddad, T. *Macromolecules* **2004**, *37*, 5211-5218.
- (46) Drazkowski, D.; Lee, A.; Haddad, T.; and Cookson, D. *Macromolecules* **2006**, *39*, 1854-1863.
- (47) Drazkowski, D., Lee, A., Haddad, T. *Macrmolecules* **2007**, *40*, 2798-2805.
- (48) Fu, B.; Hsiao, B.; Pagola, S.; Stephens, P.; White, H.; Rafailovich, M.; Sokolov, J.; Mather, P.; Jeon, H.; Phillips, S.; Lichtenhan, J.; and Schwab, J. *Polymer*, **2001**, *42*, 599-611.
- (49) Pyun, J.; Matyjaszewski, K.; Wu, J.; Kim, G.; Chun, S.; and Mather, P. *Polymer*, **2003**, *44*, 2739-2750.
- (50) Zheng, L., Hong, S., Cardoen, G., Burgaz, E., Gido, S., Coughlin, E.B. *Macromolecules* **2004**, *37*, 8606-8611.

## CHAPTER 2

### SYNTHESIS AND CHARACTERIZATION OF ETHYLENE-PROPYLENE-POSS THERMOPLASTIC ELASTOMERS

#### 2.1. EPDM background

Ethylene-propylene diene monomer (EPDM) elastomers comprise a family of weather, chemical, and heat resistant elastomers.<sup>1-3</sup> The strong weather and chemical resistance of EPDMs are due to the completely saturated polymer backbone. These elastomers are synthesized using ethylene and propylene, along with a diene monomer, such as ethylidene norbornene, dicyclopentadiene, or 1,4-hexadiene. The remaining double bonds from the diene are used for peroxide or sulfur curing. Applications for these materials include seals for automotive trunks, doors, along with roofing membranes, hoses, tubing, wire and cable insulations, tire sidewalls, and footwear.



**Figure 2.1.** (L) Structure of EPDM, with ethylidene norbornene as the diene (M) Car seal made from EPDM<sup>4</sup> (R) Roofing material made from EPDM<sup>5</sup>

Each different component of these elastomers are very important. Ethylene gives strength to the terpolymer. Ideally, 40-70 mol percent of ethylene is incorporated. High ethylene containing EPDMs have better high temperature stability and better mechanical properties, but suffer from lower solubility before curing. Propylene is used to disrupt the

crystallinity of the polymer, with approximately 30 mol percent needed. Longer alkyl chain  $\alpha$ -olefins, such as 1-hexene and 1-butene, completely disrupt the crystallinity at lower levels of incorporation, but are not used due to their higher monomer costs and lower incorporation rates. The dienes, which are used for subsequent chemical crosslinking, are incorporated at low levels (0.5-3.0 mol percent), and varied to change the crosslink densities and cure rates. Ethylidene norbornene is most commonly used because it has the fastest cure rate during sulfur vulcanization, which results in EPDMs with higher modulus and crosslink density than ones using dicyclopentadiene or 1,4-hexadiene at comparable diene incorporation levels.

## **2.2. Synthesis of EPDM elastomers**

Industrially, EPDM elastomers are synthesized using Ziegler-Natta based catalysts, which are typically soluble vanadium salts. Good EPDM polymerization catalysts will synthesize materials with a high incorporation of propylene and diene, high molecular weight, a monomodal and low polydispersity (2-4), and a random incorporation of ethylene ( $C_2$ ), propylene ( $C_3$ ), and diene, to give completely amorphous materials.<sup>3</sup> Vanadium based catalysts are activated by aluminum based cocatalysts, such as ethylaluminum sesquichloride, diethylaluminum chloride, and ethylaluminum dichloride. The aluminum to vanadium ratio is very important in these polymerizations. High Al:V ratios give polymers with random distribution of monomers, narrow polydispersities, low branching and a fast cure rate. However, at low ratios of Al:V, polymers with broad polydispersities, less random monomer incorporations and high amounts of branching form.<sup>3</sup> Another disadvantage to these systems are the chlorine containing cocatalyst. During normal workup conditions, a small amount of chloride

remains in the polymer, which is difficult to remove. Therefore, further purification steps are required to obtain a desirable product. One way to alleviate this problem is to use metallocene or constrained geometry catalysts (CGC), which are activated with methaluminoxane (MAO). Recently, there has been much academic research on synthesizing EPDMs with a variety of bridged metallocene catalysts.<sup>6-22</sup> Several reviews summarize the exhaustive work on Ziegler-Natta, constrained geometry and metallocene catalyzed ethylene, propylene,  $\alpha$ -olefin, norbornene, and norbornene derivative homo-, co-, and terpolymerizations.<sup>6-9</sup> The first EPDM polymerization literature report using metallocene catalysts was from Kaminsky *et al.*, who used a bis(cyclopentadienyldimethyl) dimethyl zirconium catalyst with a methaluminoxane (MAO) cocatalyst.<sup>10</sup> Ethylene incorporations ranged from 50-80 weight percent and ethylidene norbornene incorporations ranging from 2-10 weight percent, which are in the range of useful EPDMs. Weight average molecular weights were estimated to be between 40,000 and 160,000 g/mol, with polydispersities around 1.7. Many reports on ethylene-propylene-diene polymerizations using bridged metallocene,<sup>11-18</sup> constrained geometry,<sup>19-20</sup> and other group IV metal catalysts,<sup>21-22</sup> afforded polymers with generally high molecular weights, low polydispersities (2-3) and high levels of diene incorporation. Gillis and Karpeles patented the synthesis of EPDMs using a wide variety of group IV bridged metallocene catalysts with MAO cocatalysts.<sup>23</sup> Typical results are shown in table 2.1 below.



**Table 2.1.** Ethylene-propylene-ethylidene norbornene (ENB) terpolymers synthesized using varying metallocene catalysts activated by MAO<sup>23</sup>

Catalyst	$M_w (*10^3)$ (g/mol)	PDI	$C_2/C_3$ in polymer	ENB in polymer(wt%)
Et(Ind) <sub>2</sub> ZrCl <sub>2</sub>	142	2.15	69/31	6.6
Et(Ind) <sub>2</sub> HfCl <sub>2</sub>	514	2.19	59/41	3.7
Me <sub>2</sub> Si(Ind) <sub>2</sub> ZrCl <sub>2</sub>	164	2.07	70/30	4.9
Me <sub>2</sub> Si(Ind) <sub>2</sub> HfCl <sub>2</sub>	162	2.02	68/32	12.1
Me <sub>2</sub> Si(2-MeInd) <sub>2</sub> ZrCl <sub>2</sub>	330	1.86	78/22	0.0
Me <sub>2</sub> Si(Flu) <sub>2</sub> ZrCl <sub>2</sub>	409	1.95	79/21	5.0
Ph <sub>2</sub> C(Cp-9Flu)ZrCl <sub>2</sub>	232	2.00	70/30	7.2

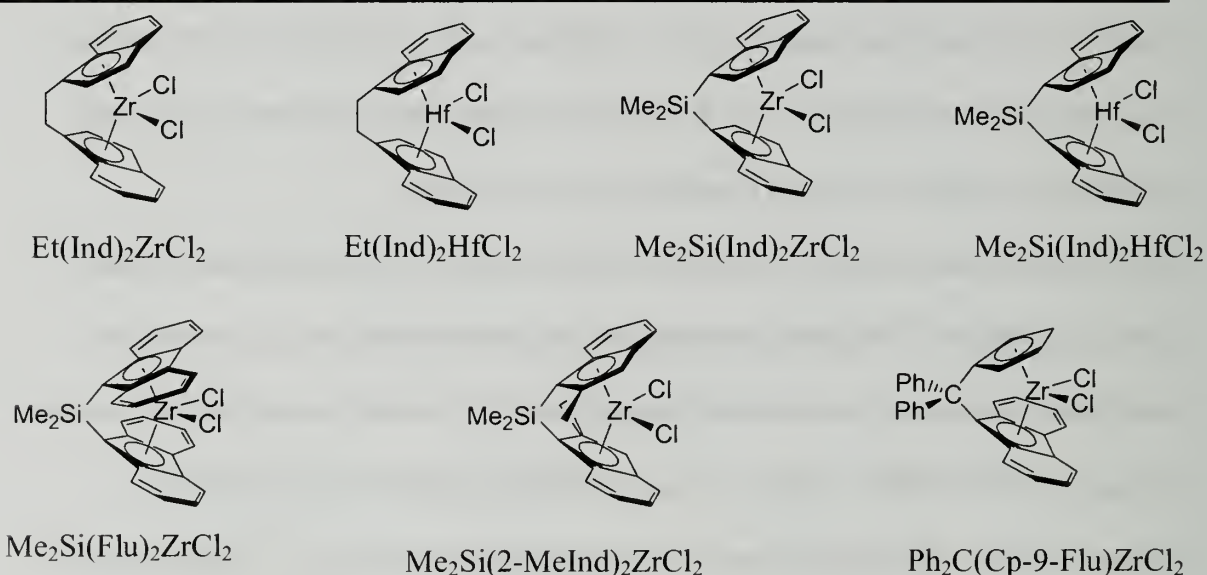


**Figure 2.2.** Structures of metallocene catalysts used in EPDM synthesis

### 2.3. POSS Elastomer Background

In previous work, POSS was incorporated into polybutadiene by a ring-opening metathesis polymerization of cyclooctadiene and cyclopentylPOSSnorbornene.<sup>24</sup> POSS was incorporated at levels ranging from 10-50 weight percent. Wide angle X-ray diffraction data shows strong POSS diffraction peaks with increasing POSS loadings. Transmission electron microscopy studies show formation of aggregates at low POSS loadings (12 wt. %), which have lengths as long as 50 nanometers. At POSS loadings of 32 weight %, a lamellar morphology was observed. This data indicates a raft-like



polymer morphology, with 2-dimensional POSS aggregates forming between amorphous butadiene regimes. This POSS particle aggregation can be considered a physical crosslink, as compared to a chemical crosslink formed via a traditional curing process. Although polybutadiene-POSS copolymers show POSS aggregation, the polymer backbone contains a high concentration of backbone olefinic groups, which give polymers with poor weatherability properties. Also, the reaction conditions allowed for the formation of copolymers with weight average molecular weights of only about 70,000 g/mol, which are not sufficient for extensive mechanical studies. Therefore, it would be advantageous to synthesize a saturated hydrocarbon elastomer containing POSS, such as in EPDM systems.

#### **2.4. Project Goals**

The goal of this project is to synthesize ethylene-propylene-POSS (EPPOSS) elastomers, varying the incorporation of POSS in the polymers. Several different peripheral groups of POSS, isobutyl, ethyl, and phenyl, will be incorporated to study the structural, physical, and mechanical properties that results from altering the periphery in these terpolymers. The properties of these polymers will be studied and compared to ethylene-propylene parent polymers and crosslinked polymers to determine what, if any advantages there may be for POSS containing thermoplastic ethylene-propylene elastomers compared to traditional EPDMs.

## 2.5. Experimental Section

### 2.5.1. Materials

Toluene, hexanes, tetrahydrofuran (THF), and triethylamine were purchased from Aldrich and purified by vacuum distillation from calcium hydride. Isobutyl-POSS-norbornene macromonomer, 1-[2-(5-norbornen-2-yl)ethyl]-3,5,7,9,11,13,15-heptaisobutylpentacyclo [9.5.1.1<sup>3,9</sup>.1<sup>5,11</sup>.1<sup>7,13</sup>]octasiloxane, Ethyl-POSS-norbornene 1-[2-(5-norbornen-2-yl)ethyl]-3,5,7,9,11,13,15-heptaethylpentacyclo [9.5.1.1<sup>3,9</sup>.1<sup>5,11</sup>.1<sup>7,13</sup>]octasiloxane, and trisilanol-Phenyl-POSS 1,3,5,7,9,11,14-Hepta-phenyltricyclo[7.3.3.1<sup>5,11</sup>]heptasiloxane-endo-3,7,14-triol were purchased from Hybrid Plastics, and used as received. Norbornylethyl trichlorosilane was purchased from Oakwood Products and used as received. The polymerization catalyst, ethyl(bis-indenyl)hafnium dichloride was purchased from Boulder Scientific. Methaluminoxane (MAO), 10%, was purchased from Albemarle.

### 2.5.2. Synthesis of PhPOSSnorbornene

In an example reaction, at room temperature, 1.07 mmol(1 g) of trisilanol-Phenyl-POSS was stirred in 30 mL of THF in a 100 mL round bottom flask with a septum under a nitrogen atmosphere. Next, 1.09 mmol (0.280 g) of norbornenylethyl trichlorosilane was added. Finally, 3.35 mmol (0.339 g) of triethylamine was added dropwise; clouding of the reaction solution was immediately observed. The reaction was stirred overnight. In the work-up, the solvent was removed in vacuo, and the resulting solid was redissolved in diethyl ether. The solution was filtered to remove the triethylamine-HCl salt, and precipitated into excess acetonitrile. Isolated yields were greater than 75%. NMR resonances: <sup>1</sup>H NMR(400 MHz, CD<sub>2</sub>Cl<sub>2</sub>, ppm): δ 7.6-7.3 (Aromatic, 5H's), 6.04

(Olefin, 1H), 5.97 (endo), 5.82 (Olefin, 1H), 2.74 (1H), 2.68 (1H), 2.50 (endo), 2.01 (1H), 1.81(1H), 1.31 (1H), 1.28 (2H's), 1.10 (endo) 0.85 (2H's), 0.46 (2H's).  $^{13}\text{C}$  NMR:  $\delta$  133.1, 131.2, 129.7, 129.4, 126.8, 48.4, 43.8, 41.4, 40.8 (endo), 40.3, 31.2, 26.4, 9.6.  $^{29}\text{Si}$  NMR:  $\delta$  -78, -65.

### 2.5.3. Polymerization of ethylene-propylene-POSS terpolymers

Reactions were performed in an Autoclave Engineers Zipperclave 0.5 liter stainless steel reactor, with controlled heating, gas flow, and mechanical stirring.<sup>25,26</sup> Prior to polymerization, the reactor was heated to 70 °C, purged with nitrogen gas for 90 minutes, and cooled to room temperature. In an inert atmosphere drybox, a solution of POSS in toluene was prepared; also added was 1 mL of MAO to scavenge any impurities. Separately, a solution of 15 mg of ethyl(bis-indenyl)hafnium dichloride and MAO, with a 1000:1 MAO to catalyst ratio, was prepared and aged 30 minutes before injection into the reactor. The POSS solution was added to the reactor and stirred with ethylene and propylene gas. The reactor was stirred at 1250 rpm and heated to 40°C. Each reagent gas was allowed to flow into the reactor by separate mass flow controllers. The total pressure was set at 50 psi with an apparent 50:50 gas ratio. Next, the catalyst solution was added to the reaction mixture. Ethylene and propylene gas were continually allowed to flow into the reactor to maintain a reactor pressure of 50 psi. Gas flow was monitored through a customized LabView® automated computer program. The reactions were stopped by releasing the pressure in the vessel and precipitating the polymer in a solution of 10%HCl/methanol. Residual POSS monomer was removed by consecutive precipitations of a toluene/polymer solution into ethyl acetate. The terpolymers were filtered and dried in a vacuum oven at 50°C overnight.

#### **2.5.4. Polymer Characterization**

$^1\text{H}$  NMR spectra were obtained in chloroform- $d$  or methylene chloride- $d_2$  on a Bruker DPX-300 FT-NMR spectrometer operating at 300 MHz.  $^{13}\text{C}$  NMR spectra were obtained at 90°C in tetrachloroethane- $d_2$  on a Bruker 400 FT-NMR spectrometer operating at 100 MHz.  $^{29}\text{Si}$  NMR spectra were obtained in tetrachloroethane- $d_2$  on a Bruker 400 FT-NMR spectrometer operating at 80 MHz. Gel permeation chromatography data was obtained using a Polymer Laboratories PL-GPC 50 Integrated GPC System, using THF as the mobile phase. Molecular weights were calibrated against narrow molecular weight polystyrene standards.

#### **DSC**

Differential scanning calorimetry was performed under a nitrogen atmosphere on a DuPont Instruments DSC 2910. Samples were cooled to -110°C and heated at 10°C/min. Data was obtained on second heating.

#### **TGA**

Thermal gravimetric analysis was performed using a Mettler-Toledo TGA/SDTA851°. Samples were heated at a rate of 10°C/min up to 800°C in an air atmosphere.

#### **WAXD**

Wide angle X-ray diffraction patterns were obtained on a PANalytical X'Pert PRO instrument in reflectance mode. Samples for this study were prepared by dissolving the polymer in a toluene solution, and casting it onto a glass slide. The solvent was allowed to evaporate over 2 hours. Residual solvent was driven off by heating the sample at 40°C for 24 hours in a vacuum oven.



## **DMA**

Dynamic mechanical analysis was performed on a TA Instruments AR 2980 Dynamic Mechanical Analyzer, in tensile mode, using a frequency of 1 Hz. The samples were prepared in a manner similar to that for WAXD studies.

## **Rheology**

Rheological studies were performed in a TA Instruments AR 2000 rheometer, using a parallel plate geometry. Samples were prepared by dissolution in toluene, and casting films in aluminum pans. The films were allowed to form over 2 days. The films were dried in a vacuum oven at 45°C for at least 24 hours.

## **TEM**

Samples for TEM were prepared as in rheology studies. Samples were microtomed at -120°C using a diamond knife, cutting 50 nm thick slices. Images were obtained using a JEOL 100CX Electron Microscope, operating at 100 kV.

## **Tensile Tests**

Samples for tensile tests were prepared by casting a film from a 10% solution in toluene. Samples were dried at 45°C overnight. Dog bones shaped specimens were cut from the film, with testing lengths of 22 millimeters and widths of 4 millimeters. Samples were pulled at a rate of 20 mm/minute. Each sample was tested 4 to 5 times, and an average of the curves was calculated. In the cyclic tests, films were pulled to 100% elongation at 20 mm/min and relaxed back to a zero displacement at the same rate. This was repeated 4 times. Next, the sample was pulled to 200% elongation and allowed to relax back to zero displacement. This was repeated 4 times. The same procedure was used at 300%

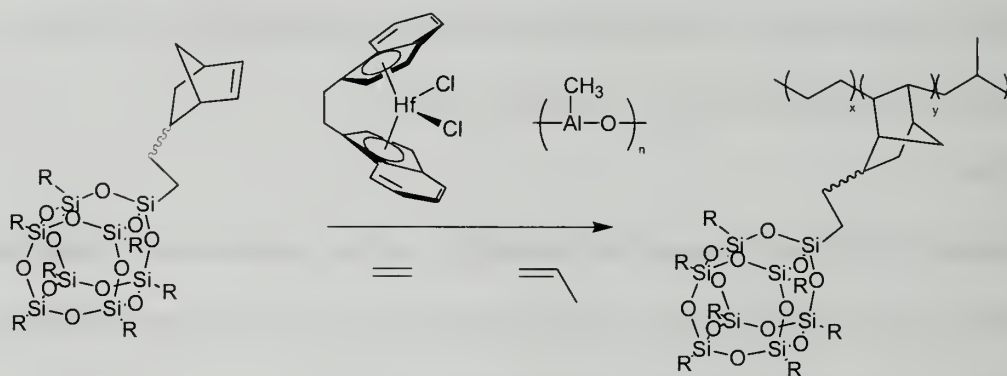


elongation. This 15 step cyclic tests was preformed on each sample twice. Experiments were preformed on a Instron 5500R.

## 2.6. Results and discussion

### 2.6.1. Reaction results

Ethylene-propylene-POSS (EPPOSS) polymers were synthesized using the metallocene catalyst, ethyl(bis-indenyl)hafnium dichloride, as shown in Scheme 2.1.



**Scheme 2.1.** EP-POSS polymerization

**Table 2.2.** Summary of Molecular Weight Data of EP-POSS Polymers

Reaction ID	POSS in Polymer Mol% <sup>a</sup>	POSS in Polymer Wt%	C <sub>2</sub> :C <sub>3</sub> by mol <sup>a</sup>	M <sub>n</sub> (g/mol) <sup>b</sup>	PDI <sup>b</sup>
EP	0	0	35:65	70,000	2.09
Ibu5	0.3	5	25:75	73,000	1.77
Ibu16	0.7	16	52:48	76,000	1.73
Ibu22	1.3	22	32:68	65,000	2.03
Ibu30	1.6	30	34:66	57,000	1.57
Ph10	0.4	10	50:50	113,000	2.07
Ph21	0.9	21	48:52	86,000	2.07
Ph30	1.4	30	50:50	75,000	1.70
Ph36	1.7	36	59:41	37,000	2.80
Et20	1.0	20	52:48	41,000	1.41
Et30	2.0	30	50:50	19,500	4.70

<sup>a</sup> As determined by <sup>13</sup>C or <sup>1</sup>H NMR in CD<sub>2</sub>Cl<sub>2</sub> or C<sub>2</sub>D<sub>2</sub>Cl<sub>4</sub>.

<sup>b</sup> As determined by GPC in THF vs. narrow molecular weight polystyrene standards.

Reaction results are shown in Table 2.2. Polymerizations took place under an apparent 50:50 ethylene to propylene ratio. According to literature precedence, the same reaction conditions produced ethylene-propylene copolymers with 59 mol percent ethylene incorporations.<sup>23</sup> The POSS periphery was altered to include isobutyl (Ibu), ethyl (Et), and phenyl (Ph) peripheries. However, the reactions using IbuPOSS had low ethylene incorporations, indicating a deviation from the expected ratio. POSS incorporations ranged from 5 to 36 weight %, with sufficiently high molecular weights and moderate polydispersities. All samples had unimodal molecular weight distributions, except for Ph36 and Et30. The Ph36 sample had two overlapping peaks, nearly identical in size. In the Et30 sample, two nearly equal peaks having a combined molecular weight of 19,500 g/mol with a polydispersity of 4.7.

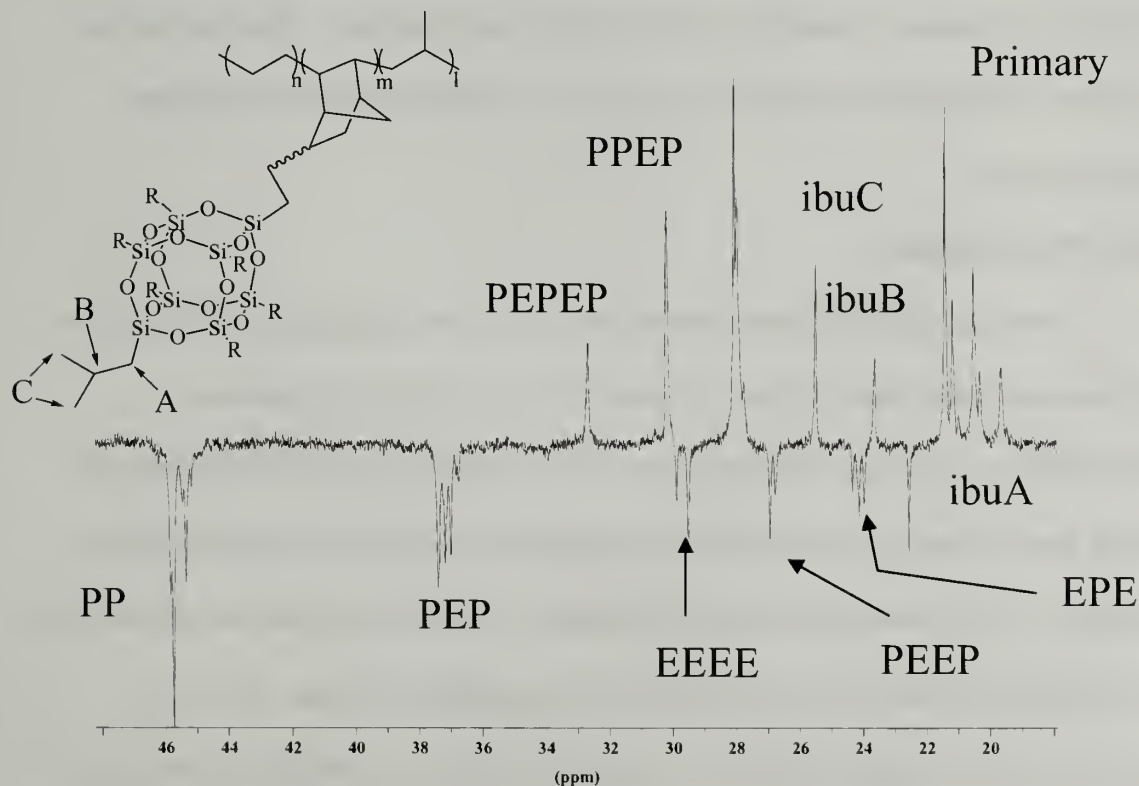


**Figure 2.3.** DEPT135 NMR of EPIbuPOSS copolymers. Peak assignments based upon literature<sup>26</sup> show ethylene(E) and propylene(P) sequences.

Polymers containing PhPOSS generally had higher molecular weights and higher than expected ethylene to propylene ratios. EtPOSS terpolymers had lower molecular weights than either IbuPOSS or PhPOSS terpolymers.

The ethylene and propylene peak assignments were taken from literature.<sup>26</sup> The presence of ethylene runs, propylene runs, alternating sequences and random sequences indicates a random ethylene-propylene microstructure, as shown in Figure 2.3. POSS incorporation was determined from the integration of the methyl peaks of the isobutyl periphery (Ibu C), and compared to the integrations of the ethylene-propylene sequence peaks. This method was also used to determine EtPOSS incorporation. In PhPOSS polymers, the POSS incorporation was determined directly by  $^1\text{H}$  NMR, as the chemical shift of the aromatic POSS proton resonances were compared to the olefinic ethylene-propylene resonances, which have chemical shifts further upfield. These values were compared to the ethylene-propylene ratio from  $^{13}\text{C}$  NMR to determine monomer incorporations.

### **2.6.2. WAXD studies**

Wide angle X-ray diffraction was used to study the aggregation of POSS in the ethylene-propylene matrix. Figure 2.4 shows the X-ray diffraction patterns of EPIbuPOSS terpolymers. The bottom trace is an ethylene-propylene (EP) copolymer. Going from the bottom trace upwards, the IbuPOSS incorporation in the terpolymers increases. The top trace is the IbuPOSS monomer. The EP copolymer has a broad peak centered at a  $2\theta$  value of 18, which indicates an amorphous polymer. There are, however, two sharp peaks within this broad peak, indicative of ethylene crystallization.<sup>27</sup>

These peaks are only observed in the EP and EPIbu22 samples, indicating an amorphous EP polymer with all other samples.

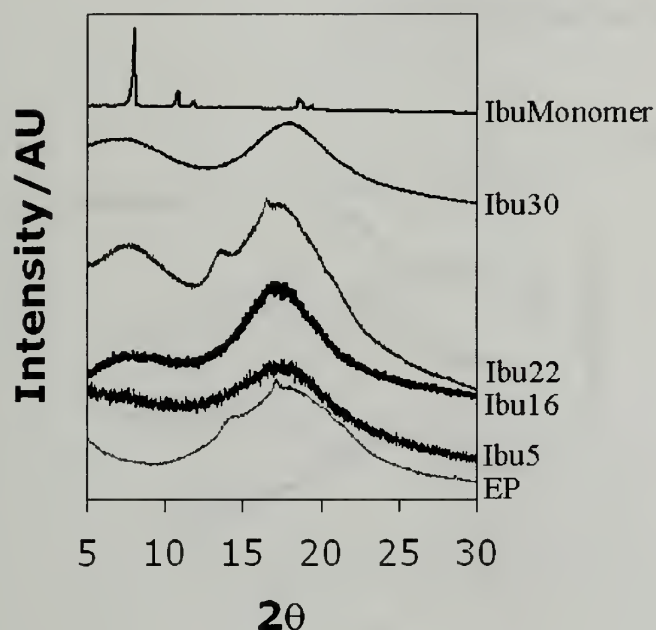


**Figure 2.4.** Wide angle X-ray diffraction pattern of EPIbuPOSS polymers.

The IbuPOSS monomer has the most intense diffraction peak at a  $2\theta$  value of 8, which is indicative of POSS monomer crystallization, as POSS monomers crystallize into three-dimensional hexagonal arrays. However, when POSS is chemically incorporated into polymers, their packing is constrained to two-dimensional sheets due to geometric constraints of attaching a POSS pendent group to a polymer chain. This results in broadening of the X-ray diffraction peaks. In the case of these IbuPOSS polymers, WAXD patterns show broad diffraction peaks centered at a  $2\theta$  value of 8. This suggests either POSS dispersion within the EP polymer matrix or the formation of very small POSS aggregates. Although it is of interest that IbuPOSS disperses within the EP matrix, this study requires POSS aggregation to determine their applicability as physical crosslinks for thermoplastic elastomers. Therefore, the POSS periphery was altered to



chemical moieties with less favorable interactions with ethylene-propylene elastomers, namely a phenyl and ethyl periphery. WAXD patterns of the series of EPhPOSS (left) and EPtPOSS (right) samples prepared are shown in Figure 2.5.

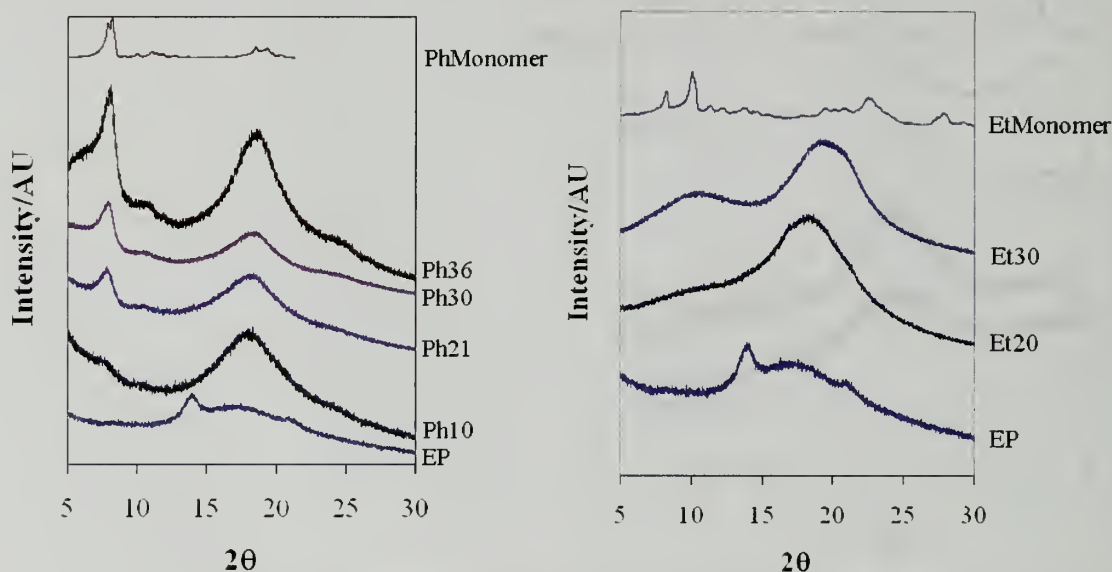


**Figure 2.5.** Wide angle X-ray diffraction data of EPhPOSS (left) polymers and EPtPOSS (right) terpolymers.

In PhPOSS polymers, as the POSS incorporation is increased, the diffraction peak at a  $2\theta$  value of 8 increases in intensity, with much sharper diffraction peaks than in the IbuPOSS polymers. This is indicative of POSS crystallization. As was observed with the IbuPOSS copolymers, EtPOSS polymers show broad diffraction peaks, indicating EtPOSS also disperses within the EP matrix. This is of great interest, as by simply altering the POSS periphery, POSS can be engineered to either disperse or aggregate within a specific polymer matrix. The polymer films prepared for these studies further reinforce this interpretation. The IbuPOSS and EtPOSS polymers were softer than the EP parent polymer, indicating that dispersed POSS acts as a plasticizer, rather than as



physical crosslinks. These two samples also lacked sufficient strength for DMA studies, unlike the PhPOSS polymers.

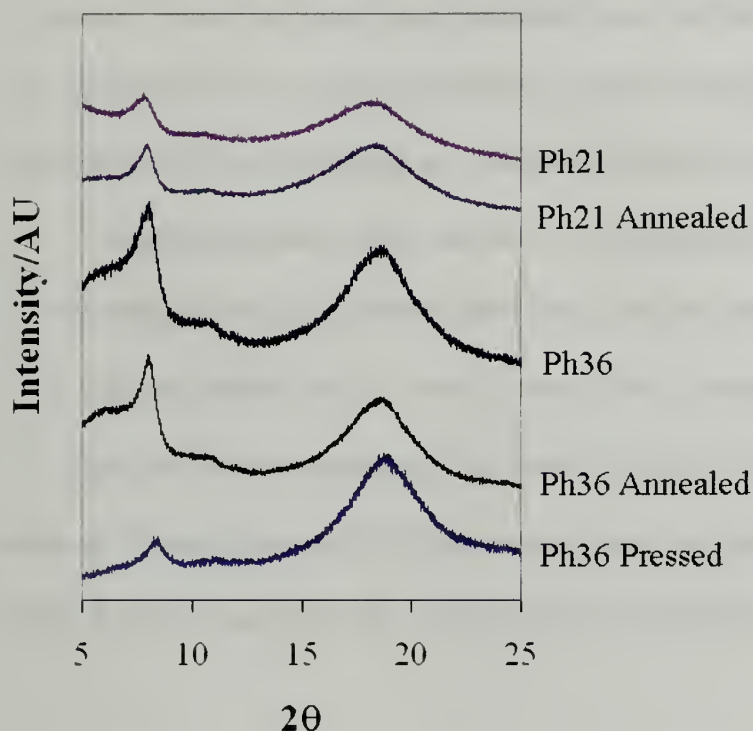


**Figure 2.6.** WAXD patterns for EPhPOSS copolymers by different preparation methods.

The sample preparation method was also studied to determine if POSS aggregation could be driven by thermal annealing or slow solvent evaporation. Samples were cast from toluene solutions, allowing for either fast evaporation of solvent (2 hours), or slow evaporation (7 days). They were also prepared by pressing (150°C at 5000 psi for 5 minutes) or annealing (120°C for 7 days). The WAXD results are shown in Figure 2.6. The EPh36 samples show sharper diffraction peaks at  $2\theta$  values of 8 by both annealing and pressing the samples, which indicate a more ordered structure in the polymer films. In both the annealed and pre-annealed EPh36 sample, there is a sharp diffraction peak preceded by a broader peak, indicating the existence of both POSS

aggregates and either smaller aggregates or dispersed POSS particles. This broad peak does not appear in the pressed sample. In the EPPH21 sample, annealing the sample resulted in a sharper POSS diffraction peak, indicating larger aggregate sizes. Although altering the preparation method had an impact in PhPOSS polymers, it had no impact on POSS aggregation in EtPOSS and IbuPOSS polymers, as peripheral interactions with the EP domain allow only for POSS dispersion or formation of only small aggregates.

Using Scherer's equation, the sizes of the POSS domains can be estimated from WAXD data. In Scherer's equation,  $L = 0.9\lambda / \beta \cos\theta$ , where  $L$  is the domain length,  $\lambda$  is the wavelength of the X-ray,  $\beta$  is the peak width at half maximum, and  $\theta$  is the angle. This calculation has previous been preformed to estimate POSS domain sizes.<sup>28,29</sup> In these calculations, it is assumed that POSS has a 15Å diameter. The results are shown in Table 2.3.

**Table 2.3.** Estimation of POSS domain sizes using Scherer's Equation

Sample	Domain Size(nm)	~POSS per domain
Ph36	5.3	3-4
Ph36annealed <sup>a</sup>	6.3	4-5
Ph36pressed <sup>b</sup>	9.5	6-7
Ph30	7.8	5-6
Ph21	7.1	4-5
Ph21annealed <sup>a</sup>	9.5	6-7
Et30	1.1	1
Ibu30	2.1	1-2
Ibu22	2.7	1-2
Ibu16	1.3	1

<sup>a</sup> Film was annealed at 120 °C in a vacuum oven for 7 days.

<sup>b</sup> Film was formed by pressing the raw sample at 150 °C and 5000 psi for 5 minutes.

This method simply estimates the largest domain size, with the number of POSS molecules it takes to fill a domain this size. POSS aggregates could also form in other

directions, with the other dimension having either one or two POSS cubes. Therefore, the number of POSS molecules per domains is probably larger than this estimated value. These results show that the PhPOSS copolymers have larger domain sizes than the EtPOSS and IbuPOSS copolymers, as Ph21, Ph30, and Ph36 samples have domain lengths of 7.1, 7.8, and 5.3 nanometers respectively. The length of all of the ethyl or isobutyl POSS periphery polymers, however, were on the order of 1-2 POSS molecules, proving these sample lack POSS aggregation. Larger domain sizes can be driven in the PhPOSS polymers by annealing or by pressing. For example, the Ph21 domain length increases from 7.1 to 9.5 nanometers by annealing the sample.

### 2.6.3. Thermal characterization

A summary of the thermal characterization of all EPPOSS terpolymers is shown in table 2.4.

**Table 2.4.** Thermal characterization of EPPOSS terpolymers

Entry	Wt. % POSS	T <sub>g</sub> (DSC)/°C	2% Decomp. Temp./°C	Char yield	Theoretical Char yield
EP	---	-44	243	3.5%	0%
Ibu5	5	-38	216	13.9%	4.1%
Ibu16	16	-47	329	6.2%	7.2%
Ibu22	22	-42	306	10.5%	11.2%
Ibu30	30	-42	183	24.8%	15.4%
Ph10	10	-51	250	9.6%	3.8%
Ph21	21	-52	327	10.0%	8.1%
Ph30	30	-49	281	19.0%	11.6%
Ph36	36	-48	308	19.2%	13.9%
Et20	20	-46	277	11.7%	11.3%
Et30	30	-50	250	9.6%	16.9%

<sup>a</sup> DSC data was obtained on second heating, heating from -100-200°C, at 10°C/min.

<sup>b</sup> TGA data was obtained by heating to 800°C at 20°C/min.

<sup>c</sup> Theoretical char yields were calculated assuming a complete conversion of POSS to SiO<sub>2</sub>.

All data from DSC was obtained on second heating, where only a single glass transition temperature was observed from -110 to 200°C for EPPOSS samples. The DSC data shows a surprising invariant relationship between  $T_g$  and POSS incorporation. Generally in literature reports, the incorporation of POSS into low  $T_g$  polymers causes a increase in  $T_g$  with increasing POSS loading, as the large bulky side POSS chain slows polymer mobility. The ethylene to propylene ratio varies in most of the different polymers, which affects the glass transition temperature. As the propylene content in an ethylene-propylene copolymer increase from 50 to 70%, the  $T_g$  increases. The ethylene to propylene content varies greatly in the IbuPOSS copolymers. In the PhPOSS and EtPOSS copolymer, the ethylene to propylene ratio appears to be closer, but there is an inherent error involved in the determination of this ratio by quantitative  $^{13}\text{C}$  NMR. This could account for the invariant  $T_g$  values.

The thermal gravimetric analysis data is shown in table 2.4, which was performed under an air atmosphere. Here, both the 2% decomposition temperature and char yields are reported. The literature trend shows an increase in decomposition temperature of POSS containing copolymers versus the homopolymer.<sup>30</sup> In these EPPOSS polymer, mixed results are observed. In the best case, EPIbu16 shows a greater than 80 °C increase in 2% decomposition temperature versus the ethylene-propylene homopolymer. There are also, however, several samples that show only moderate increases in decomposition temperature. The EtPOSS copolymers show the lowest decomposition temperatures. This is expected, as EtPOSSnorbornene has a 2% decomposition temperature of 193°C. The increase in decomposition could be due to POSS aggregating at the surface of the material. POSS not only decomposes at a higher temperature than



ethylene-propylene copolymers, but when POSS decomposes under an air atmosphere, it is able to form silica.<sup>31</sup> Silica is stable at temperatures much higher than the 800°C used in these studies. Therefore, POSS could form a silica layer at the surface, which could protect the underlying polymeric material from decomposition.

Another important factor in TGA studies of POSS containing polymers is the char yield. The char yield should increase with increasing POSS loadings, as there are more POSS cages able to form silica char. The EP copolymer shows a low char yield, as completely saturated hydrocarbon polymers form little char. Other than a few data points, an increase in char yield with increasing POSS loading is observed. A theoretical char yield can also be calculated, assuming a complete conversion of POSS to silica. Comparing these calculations to the actual values, there are cases in which less char is formed than expected, indicating an incomplete conversion of POSS to silica. There are also cases where the char is great than expected, especially with the PhPOSS polymers. Aromatic rings are also to form char, which could account for the higher than expected char yields. There could also be a small amount of char forming from the ethylene-propylene backbone.

#### **2.6.4. Dynamic mechanical analysis studies**

Films of EPPhPOSS polymers were prepared for dynamic mechanical analysis studies. The results of these studies are shown in figure 2.7. The PhPOSS polymers show promising results. The storage modulus in the glassy region has an invariant relationship with POSS loading, as Ph21 has the highest modulus, followed by Ph10, Ph36, Ph30 and EP. This could be due to the various copolymer configurations at sub- $T_g$



temperatures. Although, the EPPh36 data was obtained on second heating, the trend still fits with all samples on both the first and second heating.

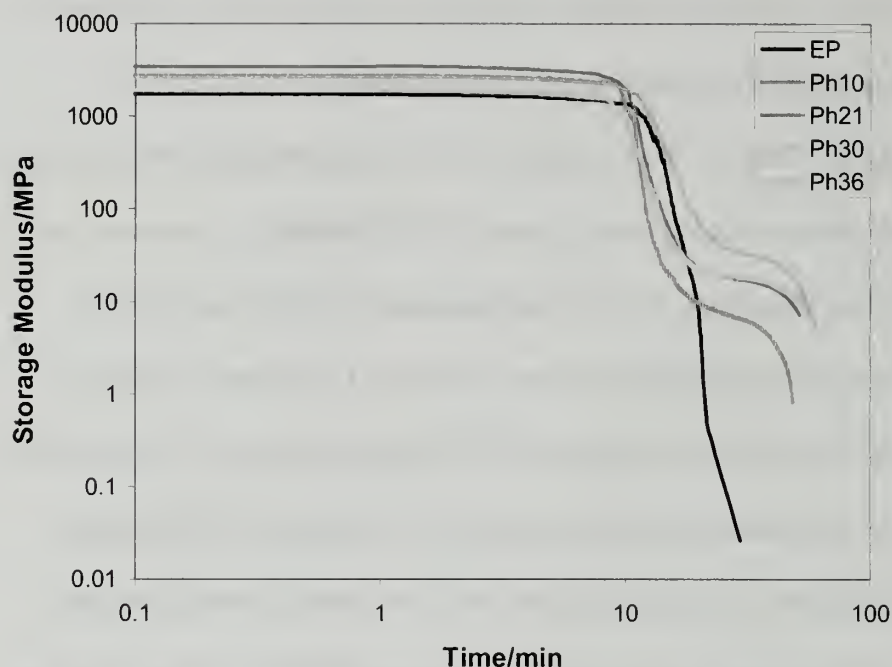


**Figure 2.7.** Dynamic mechanical analysis of EPPhPOSS polymer samples from -100 to 200°C. Plot shows the storage modulus as a function of time (temp = -100 + time\*5). Samples were heated from -100 to 200 °C at 5 °C per minute.

Also, all other samples show the same mechanical results in the glass transition region, the rubber plateau region, and the rubbery flow region on first and second heating. The glass transition temperatures are more in line with expectations based on literature precedence, as the  $T_g$  increases with increasing POSS loading. The EP copolymer has a higher value, which is due to different ethylene to propylene ratio than the EPPhPOSS copolymers. The rubbery plateau region is important to determine if POSS is acting as a physical crosslink. Crosslinked materials show an extension of the rubbery plateau region and an increase in the modulus of the rubbery plateau region as compared to the non-crosslinked polymer counterpart.<sup>32</sup>

**Table 2.5.** Dynamic Mechanical Analysis Data

Sample	T <sub>g</sub> /DSC(°C)	T <sub>g</sub> /DMA(°C) <sup>a</sup>	Rubbery Plateau Region/°C	G' at 25°C/MPa
EP	-44	-24		0.3
Ph10	-51	-46	-28 to 93	7.2
Ph21	-52	-45	-14 to 135	18.3
Ph30	-49	-40	-15 to 135	19.2
Ph36	-48	-31	-1 to 140	37.1

<sup>a</sup> Determined from the maximum of  $\tan \delta$

The storage modulus in the rubbery plateau region increases with increasing POSS loading, with Ph36 having the highest modulus, Ph30 and Ph21 are nearly equal, and Ph10 being the lowest. At room temperature, Ph36 shows a significant increase in storage modulus over the EP copolymer, with values of 37.1 MPa and 0.3 MPa respectively. These values relate to the size of POSS aggregate domains, as determined from WAXD studies. The Ph30 sample has the largest domain size of 7.8 nm, followed by Ph21 with 7.1 nm and Ph36 at 5.3 nm. Although Ph30 has a higher POSS incorporation than Ph21, it has larger domain sizes, thus fewer crosslink junctions. The Ph21 sample has more crosslink junctions, which results in similar modulus values as Ph30. Although Ph36 has a slightly higher POSS incorporation, it has much higher storage modulus values because it has smaller domain sizes, thus more crosslinking junctions than Ph21 or Ph30. This data demonstrates the strong increase in tensile properties with the addition of POSS to copolymers.

The transition of the samples from the rubbery plateau region to the rubbery flow region can correlate to the dispersion of the POSS aggregates. The Ph10 sample has the lowest value of 93 °C (Table 2.5). The other samples have values between 135-140 °C, showing higher temperatures are required to disperse polymers with a higher number of crosslink junctions and/or larger POSS domain sizes. The length of the rubbery plateau

region increases greatly with the POSS incorporation, as compared to the EP parent polymer. Therefore, the addition of POSS aggregates creates a larger rubbery plateau region. This result indicates that POSS acts as a physical crosslink for thermoplastic elastomers, assuming POSS aggregation in the copolymers.

The method of preparation of the EPh36 polymer films provide materials with different mechanical properties. Dynamic mechanical analysis data of EPh36 was obtained on samples prepared by fast and slow solvent evaporation methods, as well as melt pressing. The results are shown in figure 2.8. Each sample was cooled to  $-100^{\circ}\text{C}$ , heated to  $200^{\circ}\text{C}$ , cooled back down to  $-100^{\circ}\text{C}$ , and heated back to  $200^{\circ}\text{C}$ . All samples were completely soluble after second heating, indicating no chemical crosslinking occurred. The fast and the slow evaporation methods show similar results. In the case of the fast evaporation method during the first heating, the storage modulus is relatively low. When the sample is heated above  $110^{\circ}\text{C}$ , there is an increase in the storage modulus. This is indicative of a change in the microstructure of the polymer. According to WAXD studies, the Ph36 sample contains larger POSS aggregates, as well as small aggregates or dispersed POSS.

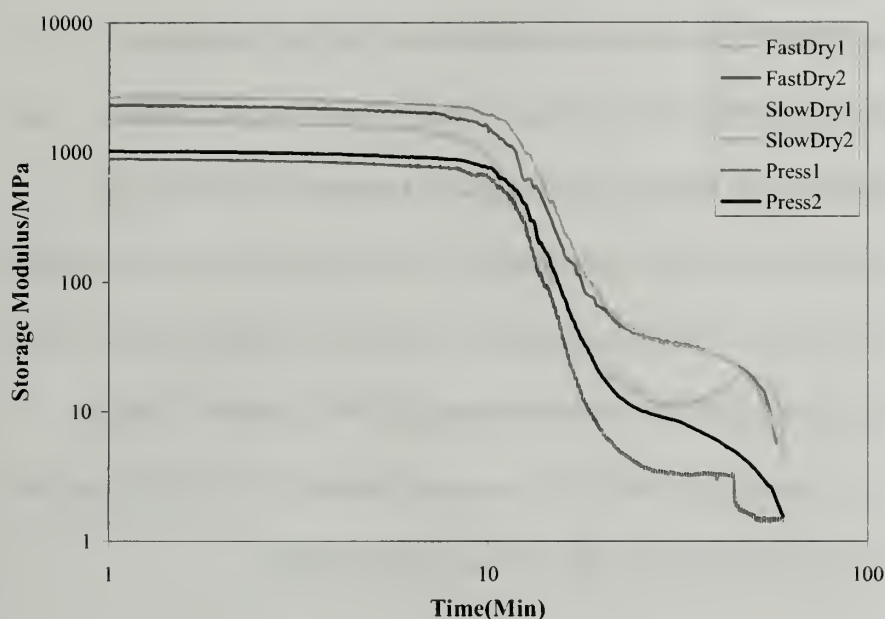


**Figure 2.8.** Dynamic mechanical study of EPPH36 polymers, varying polymer film preparation techniques, including a slow evaporation method(7 days), fast evaporation(2 hours), and by pressing the sample at 5000 psi at 150°C. Each sample was heated from -100°C to 200°C twice, at a rate of 5°C/minute, using a frequency of 1 Hz and with an initial force of 0.05 N. This plot measures the storage modulus as a function of time (temperature = -100 + 5time).

The increase in the modulus of this material could be due to the formation of POSS aggregates from these small aggregates or dispersed POSS molecules. Above 160 °C, the storage modulus drops off, indicating a dispersion of POSS aggregates. The sample prepared by the slow evaporation method shows similar results, as the storage modulus of the sample increases over 110 °C, and up to 200 °C. Upon second heating, the results change drastically. The storage modulus in the glassy region increases with both evaporating technique samples, showing similar values. This remains true across the other regions of the graphs, as much stronger tensile properties are obtained with the more ordered POSS polymers.



This study shows different evaporation methods produces samples that need to be heated and strained to produce microstructures conducive to stronger mechanical properties. The samples prepared by the pressing method produce different results. The first heating shows relatively low mechanical properties. Upon second heating, the pressed sample has a slightly higher storage modulus, which remains lower than the other samples on their second heating. The pressed sample might have a higher density, thus lower mobility, making it more difficult for the ordering of POSS domains. This is supported by the  $T_g$  of the materials. The  $T_g$  of the pressed sample is 8°C higher than the other samples, indicating less free volume, thus a more dense material.

#### **2.6.5. Rheology**

A series of the samples were also studied using rheology. Strain sweeps were performed on EP, EPPH10, EPEt20, EPIbu30, and EPPH30 at varying temperatures. Each sample was in the linear viscoelastic regime. The results are presented graphically in Figures 2.9 and 2.10. The strain sweeps were performed to measure and compare the storage and loss modulus of each polymer sample to observe polymer mechanical properties at different temperatures, as well as the temperature range in which the loss modulus becomes greater than the storage modulus.



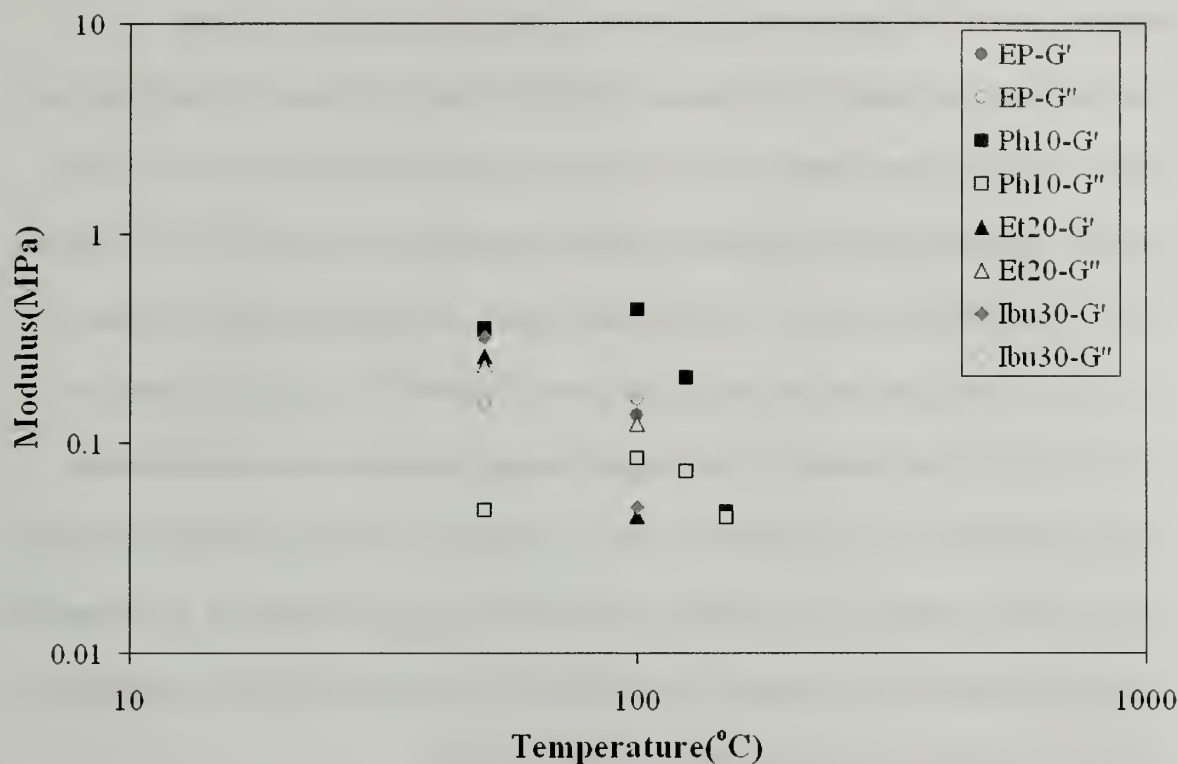


**Figure 2.9.** Rheology data of EP and EPPOSS polymer samples. Each test measures the storage modulus( $G'$ ) and loss modulus( $G''$ ) as a function of percent strain of each sample at varying temperatures. Each sample was in the linear viscoelastic regime.

This crossover point marks the temperature at which the elastomer changes over from the rubbery plateau region to the rubbery flow region. This is an important parameter to test the effectiveness of POSS as a physical crosslink, as an increase in rubber plateau region is an indication of a crosslinked system. At 50 °C, the EPPh30 sample has the highest storage modulus, and the smallest  $\tan \delta$ , showing the storage modulus is higher than the loss modulus, as  $\tan \delta = G''/G'$ . Each sample remains in the rubbery plateau region. As the temperature is increased to 100 °C, each sample is in the rubbery flow region, except for EPPh10 and EPPh30. The EPPh10 sample is further heated to 125 and 150 °C. Even at 150 °C, the sample remains in the rubbery plateau region. The EPPh30 sample shows this behavior up to 200 °C. This corroborates the WAXD and DMA data, as EPPhPOSS

samples show POSS aggregation, which acts as physical crosslinks for these thermoplastic elastomers, but EPIbu and EPETPOSS samples disperse within the polymer matrix, which does not improve the mechanical properties of the EP copolymers. The data also suggests PhPOSS aggregates disperse at temperatures around 150°C. When the EPPh10 and EPPh30 samples are heated and strained, the storage modulus increases up to 125 °C. This is predicted by theories in rubber elasticity.<sup>32</sup> The EPPh30 sample was cooled to 50 °C, and reheated. Upon second heating, the sample shows an increase in storage modulus of at least three fold. This is indicative of a change in the microstructure of the system, probably a rearrangement or formation of POSS aggregates. These samples remained completely soluble upon second heating, indicating the increase of modulus is not due to chemical crosslinking between polymer chains.

These mechanical studies can be compared to the DMA studies. If it is assumed that the polymer is incompressible, then  $3G' = E'$ . However, in these polymer samples, the shear storage modulus ( $G'$ ) is on the order of five times lower than the tensile storage modulus ( $E'$ ). Therefore, these materials are anisotropic, as they have stronger material properties under tensile strain than under shear strain.

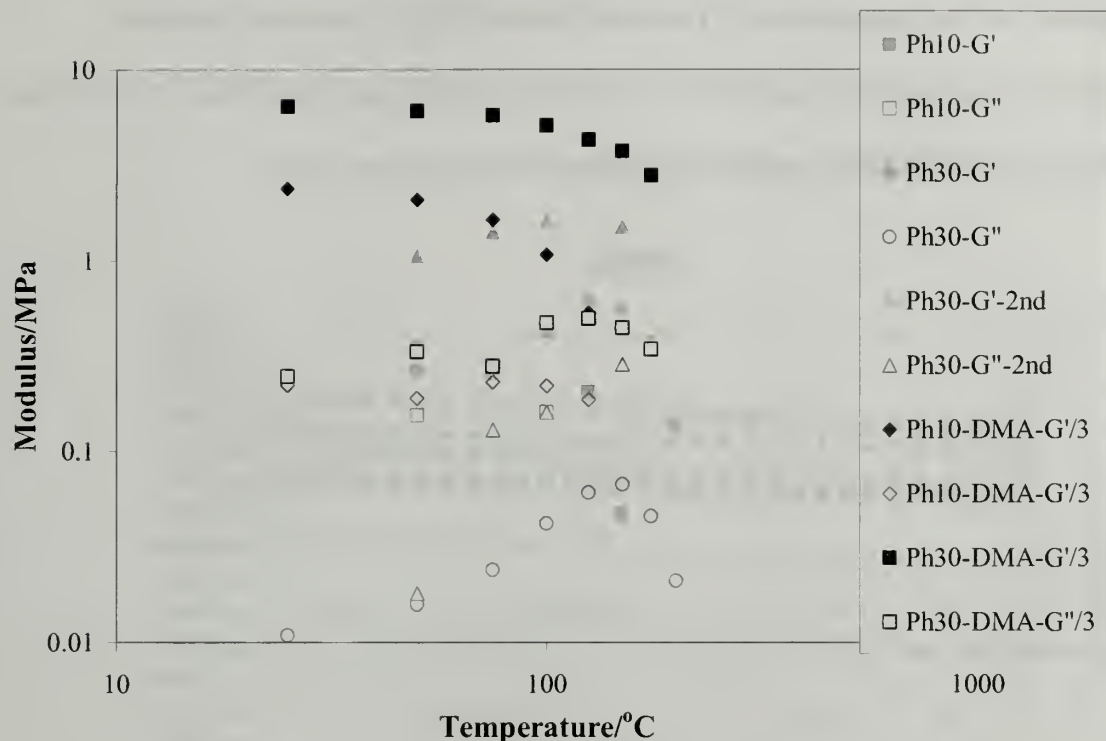


**Figure 2.10.** Rheology data of EPPOSS polymer samples. Each test measures the storage modulus( $G'$ ) and loss modulus( $G''$ ) as a function of percent strain of each sample at varying temperatures. Each sample was in the linear viscoelastic regime. The Ph10 and 30- $E'/3$  samples are from DMA data, and comparing to rheology data by dividing values by 3, as  $E' = 3G'$ .

Frequency sweeps were also performed on polymer samples EPPh30, EPIbu30, and EPPh10 as shown in figures 2.11, 2.12, and Appendix C, respectively. Frequency sweeps give information about the response of polymeric material at different frequencies, which are related to time. High frequencies are related to short times, and low frequencies are related to long times.<sup>32</sup> In the EPPh30 sample, the storage modulus remains approximately the same across the frequency range, indicating a solid material that retains its properties at high times (low frequencies). This is true for the polymer sample in a high temperature range, up to at least 175 °C. The sample at 200 °C has the

same material response, but the modulus has decreased significantly compared to the sample at the other temperatures. This study shows EPh30 has strong material properties at temperatures up to 175 °C. Therefore, the physical crosslinks created by the aggregation of PhPOSS is stable at high temperatures and long times.

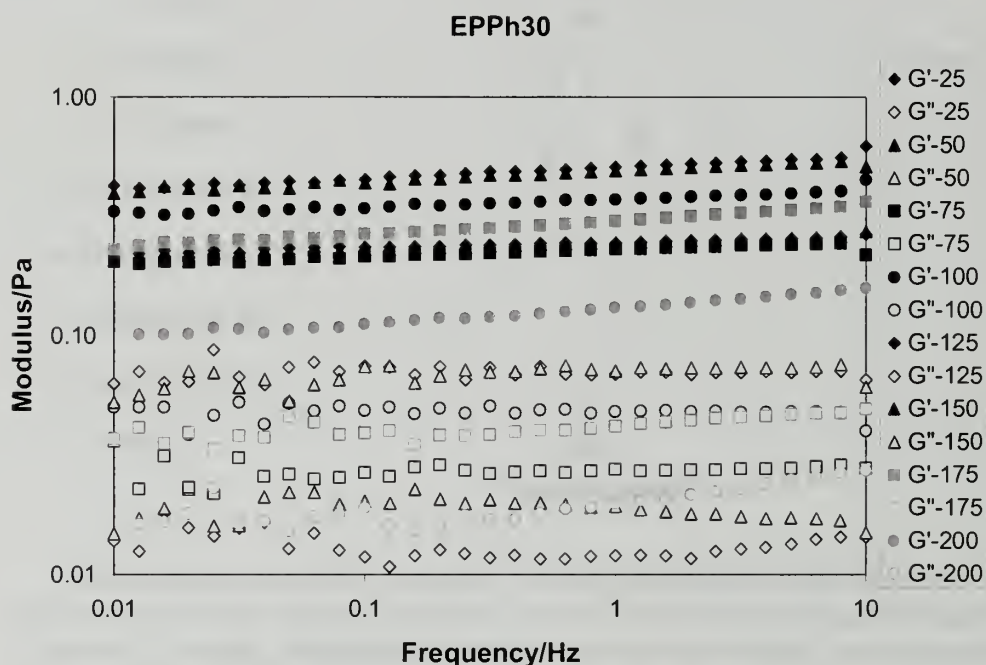


**Figure 2.11.** Frequency sweeps of EPh30 at varying temperatures, from 25 °C to 200 °C.

The Ibu30 sample shows a different behavior, which is expected, as IbuPOSS disperses within the EP matrix. At 50 °C the sample remains in the rubbery plateau region at high frequencies, as the storage modulus is higher than the loss modulus. As the frequency is decreased, the material response changes, as shown by the decrease in storage modulus. The storage modulus and loss modulus become nearly equal at 0.01 Hz. As the sample is heated to 100 °C, it becomes even more liquid like, noted by the decrease in modulus while decreasing the frequency. Comparing Ph30 to Ibu30, the frequency sweeps

confirm the positive material property gains by POSS aggregation as compared to POSS dispersion.

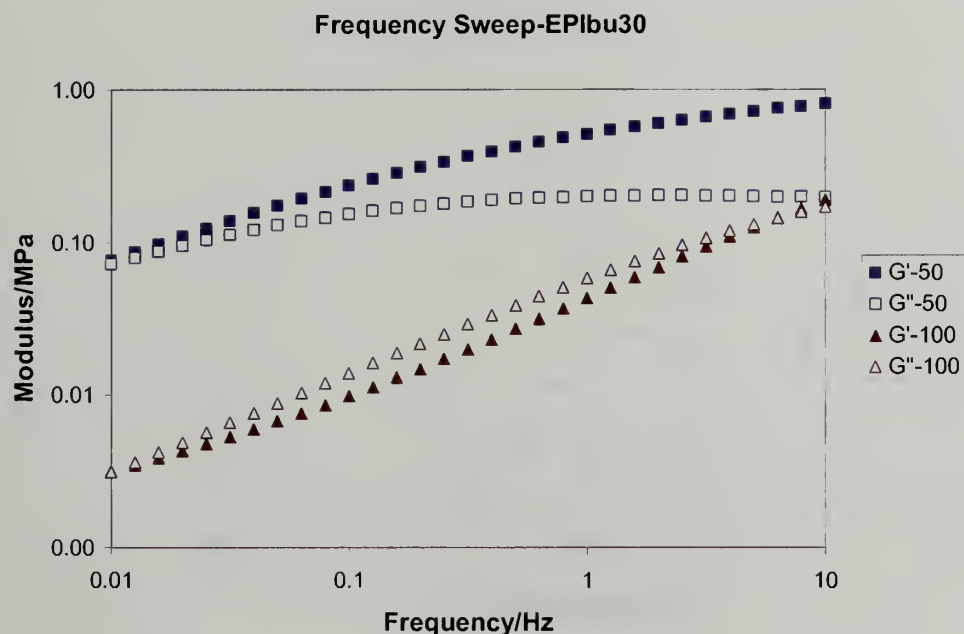


**Figure 2.12.** Frequency Sweep of EPIbu30, at 50 °C and 100 °C.

Frequency sweeps were also preformed with Ph10 (Appendix C). These results are similar to Ph30. There was little change in the storage modulus at 25 °C with various frequencies. At 50 and 100 °C, the modulus decreased slightly at low frequencies. A more significant drop in modulus does not occur until 150°C. Comparing Ph10 and Ph30, the Ph30 sample has higher storage modulus values at various frequencies up to 175 °C, whereas only between 100 to 150 °C for the Ph10 sample. Therefore, the addition of a higher amount of PhPOSS allows for not only a higher storage modulus, but also physical crosslinks which are stable at higher temperatures.

The molecular weight between crosslinks ( $M_c$ ) can be estimated using the equation  $M_c = \rho RT/G$ , where  $\rho$  is the density (assumed to be 1 g/mL),  $R$  is the universal



gas constant,  $T$  is the temperature, and  $G$  is the storage modulus. Figure 2.13 shows the molecular weight between crosslinks as a function of temperature for Ph10 and Ph30.

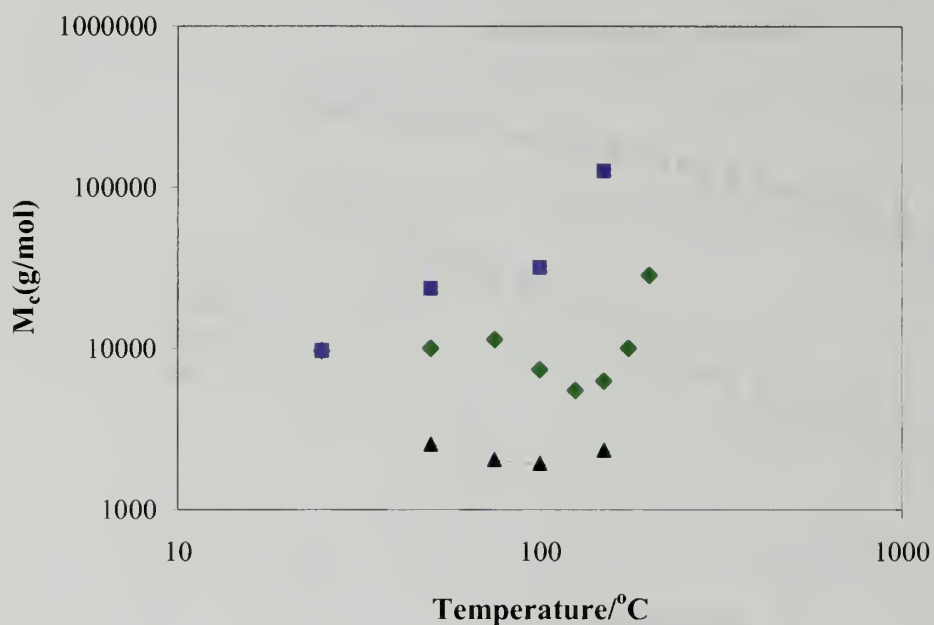


**Figure 2.13.** Molecular weight between crosslinks for EPh10 (top curve), EPh30 samples (middle curve), and EPh30 on second heating, assuming a polymer density of 1 g/mL.

As the temperature of the samples is increased from 25 to 100 °C, each curve shows different results. The Ph10 sample shows a decrease in the  $M_c$  with increased temperature. The POSS aggregates disperse at a temperature between 100 and 150 °C, as marked by a large increase in  $M_c$ . These are close to DMA values, where the end of the rubbery plateau region was estimated to be at 93 °C. At 50 °C, the  $M_c$  relates to 700 monomers between crosslinks, assuming all POSS cubes act as a physical crosslink. The Ph30 sample, however, shows an increase in  $M_c$  when the sample is heated to 125 °C. The POSS finally disperses at temperatures above 150 to 175 °C, as marked by a sharp increase in the  $M_c$ . The sample shows 200 monomers between crosslink. During the

second run of EPPh30, the mechanical strength increases, and the  $M_c$  also increases to values akin to 80 monomers between crosslink.

#### **2.6.6. Tensile tests**

Tensile tests were performed on each of the samples, as dog bones were cut from solvent cast films from toluene. The results are shown in figure 2.14. The stress-strain relationship of EPPOSS polymers are typical of elastomers.<sup>32</sup> The EP parent polymer curve lies between Ph30 and Ph21. Although it would normally be expected that the EP sample would lie below Ph10, this result is not surprising, as WAXD studies show the EP parent polymer is semi-crystalline. Therefore, the elastic modulus of the polymer will be higher than that of an amorphous copolymer due to polyethylene crystallites. Other than the EP sample, the EPPhPOSS curves show an expected trend of an increase in elastic modulus with an increasing POSS incorporation, as increasing the number of POSS cages will increase the number of physical crosslinks, thus increasing the elastic modulus.

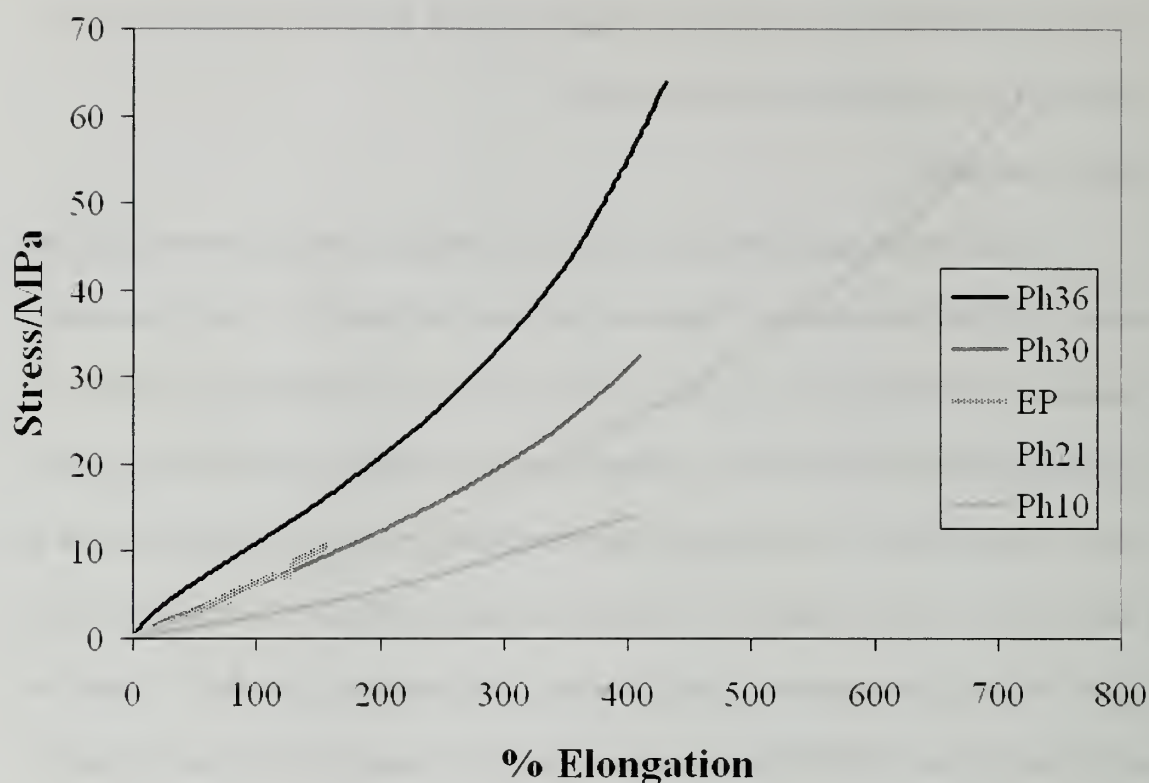


**Figure 2.14.** Tensile tests on EP and EPPhPOSS polymers, pulled at a rate of 20 mm/min. Each sample was tested 4 times, and the graph values represent an average of the combined tests.

Another property seen in these elastomers is the ‘Payne effect’.<sup>33-36</sup> Elastomers that show the Payne effect have non-linear viscoelastic behavior, as the modulus at low strain amplitudes is higher than the modulus at high strain amplitudes. This effect is commonly seen in filled elastomers, and is believed to occur due to filler deagglomeration and breakdown of the filler at low strains, thus lowering the modulus at higher strains.<sup>34-35</sup> In these EPPhPOSS polymers, the modulus decreases at increasing strains, and finally increase at higher strains before they break. Although not studied further, this initial decrease could be due to deaggregation of some POSS cubes from their domains, thus decreasing the modulus of the material. The Payne effect is seen most strongly in the EPPhPOSS copolymers with the highest POSS loading. If the Payne effect is caused by

deaggregation of some POSS molecules, it is expected that at higher loadings, the Payne effect would be more apparent, as there are more POSS cubes to deaggregate.

**Table 2.6.** Tensile properties of EP and EPPhPOSS samples from tensile tests.

Sample	Elongation at Break	Elastic Modulus/MPa
EP	170%	10.2
Ph10	472%	5.1
Ph21	723%	10.2
Ph30	448%	13.4
Ph36	450%	19.3

The percent elongation at break of elastomers is typically in the range of 500-700%. Most of the EPPhPOSS elastomers lie just below this range, at 450-470%. The EPPh21 sample, however, has an elongation at break of 720%. This polymer may have an ideal combination of POSS loading and crosslink sites, as compared to the other EPPOSS elastomers. These strong properties help support the indication that POSS aggregates behave as physical crosslinks for thermoplastic elastomers. This data could be fully supported by the EP parent polymer, as the elongation at break is much lower (170%). However, the semi-crystalline nature of the polymer will play a role in the percent elongation at break, and does not unequivocally prove the role of POSS in the elastomers based on this tensile study. Another important factor is the molecular weight of the samples. As the PhPOSS incorporation is increased in the polymers, the molecular weight decreases. Despite this, the mechanical properties remain strong at all levels of POSS incorporation.

Cyclic tensile tests were also preformed on each of the EPPhPOSS samples, to determine possible hysteresis in the polymer samples. A typical result is shown in figure 2.15.

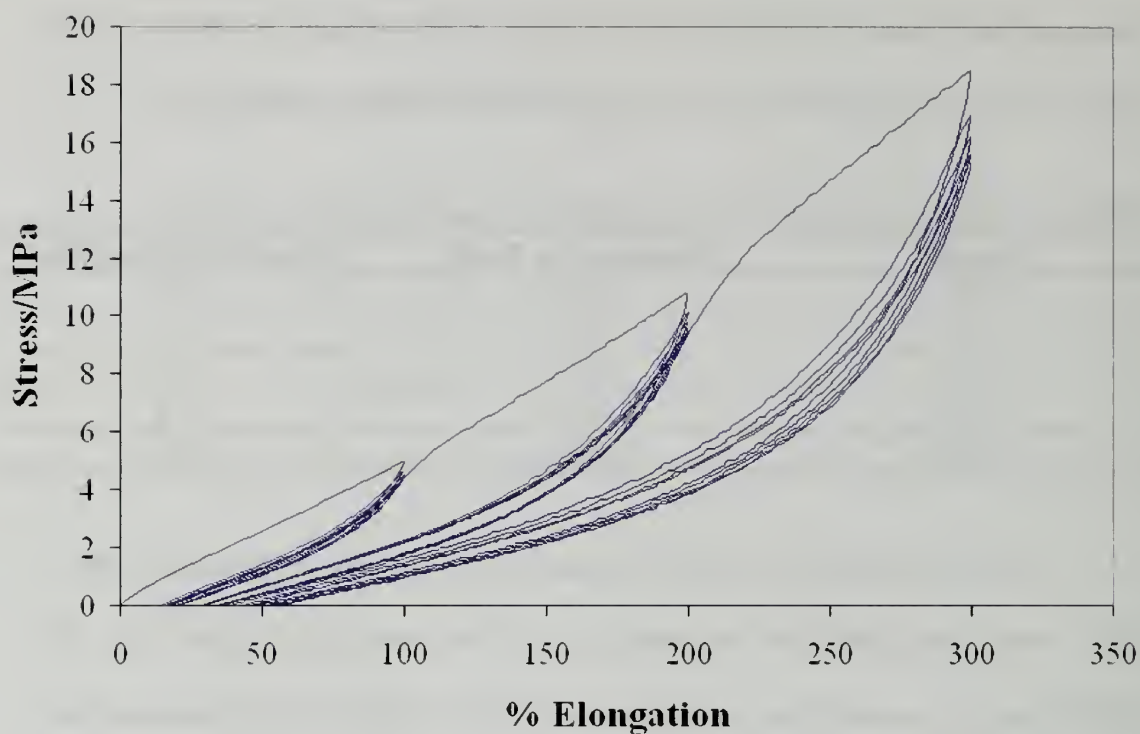


**Figure 2.15.** Cyclic tensile tests on an EPh21 dog bone sample. During the test, a sample was stretched to 100% elongation and allowed to relax back to zero displacement five consecutive times at a rate of 20 mm/min. Next, the sample was stretched 200% elongation, where the same 5 cycles were run. This was followed by 5 cycles at 300% elongation.

The EPhPOSS samples show intriguing results. After the first cycle at each elongation, the sample does not return to its initial length, as the elastomers display hysteresis.

However, the concurrent four cycles show very little hysteresis, and are similar to each other. This is clear example of the Mullins effect, which occurs in positively reinforced filled elastomers.<sup>32,37</sup> This effect is observed at each elongation, and also occurs in the other EPhPOSS samples. This effect could be due to the formation of an equilibrium physical structure after the first elongation. Upon concurrent elongations, a new equilibrium value is reached. This equilibrium value changes once again when the sample is elongated to higher values.



The main difference between the material response of the different EPPOSS samples are the relative deformations. Also, the EPPh10 sample breaks during the 12<sup>th</sup> cycle. The EPPh10 sample has a final deformation of 38%, whereas Ph10 has a final deformation value of 37%, Ph30 is 75%, and Ph36 is 88%. The results of these samples are shown in appendices E and F. As the POSS incorporation in the polymer is increased, there is a higher volume fraction of a glassy phase. Because of this, the material is less elastic at higher loadings, as indicated by these final deformations.

Overall, the EPPOSS polymers show strong mechanical properties. The increase in the length of the rubbery plateau region and the increase in modulus in the rubbery plateau region, as compared to the EP copolymers indicate POSS is acting as a physical crosslink. These materials are advantageous over crosslinked EPDM elastomers, as they are able to be reprocessed, while retaining strong mechanical properties.

#### **2.6.7. TEM**

TEM images were obtained to observe the structures formed in the EPPOSS polymers.

An image is shown in figure 2.17.



**Figure 2.16.** TEM image of EPPH30 polymers, viewed with natural contrast.

Transmission electron microscopy can be used to visualize POSS aggregates in copolymers. These images were obtained without staining. Image contrast can be obtained due to the contrast between the silicon based POSS cages and the hydrocarbon based polymers. The length of the POSS aggregates in the EPPH30 sample is on the order of 8 nanometers, as determined by WAXD. In TEM, these aggregates are expected to be quite small. In these images, POSS aggregates are shown as small black spots. These POSS aggregates are randomly oriented in this polymer sample, and were on the expected size scale. These images confirm POSS aggregates form and are randomly dispersed in the polymer matrix, which is expected for a physically crosslinked polymer.

## 2.7. Conclusions

The synthesis of novel ethylene-propylene-POSS terpolymers allows for the study of POSS aggregation in a mechanically robust and amorphous ethylene-propylene polymer matrix. Polymerizations using a hafnium based metallocene catalyst afforded terpolymers with sufficiently high molecular weights, relatively low polydispersities, varying POSS incorporations and peripheries, and varying ethylene to propylene ratios. Thermal studies of the terpolymers show an invariant relationship between POSS incorporation and glass transition temperature, due to the varying E/P ratios. Thermal gravimetric analysis studies show an increase in decomposition temperature by incorporating POSS, but an invariant relationship between the quantity of POSS incorporation and decomposition temperature. Aggregation studies by WAXD studies suggest POSS disperses within the ethylene-propylene matrix with the isobutyl and ethyl peripheries, but aggregates with the phenyl periphery. This is reinforced by mechanical tests. Terpolymers with the isobutyl and ethyl peripheries were not sufficiently strong for this mechanical test, suggesting POSS acts as a plasticizer when dispersed within the polymer matrix. However, EPhPOSS elastomers show strong mechanical properties. The storage modulus of the terpolymers increases with increasing POSS loading in the rubbery plateau region, as compared to the ethylene-propylene parent polymer. The length of the rubbery plateau region also increases drastically, as compared to the ethylene-propylene parent polymer, indicating POSS acts as an effective physical crosslink for use as thermoplastic elastomers. Tensile studies of EPhPOSS polymers show an increase in the elastic modulus with increasing POSS loading, as well as elongations at break as high as 720%. These elastomers also show the Payne effect, as

the low amplitude modulus is higher than the high amplitude modulus. Cyclic test on the EPPhPOSS elastomers show hysteresis on initial deformations. However, concurrent cycles show indications of the Mullins effect. These mechanical tests shown POSS acts a physical crosslink, which can be utilized in thermoplastic elastomers.

## 2.8. References

- (1) Bhowmick, A. and Stephens, H. *Handbook of Elastomers*, 2<sup>nd</sup> Ed. Marcel Dekker, Inc., New York, 2001.
- (2) Odian, G. *Principles of Polymerization*, 3<sup>rd</sup> Ed. Wiley Interscience & Sons, Inc. New York, 1991.
- (3) Salamore, J. *Polymer Materials Encyclopedia* 1996, 2264-2271.
- (4) The Automobile Trimmings Co. <http://www.automobiletrim.com/door-seal-rubber.html>
- (5) Firestone [http://www.firestonebpe.com/roofing/rubbergard/\\_en/index.shtm](http://www.firestonebpe.com/roofing/rubbergard/_en/index.shtm)
- (6) Möhring P., and Coville, N. *Journal of Organometallic Chemistry* **1994**, 479, 1-29.
- (7) Brintzinger, H., Fischer, D., Mülhaupt, Rieger, B., and Waymouth, R. *Angewandte Chemie, International Edition* **1995**, 34, 1143-1170.
- (8) McKnight, A., and Waymouth R. *Chemistry Reviews* **1998**, 98, 2587-2598.
- (9) Britovsek, G., Givson, V., and Wass, D. *Angewandte Chemie, International Edition* **1999**, 38, 428-447.
- (10) Kaminsky, W. and Miri, M. *Journal of Polymer Science Part A: Polymer Chemistry* **1985**, 23, 2151-2164.
- (11) Leclerc, M., and Waymouth, R. *Angewandte Chemie, International Edition* **1998**, 37, 922-925.
- (12) Galimberti, M., Piemontesi, F., Mascellani, N., Camurati, I., Fusco, O., and Destro, M. *Macromolecules* **1999**, 32, 7968-7976.
- (13) Longo, P., Siani, E., Pragliola, S., and Monaco, G. *Journal of Polymer Science Part A: Polymer Chemistry* **2002**, 40, 3249-3255.



- (14) Malmberg, A. and Löfgren, B. *Journal of Applied Polymer Science* **1997**, *66*, 35-44.
- (15) Zhengtian, Y.; Marques, M.; Rausch, M.; and Chien, J. *Journal of Polymer Science Part A: Polymer Chemistry* **1995**, *33*, 2795-2801.
- (16) Arrowsmith, D.; Kaminsky, W.; Schauwienold, A.; Weingarten, U. *Journal of Molecular Catalysis A: Chemical* **2000**, *160*, 97-105.
- (17) Kravchenko, R., and Waymouth R. *Macromolecules* **1998**, *31*, 1-6.
- (18) Fan, W., Leclerc, M., and Waymouth, R. *Journal of the American Chemical Society* **2001**, *123*, 9555-9563.
- (19) Park, S., Wang, W., and Zhu, S. *Macromolecular Chemistry and Physics* **2000**, *201*, 2203-2209.
- (20) Galimberti, M., Mascellani, N., Piemontesi, F., and Camurati, I. *Macromolecular Rapid Communications* **1999**, *20*, 214-218.
- (21) Ishii, S., Saito, J., Matsuura, S., Suzuki, Y., Furuyama, R., Mitani, M., Nakano, T., Kashiwa, N., and Fujita, T. *Macromolecular Rapid Communications* **2002**, *23*, 693-697.
- (22) Bavarian, N., Baird, M., and Parent, S. *Macromolecular Chemistry and Physics* **2001**, *202*, 3248-3252.
- (23) Gillis, D. and Karpeles, R. **US Pat 6,060,572** May 9, 2000
- (24) Zheng, L.; Hong, S.; Cardoen, G.; Burgaz, E.; Gido, S.; and Coughlin, E.B. *Macromolecules* **2004**, *37*, 8606-8611.
- (25) Gonzalez-Ruiz, R., Quevedo-Sanchez, B., Laurence, R., Coughlin, E.B., Henson, M. *AIChE Journal* **2006**, *52*, 1824-1835.
- (26) B. Quevedo-Sanchez, J. F. Nimmons, E. B. Coughlin, M. A. Henson *Macromolecules* **2006**, *13*, 4306-4316.
- (26) Kolbert, A. and Didier, J. *Journal of Applied Polymer Science* **1999**, *71*, 523-530.
- (27) Vasile, C. *Handbook of Polyolefins*, 2<sup>nd</sup> Ed. Marcel Dekker, Inc., New York, 2001.
- (28) Waddon, A., Zheng, L., Farris, R., and Coughlin, E.B. *Nano Letters* **2002**, *2*, 1149-1155.



- (29) Constable, G., Lesser, A., and Coughlin, E.B. *Macromolecules* **2004**, 37, 1276-1782.
- (30) Joshi, M. and Butola, B. *Journal of Macromolecular Science Part C-Polymer Reviews* **2004**, 44, 389-410.
- (31) Phillips, S., Haddad, T., and Tomczak, S. *Current Opinion in Solid State and Materials Science* **2004**, 8, 21-29.
- (32) Aklonis, J., and MacKnight, W. *Introduction to Polymer Viscoelasticity*, 2<sup>nd</sup> Ed. Wiley Interscience & Sons, Inc. New York, 1983.
- (33) Payne, A.R. *Journal of Applied Polymer Science* **1962**, 6, 57.
- (34) Chazeau, L. Brown, J.D., Yanyo, L.C. and Sternstein, S.S. *Polymer Composites* **2000**, 21, 202-222.
- (35) Zheng, L., Xie, A., and Lean, J. *Macromolecules* **2004**, 37, 9954-9962.
- (36) Payne, A.R. and Whittaker, R.E. *Rubber Chemistry and Technology* **1971**, 44, 440.
- (37) Mullins, L. and Tobin, N.R. *Trans. IRI*, **1956**, 33, 2.

## CHAPTER 3

### SYNTHESIS AND CHARACTERIZATION OF POLY(OCTAFLUOROPENTYL ACRYLATE)-POSS ELASTOMERS

#### 3.1. Fluoroelastomer background

Fluoropolymers are organic polymers with fluorine attached to the polymer main chain.<sup>1,2</sup> The first fluoropolymers were introduced in the 1930s, which included low molecular weight polychlorotrifluoroethylene, and high molecular weight polytetrafluoroethylene, known commonly as Teflon<sup>®</sup>. Despite high monomer costs and poor base resistance, fluoropolymers find great interest due to their excellent material properties, such as strong thermal, chemical, ageing and weather resistance, solvent inertness, low surface energy, low flammability and low moisture absorption.<sup>1,2</sup> These properties arise from the unique chemical nature of fluorine. Fluorine is the most electronegative element, has a small van der Waals radius (1.32Å) and has a strong C-F bond (485kJ/mol). Fluoropolymers are utilized in such applications as UV and graffiti resistant coatings, gaskets or o-rings in the automotive, petrochemical, and aeronautics industries, microelectronics, and perhaps the most well known application, non-stick cookware.<sup>1,2</sup>

Many fluoroelastomers are synthesized by copolymerization, or terpolymerization, with such monomers as vinylidene fluoride (VDF), tetrafluoroethylene (TFE), hexafluoropropylene (HFP), propylene (P) or fluorinated perfluoro(methylvinylethers) (PMVE), as shown in figure 1.<sup>1</sup> The two most common fluoroelastomers are tetrafluoroethylene/propylene copolymers and vinylidene

fluoride/hexafluoropropylene copolymers. TFE/propylene elastomers were introduced in 1975 by Asahi Glass Co. as AFLAS®. The elastomer generally contains 54-57 mol% of fluorine, which is less than most other fluoroelastomers. TFE/propylene elastomers have a maximum service temperature of 230°C, exceptional chemical resistance, even at high temperatures, and high electrical resistivity.

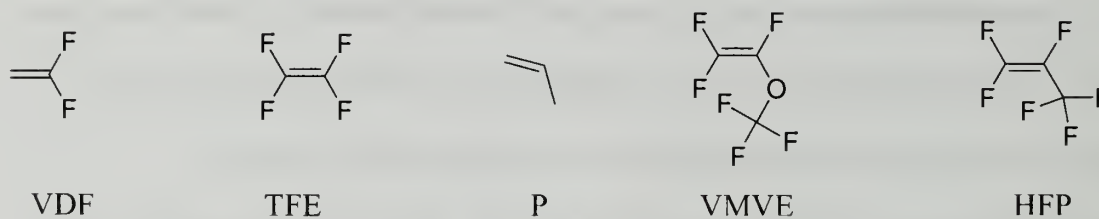


**Figure 3.1.** Common monomers used in the synthesis of fluoroelastomers

Commercially, these elastomers are synthesized using emulsion polymerization with redox catalysts at high pressures and low temperatures, employing a termonomer as a cure site monomer. Viton® and Fluorel® are copolymers of VDF and HFP produced by DuPont (1957) and 3M (1958) respectively. VDF/HFP elastomers have better high temperature stability and better oil resistance than TFE/propylene elastomers. HFP disrupts the crystallinity of the vinylidene fluoride copolymer. HFP incorporations as high as 15 mol% produce polymers which are thermoplastic in nature, while about 22 mol% is need to completely disrupt crystallinity. Fluorelastomers can be crosslinked by a number of crosslinking agents, including peroxides, diamines, and bisphenols.

Thermoplastic fluoroelastomers have also been the subject of much research.<sup>3</sup> These reports have utilized iodine transfer polymerization to synthesize triblock copolymers with a hard segment-soft segment-hard segment architecture. In one example, triblock polymers were synthesized using tetrafluoroethylene-vinylidene fluoride-hexafluoropropylene soft segments and ethylene-tetrafluoroethylene-hexafluoropropylene

or vinylidene fluoride hard segments.<sup>4</sup> By altering the composition of the hard segments, the polymeric properties can be controlled to give materials with higher thermal stability, better chemical resistance, lower glass transition temperatures, and better mechanical properties.

### **3.2. Project goals**

As mentioned previously, POSS aggregates in polybutadiene-POSS copolymers.<sup>5</sup> In chapter 2 of this thesis, POSS was also shown to aggregate in ethylene-propylene-POSS elastomers when there was a phenyl periphery surrounding the POSS cage, but not to aggregate when there was either the isobutyl or ethyl peripheries. Mechanical studies of the polymers showed that PhPOSS acts as an effective physical crosslink in the ethylene-propylene copolymers. In this chapter, POSS aggregation will be studied by varying the polymeric system, specifically in fluorinated elastomers. Because fluorine chains are repulsive, especially to hydrocarbons, they should help drive POSS aggregation, especially with the isobutyl periphery. Thermal properties will be studied, as both POSS and fluoropolymers are known to have high thermal stability. The aggregation of POSS will be studied with varying the POSS peripheries, including isobutyl, phenyl, and isooctyl substituents. Mechanical properties will be probed to determine if POSS incorporation increases the rubbery plateau region and modulus, as compared to the parent fluorinated polymer.

### **3.3. Synthetic methods**

#### **3.3.1. Materials**

POSS macromonomer 3-[(3,5,7,9,11,13,15-Heptaisobutyl-pentacyclo [9.5.1.1<sup>3,9</sup>.1<sup>5,15</sup>.1<sup>7,13</sup>]octasiloxane)]propyl methacrylate (IbuPOSSmethacrylate) was



purchased from Aldrich and 3-[(3,5,7,9,11,13,15-Heptaisooctyl-pentacyclo[9.5.1.1<sup>3,9</sup>.1<sup>5,15</sup>.1<sup>7,13</sup>] octasiloxane)]propyl methacrylate (IoPOSSmethacrylate) and 3-[(3,5,7,9,11,13,15-Heptaphenyl-pentacyclo[9.5.1.1<sup>3,9</sup>.1<sup>5,15</sup>.1<sup>7,13</sup>] octasiloxane)]propyl methacrylate (PhPOSSmethacrylate) were purchased from Hybrid Plastics, and used as received. Octafluoropentylacrylate was purchased from Oakwood Products and used as received. Reaction initiator AIBN, 2,2'-azobis(2-methylpropionitrile), was purchased from Aldrich and recrystallized from methanol and dried before use. Benzene was purchased from Aldrich and vacuum distilled over CaH<sub>2</sub> before use.

### 3.3.2. Polymerization of POSSmethacrylate and octafluoropentyl acrylate

Under a nitrogen atmosphere, a 100 mL round bottom flask, with a stir bar and septum, was charged with 1.2 mL (6.24 mmol) of octafluoropentylacrylate, 7 mg (0.043 mmol) of AIBN, 10 mL of benzene, and a predetermined amount of methacrylatePOSS. The flask was heated in an oil bath at 65 °C for 6 hours. The reaction was precipitated in hexane or methanol, depending on the POSS loading and POSS periphery. Residual POSS monomer was removed from PhPOSS copolymers by consecutive precipitations in hexane. Residual POSS monomer was removed from IbuPOSS copolymers by consecutive precipitations into an 85:15 (v:v) methanol/H<sub>2</sub>O mixture. At low POSS loading, the precipitation of POSS copolymer in hexanes completely removed residual POSS monomer.

### 3.3.3. Polymer characterization

<sup>1</sup>H NMR spectra were obtained in chloroform-*d* or methylene chloride-*d*<sub>2</sub> on a Bruker DPX-300 FT-NMR spectrometer operating at 300 MHz. <sup>13</sup>C NMR spectra were obtained



at 90°C in tetrachloroethane- $d_2$  on a Bruker 400 FT-NMR spectrometer operating at 100 MHz. Gel permeation chromatography was obtained using a Polymer Laboratories PL-GPC 50 Integrated GPC System, using THF as the mobile phase. Molecular weights were calibrated against narrow molecular weight polystyrene standards.

### **DSC**

Differential scanning calorimetry was performed under a nitrogen atmosphere on a DuPont Instruments DSC 2910. Samples were cooled to -110 °C and heated at a rate of 10 °C/min. Data was obtained on second heating, also at a rate of 10 °C/min.

### **TGA**

Thermal gravimetric analysis was performed using a Mettler-Toledo TGA/SDTA851°. Samples were heated at a rate of 10 °C/min up to 800 °C under an air atmosphere.

### **WAXD**

Wide angle X-ray diffraction patterns were obtained on a PANalytical X'Pert PRO instrument in reflectance mode. Samples for this study were dissolved in a toluene solution (20% volume), and cast onto a glass slide. Samples were dried in a vacuum oven at 40 °C for 24 hours.

### **Rheology**

Rheological studies were performed in a TA Instruments AR 2000 rheometer, using a parallel plate geometry. Samples were prepared by dissolution in toluene, and casting films in aluminum pans. The films were allowed to form over 2 days. The films were then dried in a vacuum oven at 45 °C for at least 24 hours.

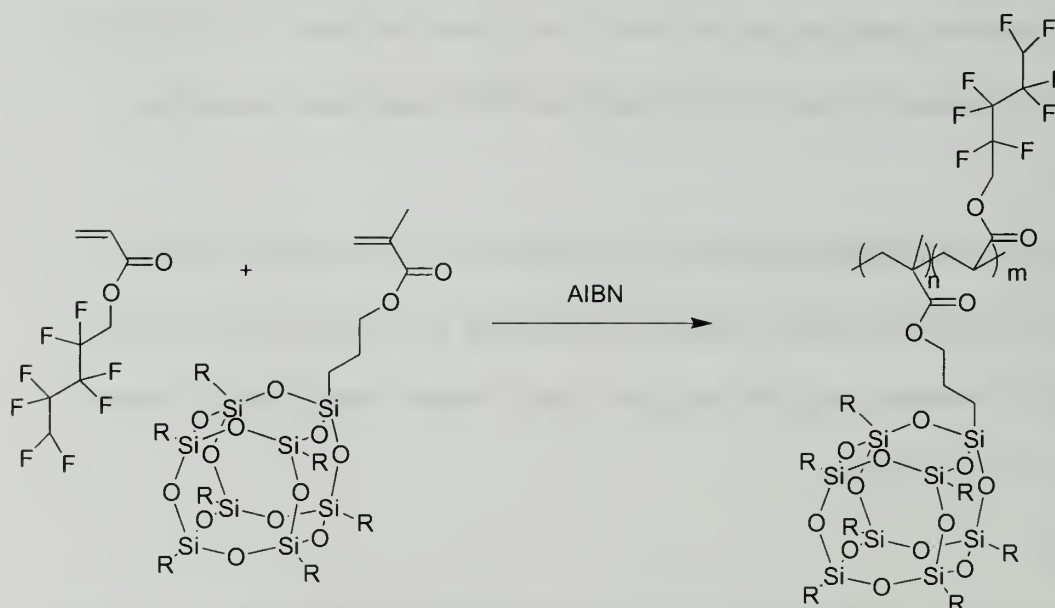
## TEM

Samples of TEM were prepared as in rheology studies. Samples were microtomed at  $-120^{\circ}\text{C}$  using a diamond knife, cutting 50 nm thick slices. Images were obtained using a JEOL 100CX Electron Microscope, operating at 100 kV.

### 3.4. Results and discussion

#### 3.4.1. Polymerization

As an introduction into fluoroelastomers containing POSS, free radical copolymerization of octafluoropentylacrylate and POSSmethacrylate was preformed, as shown in scheme 3.1.



**Scheme 3.1.** Copolymerization of octafluoropentylacrylate-POSS copolymers

Octafluoropentyl acrylate copolymers were chosen due to their robust polymerization techniques, their well-defined polymer nature, their elastomeric nature, and their presumed ability to form random copolymers with POSS. Studying the reactive ratios of two similar monomers, trifluoroethylacrylate and methyl methacrylate, it was anticipated that random copolymers would be formed, as the  $r_1$  value of trifluoroethylacrylate was

0.1 and the  $r_2$  value was 2.1.<sup>6</sup> Replacing methyl methacrylate with the more bulky POSSmethacrylate should decrease the  $r_2$  value, resulting in random copolymers. Copolymerization reaction results are shown in table 3.1.

**Table 3.1.** Octafluoropentyl acrylate-POSS copolymerization results

Rxn ID	POSS loading/ wt%	$M_n$ (g/mol) (PDI) <sup>a</sup>	POSS in Polymer/ mol%(wt%) <sup>b</sup>	Isolated Yields
POFPA	---	16,000(1.54)	---	81%
Ibu7	6.7	28,000(2.26)	2.0(7)	66%
Ibu10	12.6	64,000(1.57)	3.0(10)	79%
Ibu32	20.6	32,000(2.39)	13(32)	65%
Ibu36	30.3	53,700(1.45)	15(36)	>20%
Ph8	6.7	32,000(1.79)	2.2(8)	64%
Ph14	12.6	44,000(1.61)	4.0(14)	62%
Ph23	20.6	45,000(1.88)	7.3(23)	64%
Ph32	30.3	34,000(1.66)	11.2(32)	60%
Io6	7.9	70,000(2.30)	1.4(6)	69%
Io13	14.7	54,000(1.93)	3.2(13)	59%

<sup>a</sup>As determined by GPC, using narrow molecular weight polystyrene standards in THF.

<sup>b</sup>As determined by <sup>1</sup>H NMR, with CDCl<sub>3</sub> or CD<sub>2</sub>Cl<sub>2</sub> as solvent.

Polymerizations were stopped at relatively low conversions to reduce chain branching and crosslinking reactions. Molecular weights were low for the poly(octafluoropentylacrylate) (POFPA) homopolymer, and several copolymers with low POSS loadings. The number-average molecular weights ranged from 28,000 to 70,000 g/mol for the range of different copolymers prepared. The molecular weight, as calculated from GPC, are presumably higher than the actual values, as fluoropolymers have strongly repulsive polymer chains, thus creating a random coil with a larger radius of gyration than most polymers. This allows for faster elution in GPC as the copolymers appear larger. POSS homopolymers, on the other hand, have shown lower than expected molecular weights in GPC when compared to molecular weights determined by NMR spectroscopy. POSS incorporations were determined by <sup>1</sup>H NMR, as shown in figure 3.2.

POSS incorporations were determined by using the methyl and methylene protons of the isobutyl periphery to the methylene protons  $\alpha$  to the carbonyl on the octafluoropentyl-side chain. Internal integrations of other protons in the copolymers were consistent with the calculated POSS incorporations.

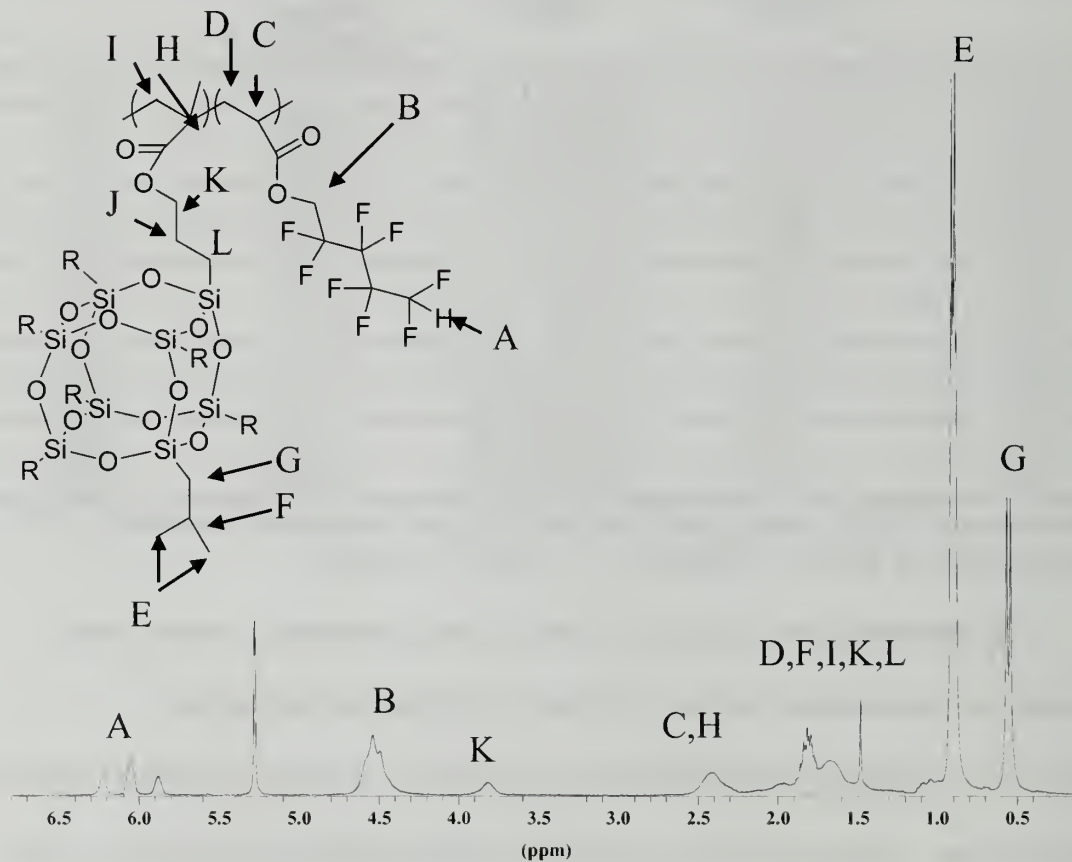


**Figure 3.2.**  $^1\text{H}$  NMR of poly(octafluoropentylacrylate-IbuPOSS) copolymer

Based on the expected reactivity ratios and the POSS feed to incorporation comparisons, it is believed that random copolymers are formed. From NMR spectroscopy, the monomer arrangement of copolymers can be determined from resonance shifts in atoms that connect different monomers. However, in the case of POSS-octafluoropentyl acrylate copolymers, resonances from backbone atoms overlap,



making it difficult to observe resonance shifts. In  $^{13}\text{C}$  NMR, it is difficult to observe POSS backbone resonances, as only a small mol % of POSS is incorporated into the copolymers, and there are very few backbone carbons per POSS molecule. POSS loadings were similar to POSS incorporations in the copolymers, reinforcing the suggestion of random copolymers. POSS incorporations ranged from 6 to 36 weight %, and could be relatively well controlled. Copolymers with IoPOSS could only be synthesized with low POSS incorporations due to the difficulty of removing IoPOSS monomer from copolymers with high POSS incorporations.

### 3.4.2. WAXD

Wide angle X-ray diffraction (WAXD) was used to study the aggregation of POSS in the prepared copolymers.<sup>5,7</sup> WAXD patterns of the POFPA-POSS copolymers are shown in Figures 3.3-3.5. Each figure shows the POFPA homopolymer diffraction pattern on the bottom with increasing POSS loading going up the graph, with POSS monomer on the top. The POFPA homopolymer shows an amorphous halo centered around a  $2\theta$  value of 18. As the IbuPOSS content is increased to 10 wt%, a POSS diffraction peak at a  $2\theta$  value of 8 is shown, indicating POSS aggregates. As the POSS content is increased to 36 wt%, the diffraction peak increases in intensity and sharpens, indicating larger POSS aggregates. In ethylene-propylene-IbuPOSS elastomers, POSS disperses within the ethylene-propylene matrix (Chapter 2). The current study shows that by changing the nature of the polymer, POSS can be tuned to aggregate in copolymers. In the PhPOSS copolymers, POSS diffraction peaks are relatively sharp at all POSS incorporations, indicating extensive POSS aggregation in the copolymers. Copolymers containing IoPOSS show broad POSS diffraction peaks, indicating small POSS



aggregates, or more likely POSS dispersion. The IoPOSS monomer is not crystalline in nature, indicating that the long isooctyl chain suppress the ability of POSS to aggregate.

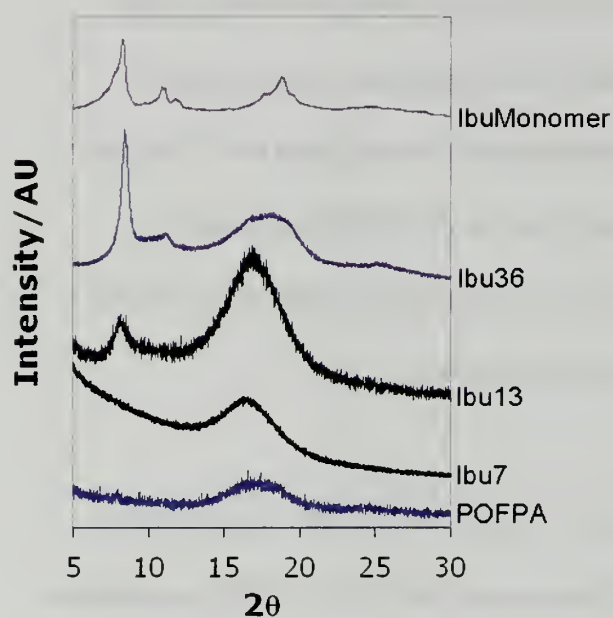


Figure 3.3. WAXD patterns of POFPA-IbuPOSS copolymers

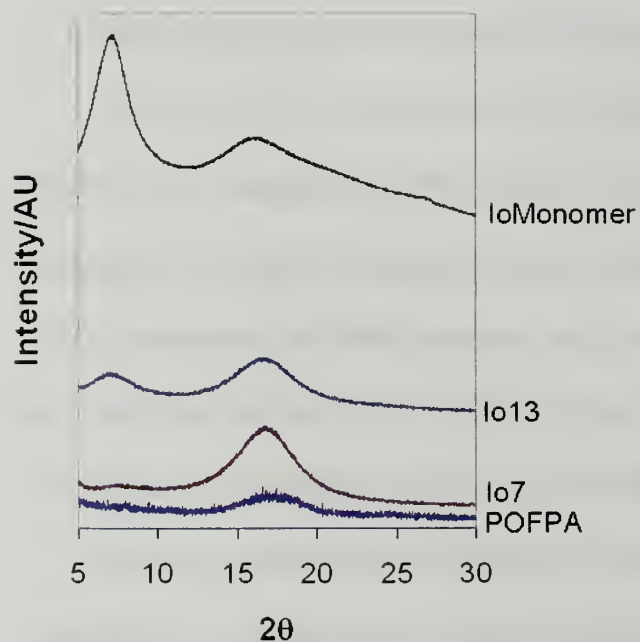
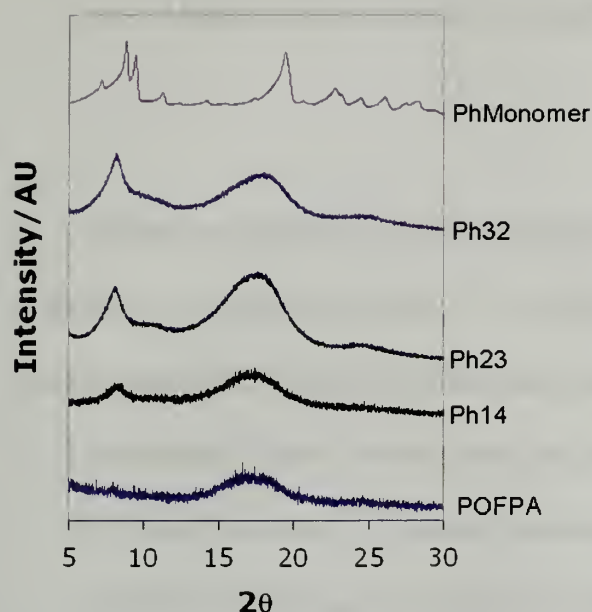


Figure 3.4. WAXD patterns of POFPA-IoPOSS copolymers



**Figure 3.5.** WAXD patterns of POFPA-PhPOSS copolymers

The approximate lateral size of the POSS aggregates was determined using Scherer's equation. It is assumed that a POSS monomer has a 1.5 nm diameter. The results are shown in Table 3.2.

**Table 3.2.** POSS domain sizes estimated using Scherer's equation

Sample	Domain Size(nm)	~POSS per domain <sup>a</sup>
Ibu36	15	10
Ibu10	8.0	5-6
Ph32	7.2	4-5
Ph23	6.0	4
Io13	3.5	2-3

<sup>a</sup> Number of POSS per domain was estimated by dividing the estimated domain size by 1.5 nm, the approximate diameter of POSS.

This study shows POSS aggregates to form the longest domain sizes with the isobutyl periphery, as Ibu36 has a domain length of 15 nm. The PhPOSS copolymers have lengths of 6-7.2 nm per domain, which are similar in size to the ethylene-propylene-PhPOSS samples. The Io13 sample may have approximately 2-3 POSS molecules per

domain. Because the monomer is not crystalline, the relative intensity could be due to non-crystalline aggregation.

### 3.4.3. Thermal characterization

The thermal characterization data is shown in table 3.3. The glass transition temperature of poly(octafluoropentyl acrylate) is -27 °C, and the polymer has a melting peak at 96 °C. However, no diffraction peaks were seen in WAXD of this homopolymer. None of the copolymers show a melting peak, indicating that POFPA crystallization is restricted to the homopolymer. Based on previous literature, it is expected that POSS will increase the glass transition temperature of the parent homopolymer, as adding a bulky side group slows the segmental movement of the copolymer chain.<sup>9</sup> In PhPOSS copolymers, the  $T_g$  increases with increasing POSS loading, with the largest jump occurring between the Ph14 and Ph23 samples. This trend also fits with the two IoPOSS copolymers. This trend does not fit with the IbuPOSS copolymers, as the  $T_g$  values remain about the same with all POSS loadings. A possible explanation is that the POSS aggregates are acting like domains in block copolymers. Thermal studies on phase separated block copolymers have shown  $T_g$  values for both blocks which are the same  $T_g$  values as the respective homopolymers. These samples do not show a  $T_g$  for the POSS block. There have been very few literature reports of  $T_g$  values for POSS blocks.

Thermal gravimetric analysis data shows the strong thermal characteristics of both the fluorinated homopolymer and POSS containing copolymers (Table 3.3). The homopolymer, POFPA, has a 2% decomposition temperature of 291 °C, which increases by the addition of POSS to the polymers. The periphery plays an important role in the decomposition temperature, but the POSS incorporation does not seem to play a

significant role. This could be related to the amount of POSS aggregated at the surface. If the amount of POSS is similar at different loadings, the thermal decomposition data should be similar.

**Table 3.3.** Thermal characterization of POSS-octafluoropentyl acrylate copolymers

Rxn ID	Wt. % POSS	T <sub>g</sub> <sup>a</sup> /°C	2% Decomp. Temp. <sup>b</sup> /°C	Char Yield <sup>b</sup> /%	Theo. Char Yield <sup>c</sup> /%
POFPA	---	-27(T <sub>m</sub> =96)	291	12.1%	---
Ibu7	7	-29	294	4.5	3.5
Ibu10	10	-28	294	10.3	5.1
Ibu32	32	---	295	18.8	16.2
Ibu36	36	-27	295	20.3	18.3
Ph8	8	-29	316	3.8	3.1
Ph14	14	-26	319	7.0	5.4
Ph23	23	-15	316	11.8	10.3
Ph32	32	-14	318	16.2	14.3
Io6	6	-26	320	2.7	2.5
Io13	13	-24	320	4.5	4.6

<sup>a</sup>As determined by GPC, with a heating rate of 10°C/minute.

<sup>b</sup>As determined by TGA, with a heating rate of 10°C/minute.

<sup>c</sup>Theoretical calculation assumes a complete conversion of POSS to SiO<sub>2</sub>.

The IbuPOSS copolymers show the lowest increase in decomposition temperature, at 295°C followed by the PhPOSS copolymers and IoPOSS copolymers, which are both in the range of 319°C. This is another important material property that depends directly upon the POSS periphery.

Another important property is the char yield. Ideally, POSS will decompose under air to form silica, SiO<sub>2</sub>. The theoretical char yields calculated in Table 3.3 are based on a complete conversion of POSS to silica. The POFPA homopolymer shows a significant char yield, which partially explains the fact that the theoretical yields are lower than the actual values. PhPOSS copolymers also show higher char than expected, as the phenyl ring can also form char. Because of the high char yields that form from the POFPA homopolymer plus POSS conversion to silica, it is expected that the char yields



will be higher than the theoretical values. However, several char yields are close to the theoretical values. One possible explanation for this is a possible POFPA scission that results in the formation of a fluoride anion, which can attack silicon, thus suppressing the formation of  $\text{SiO}_2$ , and reducing the char formed from the fluoropolymer.

#### **3.4.4. Rheology**

The mechanical properties of these materials are not expected to be strong due to the relatively low molecular weight of the copolymers. Rather, the studies will be used to determine if POSS copolymers show an increase in the length and modulus of the rubbery plateau region as compared to the homopolymer, as crosslinked elastomers are known to have an increase in the length of the rubber plateau region as well as an increase in the modulus of the material, in the rubbery plateau region.<sup>10</sup> Strain sweeps at various temperatures were performed to determine the crossover temperature of the elastomers from the rubbery plateau region to the rubbery flow region. Three plots are shown in figure 3.6, which measure the storage and loss modulus as a function of temperature.



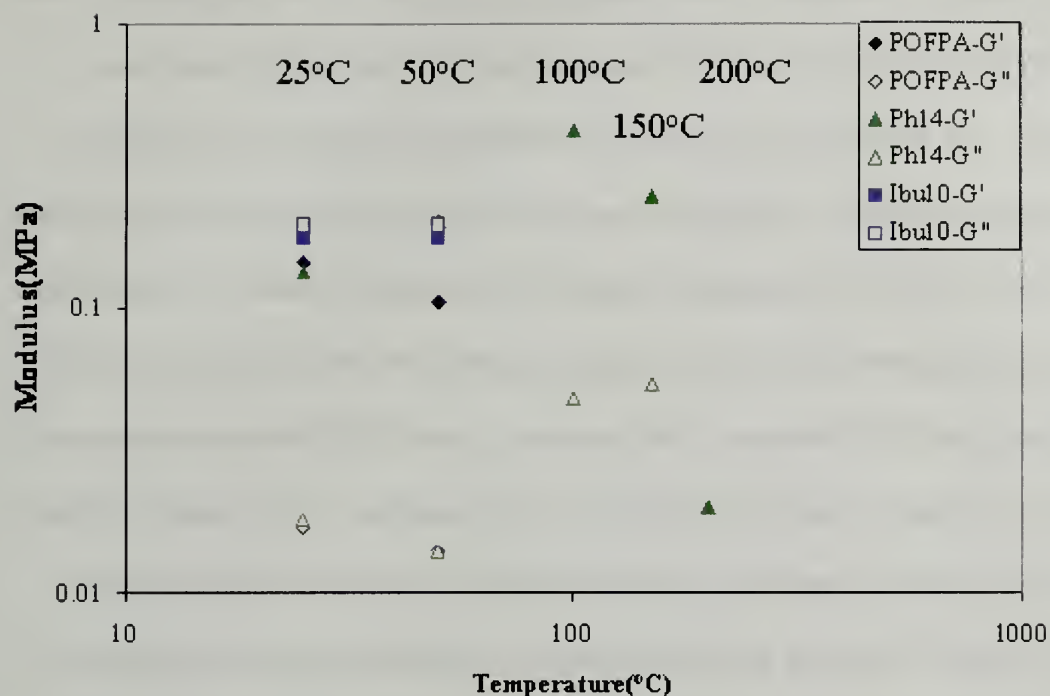


**Figure 3.6.** Modulus as a function of temperature in POFPA and POFPA copolymers.

A strain sweep was performed on three different samples, the POFPA homopolymer, and Ibu10 and Ph14 copolymers. Each sample was in the linear viscoelastic regime, allowing for a single data point at each temperature. At 25°C, Ibu10 has the highest storage modulus, but the loss modulus is higher than the storage modulus, indicating the sample already has crossed over to the rubbery flow region. The Ph14 and POFPA samples show similar behavior, with their storage modulus being much higher than the loss modulus. It is important to note that the POFPA homopolymer shows a significant melting peak at 96°C. This semi-crystalline nature of the homopolymer inherently makes this material a thermoplastic elastomer, and explains the relatively strong mechanical properties of the material at both 25 and 50 °C. The Ph10 copolymer sample shows the strongest mechanical properties at 50 °C. The storage and loss modulus of both the POFPA homopolymer and Ibu10 samples decrease at this temperature, although the

POFPA homopolymer remains in the rubber plateau region. As the temperature is raised to 100 °C, both the POFPA and Ibu10 samples flow off of the parallel plates in the rheometer. The Ph10 sample had sufficient mechanical strength to test properties at temperatures up to 200 °C. When the temperature of the sample was further raised from 25 °C to 50 °C to 100 °C, the storage modulus of the material increases. This indicates a change in the microstructure of the copolymer, possibly the formation of larger POSS domains or more POSS domains. The formation of more POSS domains corresponds to a material with more crosslinks, affording a tougher material. As the sample is heated to 150 °C, the mechanical properties remain strong and are still in the rubbery plateau region. At 200 °C, however, the storage modulus is drastically lower, and appears to be in the rubbery flow region. This displays the ability of POSS to act as a physical crosslink, as the rubbery plateau region is increased versus the homopolymer, despite the semi-crystalline nature of the copolymer.

Frequency sweeps were also performed on the polymer samples (Figures 3.7-3.9). Frequency sweeps give information about the response of polymeric material at different frequencies, which are related to time. High frequencies are related to short times, and low frequencies are related to high times.<sup>10</sup> In the POFPA homopolymer, the storage modulus remains approximately the same across the frequency range, indicating a solid material that retains its properties at high times (low frequencies). When the sample is heated to 50 °C, it has the same material response, with only a small decrease in the modulus. The Ibu10 sample shows fluid like behavior at both 25 and 50 °C. Although POSS has been shown to aggregate in POFPA-IbuPOSS copolymers, the IbuPOSS loading must be too small to drastically enhance material properties.

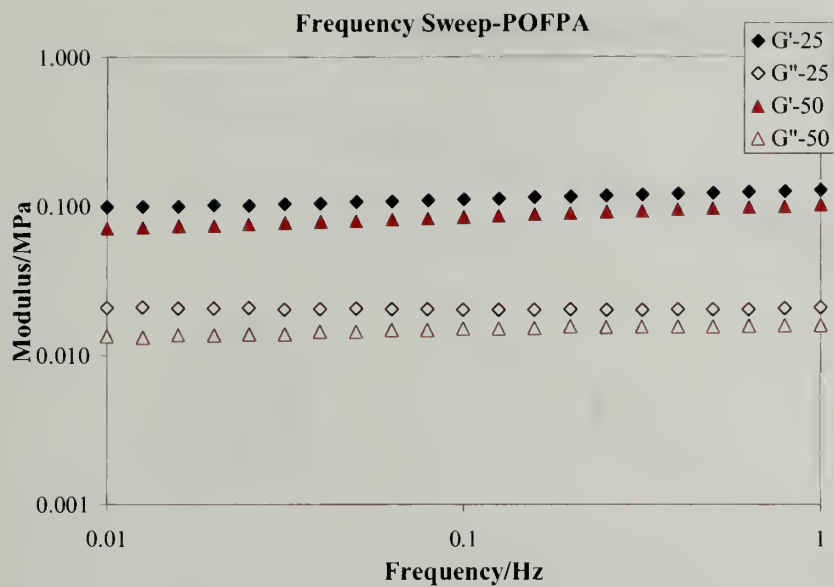


**Figure 3.7.** Frequency sweep of POFPA homopolymer sample.

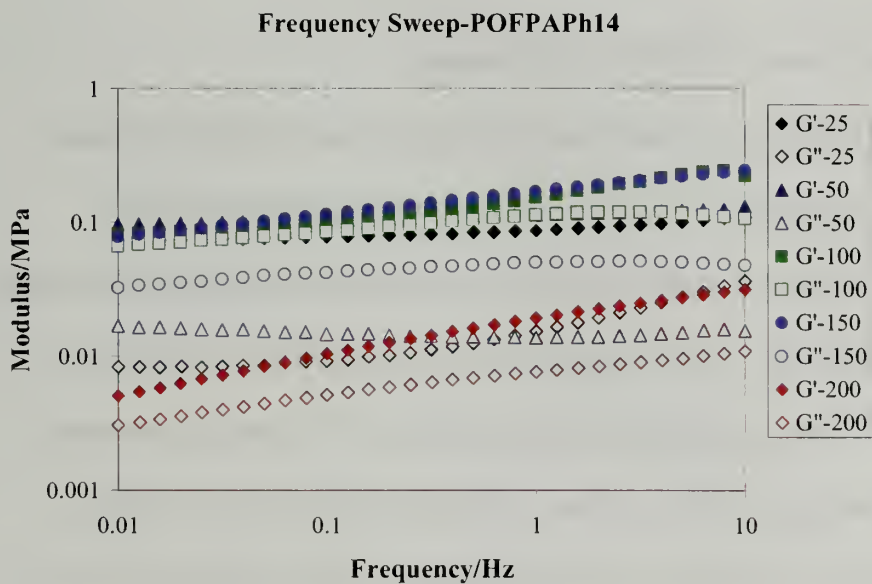


**Figure 3.8.** Frequency sweep of POFPA-Ph14 sample.

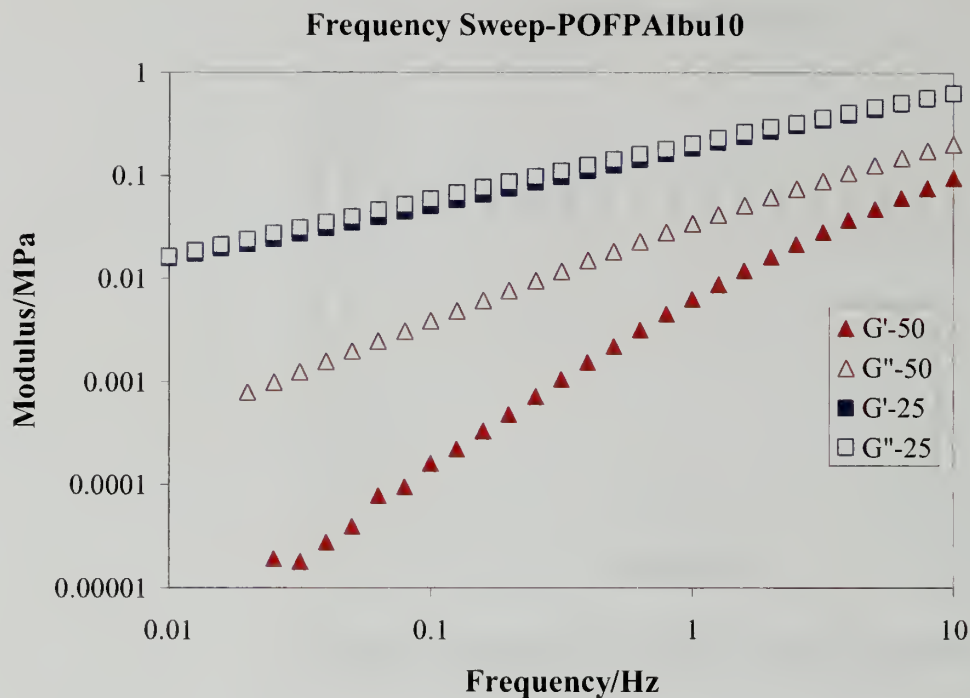


**Figure 3.9.** Frequency sweep of POFPA-Ibu10 sample.

The homopolymer has stronger material properties due to its semi-crystalline nature, making it difficult to compare the enhancement in mechanical properties by the incorporation of low loadings of IbuPOSS. The Ph14 sample has much stronger material properties. The modulus only shows a slight decrease in modulus as the frequency is changed from 10 to 0.01 Hz, indicating a solid-like material. The material properties only show a drastic change at 200 °C, as there is a larger change in modulus while decreasing the frequency. Therefore, even at small POSS loadings, POSS increases the rubbery plateau region and shows a higher modulus than the POFPA homopolymer.

The molecular weight between crosslinks ( $M_c$ ) was estimated from the rheological data using the equation  $M_c = \rho RT/G$ . The average molecular weight between crosslinks between 50-150°C was 24,000 g/mol, or 87 monomer units between crosslinks.

Therefore, on average, Ph14 has 2 or 3 crosslink junctions per polymer chain. The POSS aggregates disperse at a temperature between 150 and 200 °C.

#### **3.4.5. TEM**

Transmission electron microscopy was used to observe the POSS aggregates forming in the copolymers. Typical results are shown in figure 3.10 below. Transmission electron microscopy can be used to visualize POSS aggregates in copolymers. The length of the POSS aggregates in the Ibu36 sample are on the order of 15 nanometers, as determined by WAXD. In TEM, these aggregates are expected to be the same. These images were obtained without staining. Image contrast can be obtained without staining due to the contrast between the silicon based POSS cages and the hydrocarbon based polymers. In these images, POSS aggregates are shown as small black spots. These POSS aggregates are randomly oriented in the polymer sample. These images confirm POSS aggregates form and are randomly dispersed in the polymer matrix, which is expected for a crosslinked polymer.



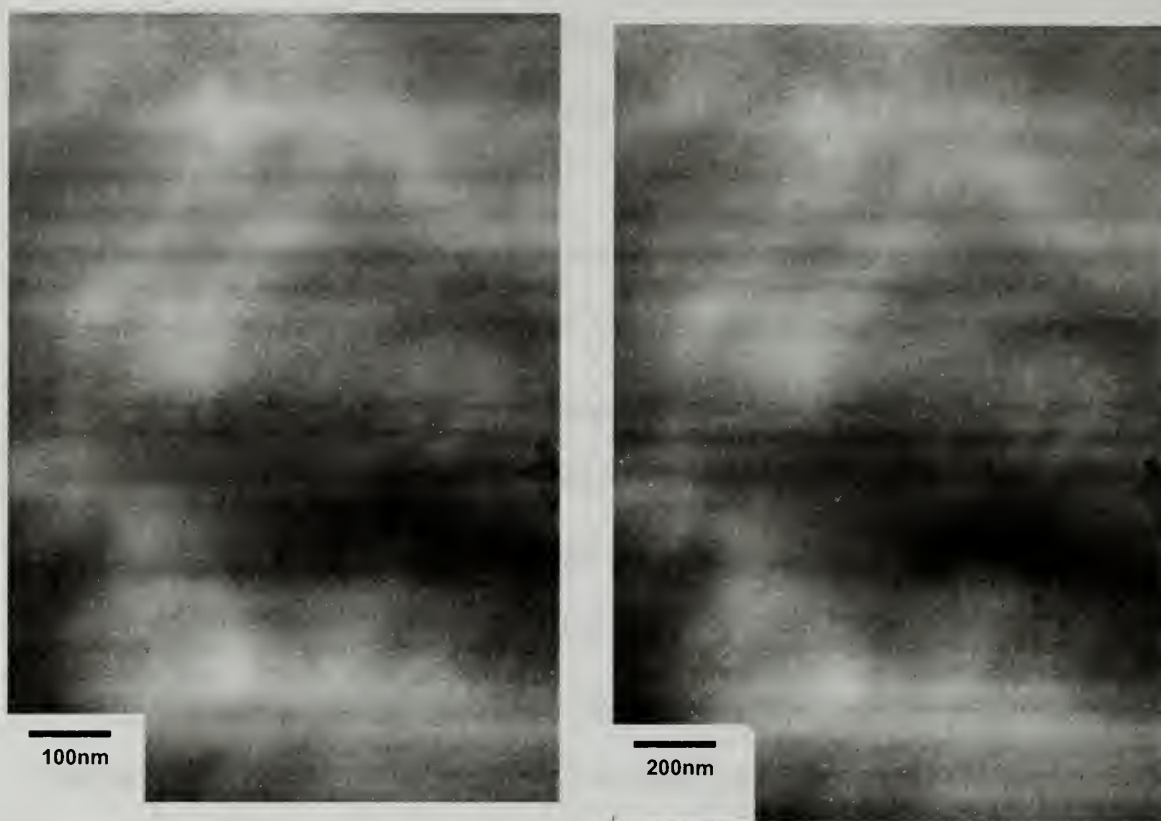


**Figure 3.10.** TEM images of POFPA-Ibu36 sample.

### 3.5. Conclusions

The synthesis of poly(octafluoropentylacrylate)-POSS copolymers allowed for the study of POSS aggregation in fluoroelastomers and the subsequent investigation of the mechanical properties of POSS copolymers. The synthesis of the copolymers by free radical chemistry afforded copolymers with moderate molecular weights, and relatively low polydispersities while also permitting the variation of POSS peripheries. Thermal studies of these random copolymers show moderate increases in glass transition temperature with PhPOSS and IoPOSS copolymers, but no increases with IbuPOSS copolymers. Thermal gravimetric analysis data shows an increase in 2% decomposition temperature by incorporating POSS, and an increase in decomposition temperatures based on the POSS periphery, with isooctyl showing the highest decomposition

temperature, followed by phenyl and isobutyl. The aggregation of POSS in these fluorinated copolymers were also shown to be periphery dependent. Unlike ethylene-propylene-IbuPOSS copolymers, IbuPOSS was found to aggregate in these fluoroelastomer copolymers, as the chain repulsive fluorinated chains help drive POSS aggregation. POSS was also found to aggregate with the PhPOSS copolymers. The IoPOSS copolymers, however, show broad aggregation peaks, showing the non-crystalline nature of the copolymers. However, using Scherrer's equation, the domain length was estimated to be on the order of 2-3 POSS cubes, perhaps indicating non-crystalline POSS aggregation. Rheological studies of these copolymers show a significant increase in the rubbery plateau region and modulus of the POFPA-Ph14 samples as compared to the POFPA semi-crystalline homopolymer.

### 3.6. References

- (1) Améduri, B., Boutevin, B., and Kostov, G. *Progress in Polymer Science* **2001**, 26, 105-187.
- (2) Bhowmick, A., and Stephens, H. *Handbook of Elastomers*, 2<sup>nd</sup> Ed. Marcel Dekker, Inc., New York, 2001.
- (3) David, G., Boyer, C., Tonner, J., Améduri, B., Lacroix-Desmazes, P., and Boutevin, B. *Chemistry Reviews* **2006**, 106, 3936-3962.
- (4) Tatemoto, M. European Patent 399543, 1990.
- (5) Zheng, L., Hong, S., Cardoen, G., Burgaz, E., Gido, S., and Coughlin, E.B. *Macromolecules* **2004**, 37, 8606-8611.
- (6) Lide, D. *CRC Handbook of Chemistry and Physics*, 81<sup>st</sup> Ed. CRC Press, New York, 2001.
- (7) Zheng, L., Farris, R., and Coughlin, E.B. *Journal of Polymer Science Part A: Polymer Chemistry* **2001**, 39, 2920-2928.

- (8) Waddon, A., Zheng, L., Farris, R., and Coughlin, E.B. *Nano Letters* **2002**, 2, 1149-1155.
- (9) Li, G., Wang, L., Ni, H., and Pittman Jr., C. *Journal of Inorganic and Organometallic Polymers* **2001**, 11, 123-154.
- (10) Aklonis, J., and MacKnight, W. *Introduction to Polymer Viscoelasticity*, 2<sup>nd</sup> Ed. Wiley Interscience & Sons, Inc. New York, 1983.

## CHAPTER 4

### PERIPHERAL EFFECT ON POSS AGGREGATION IN POLY(DIMETHYLCYCLOOCTADIENE)-POSS COPOLYMERS

#### 4.1. Background

The synthesis of POSS molecules results in cage structures of varying sizes. Much of the literature on POSS containing polymers make use of T<sub>8</sub> cages, which contain 8 silicon atoms, 12 oxygen atoms, and 8 peripheral groups. A specific synthesis of POSS allows for the addition of one unique functional group, which can be used in polymerizations or polymer grafting reactions. The seven remaining inert peripheral groups provide solubility in common organic solvents or miscibility in polymers. Some common inert peripheral groups include cyclopentyl (Cp), cyclohexyl (Cy), phenyl (Ph), ethyl (Et), isobutyl (Ibu) and isooctyl (Io). The closed cage structure POSS analog (T<sub>8</sub>, Si<sub>8</sub>O<sub>12</sub>R<sub>8</sub>) with fluoryl-alkyl groups –CH<sub>2</sub>CH<sub>2</sub>(CF<sub>2</sub>)<sub>7</sub>CF<sub>3</sub> and –CH<sub>2</sub>CH<sub>2</sub>CF<sub>3</sub> have been prepared, but there has been no published work of incorporating their T<sub>7</sub> analogs (Si<sub>7</sub>O<sub>12</sub>H<sub>3</sub>R<sub>7</sub>) chemically onto a polymer chain.<sup>1</sup>

Outside of the current thesis work, there are no reports of systematic studies on the POSS peripheral effect on aggregation in completely amorphous polymer systems. Haddad *et al.* explored different cyclic peripheries and an isobutyl periphery in SBS-POSS elastomers.<sup>2-4</sup> PhPOSS had the most influential effect on the SBS-POSS polymers, as it interacts with the styrene phase, acting as a plasticizer. Addition of PhPOSS to the polymer decreased the *d* spacing and the order-to-disorder transition temperature, with respect to the SBS parent polymer. Cyclohexenyl, cyclopentyl, and cyclohexylPOSS



were also incorporated to these SBS triblocks in the butadiene regime. These polymers also showed a decrease in the  $d$  spacing and the order-to-disorder transition temperature, but to a lesser magnitude. When the isobutyl periphery was grafted to the polymer, POSS was distributed within the butadiene regime, thus swelling it.<sup>4</sup> Unlike the current thesis work, these SBS-POSS elastomers have competing factors of POSS aggregation and butadiene phase segregation.

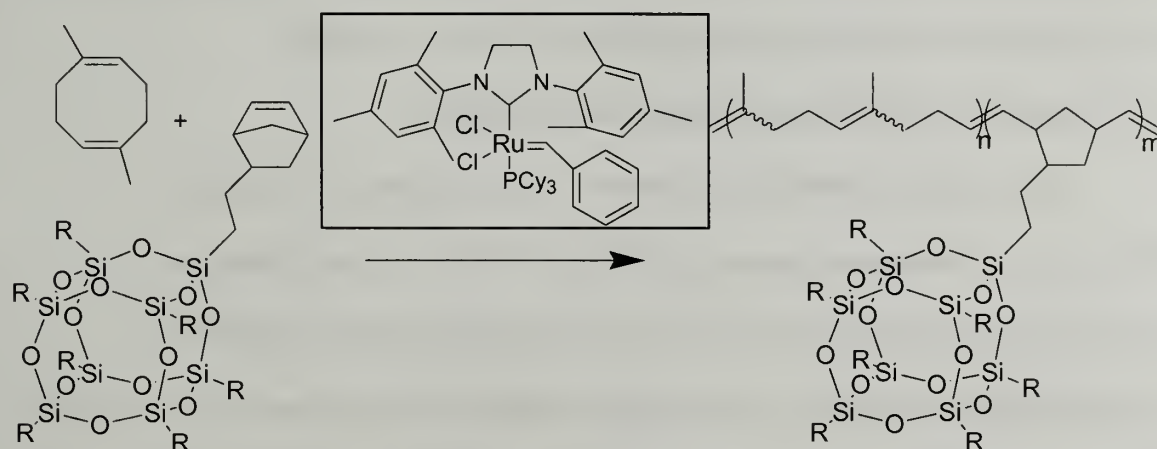
In Chapter 2 and 3 of this thesis, the aggregation of POSS was studied in a saturated hydrocarbon polymer (EP) and a hydrocarbon repulsive fluoropolymer. In the EP copolymers, only the phenyl periphery was shown to aggregate, whereas the ethyl and isobutyl peripheries dispersed within the polymer matrix. In the fluoropolymer, POSS was shown to aggregate with both the isobutyl and phenyl peripheries, but not with the isooctyl periphery, presumably due to the non-crystalline nature of isooctylPOSS.

To study the peripheral effect, an ideal system would have a uniform polymer chain, where only the POSS peripheral substituent is altered. Along with this, a different polymeric backbone than the saturated hydrocarbon ethylene-propylene and fluoroacrylate copolymers allows for the further exploration of POSS aggregation in differing elastomeric systems. One such polymer system is polyisoprene. Unlike the ethylene-propylene copolymers, polyisoprene has unsaturation in the polymer backbone. Also, if it is synthesized specifically to have a complete 1,4-structure, polyisoprene will have a more uniform backbone structure. Because of these differences, the polymeric chain should interact differently with POSS than in saturated hydrocarbons.



## 4.2. Project goals

In this study, the effect of the periphery of POSS in a copolymer will be studied. The copolymer will be amorphous, as crystallization of the comonomer in semi-crystalline POSS copolymers could affect POSS aggregation.<sup>5</sup> POSS peripheral groups will be changed to include ethyl, cyclopentyl, isobutyl, and phenyl. In a previous study, polybutadiene-POSS elastomers were prepared using the cyclopentyl periphery. Studies of the copolymers show POSS aggregation, and at high POSS incorporations, a raft-like morphology is formed.<sup>6</sup> In this study, a similar amorphous polymer containing POSS will be used to determine if changing the periphery has a major effect on POSS aggregation. One ideal matrix candidate is a polyisoprene-like polymer, produced by the ring-opening metathesis polymerization (ROMP) of 1,5-dimethyl-1,5-cyclooctadiene. This polymer has previously been prepared using Grubbs second generation catalyst.<sup>7</sup> POSS can easily be polymerized and copolymerized by ROMP in high yields.<sup>5</sup> This allows us to explore a polymer chain with degrees of unsaturation in the polymer backbone, making it chemically different from the EP polymers.



**Scheme 4.1.** Polymerization of polyisoprene like-POSS copolymers

### 4.3. Experimental

#### 4.3.1. Materials

The monomer 1,5-dimethyl-1,5-cyclooctadiene was purchased from TCI America, and was vacuum distilled over  $\text{CaH}_2$  prior to use. POSS macromonomers, IbuPOSS, 1-[2-(5-norbornen-2-yl)ethyl]-3,5,7,9,11,13,15-heptaisobutylpentacyclo [9.5.1.1<sup>3,9</sup>.1<sup>5,11</sup>.1<sup>7,13</sup>]octasiloxane, EtPOSS-norbornene 1-[2-(5-norbornen-2-yl)ethyl]-3,5,7,9,11,13,15-heptaethylpentacyclo [9.5.1.1<sup>3,9</sup>.1<sup>5,11</sup>.1<sup>7,13</sup>]octasiloxane, CpPOSS-norbornene 1-[2-(5-norbornen-2-yl)ethyl]-3,5,7,9,11,13,15-heptacyclopentylpentacyclo [9.5.1.1<sup>3,9</sup>.1<sup>5,11</sup>.1<sup>7,13</sup>]octasiloxane and trisilanol-PhPOSS 1,3,5,7,9,11,14-Hepta-phenyltricyclo[7.3.3.1<sup>5,11</sup>]heptasiloxane-endo-3,7,14-triol were purchased from Hybrid Plastics, and used as received. Norbornylethyl trichlorosilane was purchased from Oakwood Products and used as received. Reaction solvents, tetrahydrofuran and methylene chloride were purchased from Aldrich, and vacuum distilled over  $\text{CaH}_2$  prior to use. Grubbs second generation catalyst, (1,3-Bis(2,4,6-trimethylphenyl)-2-imidazolidinylidene)dichloro(phenylmethylene)(tricyclohexylphosphine)ruthenium, and ethyl vinyl ether were purchased from Aldrich, and used as received.

#### 4.3.2. Synthesis of PhPOSSnorbornene macromonomer

The synthesis of PhPOSS-norbornene, 1-[2-(5-norbornen-2-yl)ethyl]-3,5,7,9,11,13,15-heptaphenylpentacyclo [9.5.1.1<sup>3,9</sup>.1<sup>5,11</sup>.1<sup>7,13</sup>]octasiloxane was synthesized as described in chapter 2 from the reaction of trisilanol-PhPOSS and norbornylethyltrichlorosilane. In an example reaction, at room temperature, 1.07 mmol (1 g) of trisilanolPhenyl-POSS was stirred in 30 mL of THF in a 100 mL round bottom flask with a septum under a nitrogen atmosphere. Next, 1.09 mmol (0.280 g) of

norbornenylethyltrichlorosilane was added. Finally, 3.35 mmol (0.339 g) of triethylamine was added dropwise, clouding the reaction solution. The reaction was left to stir overnight. In the work-up, the solvent was removed in vacuo, and the products were redissolved in diethyl ether. The solution was filtered to remove the triethylamine-HCl salt, and precipitated into excess acetonitrile. Isolated yields were greater than 75%. NMR resonances:  $^1\text{H}$  NMR(400 MHz,  $\text{CD}_2\text{Cl}_2$ , ppm):  $\delta$  7.6-7.3 (Aromatic, 5H's), 6.04 (Olefin, 1H), 5.97 (endo), 5.82 (Olefin, 1H), 2.74 (1H), 2.68 (1H), 2.50 (endo), 2.01 (1H), 1.81(1H), 1.31 (1H), 1.28 (2H's), 1.10 (endo) 0.85 (2H's), 0.46 (2H's).  $^{13}\text{C}$  NMR:  $\delta$  133.1, 131.2, 129.7, 129.4, 126.8, 48.4, 43.8, 41.4, 40.8 (endo), 40.3, 31.2, 26.4, 9.6.  $^{29}\text{Si}$  NMR:  $\delta$  -78, -65.

#### 4.3.3. Polymerization

Polymerizations were set up in an inert atmosphere drybox. In a 25 mL reaction tube with a stir bar, solutions of 1.05 mL of 1,5-dimethyl-1,5-cyclooctadiene, POSS-norborenene macromonomer, and 10 mg of Grubbs second generation catalyst in methylene chloride were added. The tubes were sealed, taken out of the dry box, then heated and stirred in an oil bath at 55°C for 24 hours. The reaction was stopped by addition of a solution of a trace amount of ethyl vinyl ether in methylene chloride. The polymer was precipitated in methanol, and dried in vacuum oven at 40°C for 24 hours.

#### 4.3.4. Polymer characterization

$^1\text{H}$  NMR spectra were obtained in chloroform- $d$  or methylene chloride- $d_2$  on a Bruker DPX-300 FT-NMR spectrometer operating at 300 MHz.  $^{13}\text{C}$  NMR spectra were obtained at 90°C in tetrachloroethane- $d_2$  on a Bruker 400 FT-NMR spectrometer operating at 100 MHz. Gel permeation chromatography was obtained using a Polymer

Laboratories PL-GPC 50 Integrated GPC System, using THF as the mobile phase.

Molecular weights were calibrated against narrow molecular weight polystyrene standards.

## **DSC**

Differential scanning calorimetry was performed under a nitrogen atmosphere on a DuPont Instruments DSC 2910. Samples were cooled to -110°C and heated at a rate of 10°C/min. Data was obtained on second heating.

## **TGA**

Thermal gravimetric analysis was performed using a Mettler-Toledo TGA/SDTA851°. Samples were heated at a rate of 10°C/min up to 800°C in an air atmosphere.

## **WAXD**

Wide angle X-ray diffraction patterns were obtained on a PANalytical X'Pert PRO instrument in reflectance mode. Samples for this study were prepared by dissolving the polymer in a toluene solution, and casting it onto a glass slide. The solvent was allowed to evaporate over 2 hours. Residual solvent was driven off by heating the sample at 40°C for 24 hours in a vacuum oven.

## **4.4. Results and discussion**

### **4.4.1. Polymerization**

Reactions were performed at 55 °C, as trisubstitued cyclic olefins require elevated temperatures to produce polymer with sufficient molecular weight. The reactions were performed for 24 hours to promote cross-metathesis.<sup>6</sup> The polymerization reaction results are shown in table 4.1.



**Table 4.1.** Reaction results of DMCOD-POSS copolymers

Reaction ID	POSS in feed/wt%	POSS in polymer/mol% <sup>a</sup>	POSS in polymer/wt%	Mn(PDI) <sup>b</sup>	Percent Yield
DMCOD	---	---	---	87,000(1.85) <sup>c</sup>	57
Ibu11	7	1.8	11	58,000(2.21)	84
Ibu26	14	4.8	26	56,000(2.76)	64
Ibu36	25	7.5	36	42,000(1.81)	68
Ibu48	33	11.9	48	50,000(2.40) <sup>c</sup>	54
Ph10	8	1.4	10	38,000(1.81)	61
Ph18	14	2.6	18	56,000(1.93)	57
Ph35	25	6.3	35	39,000(2.54) <sup>c</sup>	45
Et14	11	2.8	14	49,000(2.41)	47
Et41	33	7.8	41	55,000(2.40) <sup>c</sup>	59
Cp16	13	2.3	16	139,000(1.58) <sup>c</sup>	86
Cp37	22	5.2	37	77,000(1.78) <sup>c</sup>	69
Cp46	36	7.4	46	47,000(2.05) <sup>c</sup>	35

<sup>a</sup> POSS incorporation determined by <sup>1</sup>H NMR.

<sup>b</sup> Molecular weight information determined by GPC in THF, calibrated from narrow polystyrene standards.

<sup>c</sup> Copolymers have 2-6% of a low molecular weight peak ( $M_n$ =2000-5000 g/mol)

The synthesized polymers had a range of molecular weights from 38,000 to 139,000 g/mol, with polydispersities ranging from 1.67 to 2.76. The GPC traces show unimodal molecular weight distributions for all polymers, except Ibu48 and Ibu36, which had a small, high molecular weight peak. This type of peak is also seen in the homopolymerization of POSS by ROMP. Several samples also show a low molecular weight peak, due to an oligomerization reaction that also occurs during some polymerizations. During the reactions, POSS monomer was either completely consumed, or removed in the precipitation step. POSS incorporation, as determined by <sup>1</sup>H NMR, could be controlled relatively well by varying the feed ratio.

The monomer sequence distribution in copolymers can be determined by NMR.

Blocky copolymers would be expected without cross metathesis reactions, as



POSSnorbornene reacts faster than DMCOD, due to the difficulty of ring-opening trisubstituted olefins. In this copolymer system, the DMCOD homopolymer has olefinic resonance at chemical shifts of  $\delta$  5.13 and 5.11 ppm, corresponding to cis and trans isomers. Poly(POSSnorbornene) homopolymers have olefinic resonances with chemical shifts at  $\delta$  5.35 and 5.25 ppm.

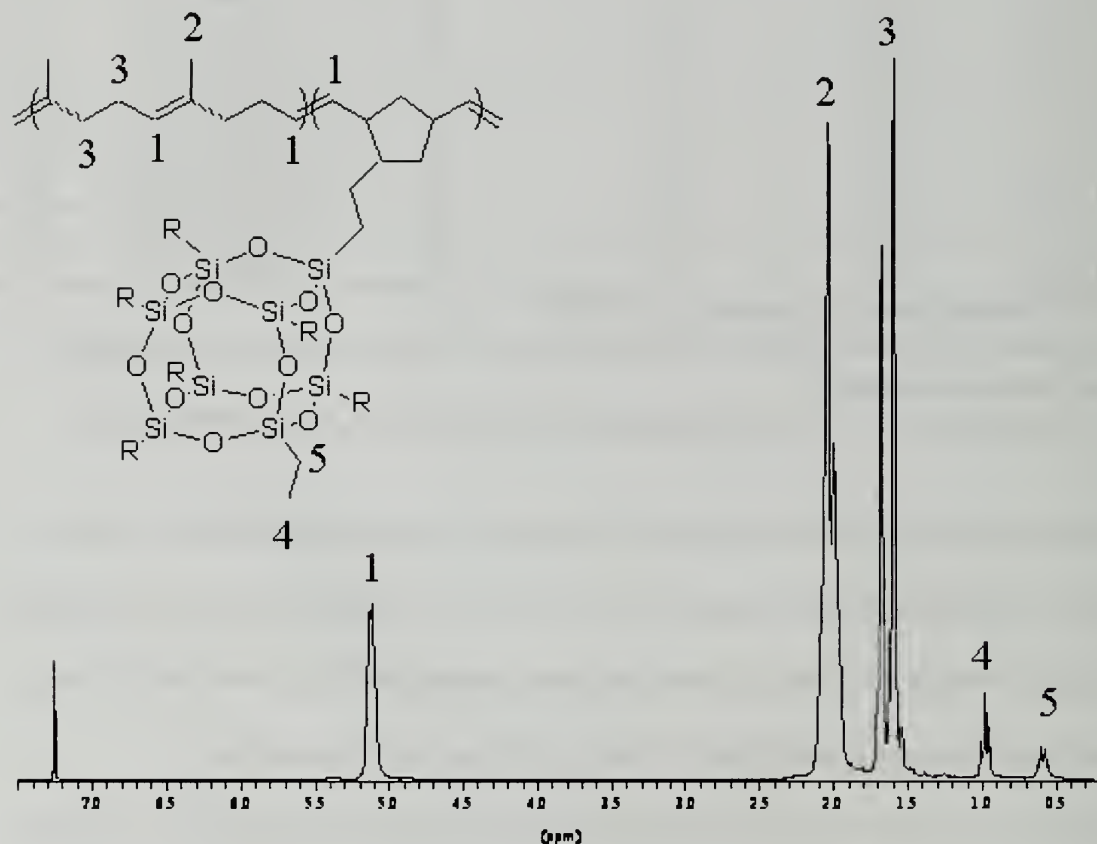


**Figure 4.1.**  $^1\text{H}$  NMR of DMCOD-EtPOSS copolymer

Copolymer samples have resonances slightly downfield from the main olefinic resonances, as shown in figure 4.2. This appears to be more of a peak tailing than well defined peaks. These peaks were also seen in the DMCOD homopolymer. These peaks could be a combination of olefinic peaks from POSS-POSS sequences or POSS-DMCOD

sequences. Also, due to the small percent of olefinic POSS protons, it is very difficult to ascertain any POSS-POSS units, especially using  $^{13}\text{C}$  NMR.

#### 4.4.2. Thermal characterization

The results of DSC and TGA studies are shown in Table 4.2.

**Table 4.2.** Thermal Characterization DMCOD-POSS Copolymers

ID	Wt% POSS	$T_g^a$ ( $^{\circ}\text{C}$ )	2% Decomp. Temp. ( $^{\circ}\text{C}$ )	Char Yield	Theo. Char Yield <sup>b</sup>
DMCOD	---	-66	203	0	---
Ibu11	11	-56	305	4	5
Ibu26	26	-56	307	10	12
Ibu36	36	---	304	7	16
Ibu48	48	-66	286	18	21
Ph10	10	-59	284	6	4
Ph18	18	-59	294	10	7
Ph35	35	-66	228	14	11
Cp13	13	-61	203	4	4
Cp37	37	-56	177	7	13
Cp46	46	---	180	18	16
Et14	14	-57	302	7	8
Et41	41	-66	203	5	18

<sup>a</sup>Glass transition temperature determined by DSC on second heating with a heating rate of  $10^{\circ}\text{C}/\text{min}$

<sup>b</sup>Theoretical char yield was determined assuming a complete conversion of POSS to  $\text{SiO}_2$

The thermal data show interesting glass transition temperature results. Based on literature precedence, the  $T_g$  is known to increase with increasing POSS loading due to the decrease of chain motion by incorporating a large, bulky POSS group. The  $T_g$  of the reference homopolymer is  $-66^{\circ}\text{C}$ . In the copolymers, there are two cases. First, some of the polymers show an increase in  $T_g$ , ranging from  $-62$  to  $-56^{\circ}\text{C}$ . Others show a  $T_g$  of  $-66^{\circ}\text{C}$ , the same as the homopolymer. In AB block copolymers, a  $T_g$  of the A block, the B block, and an intermediate  $T_g$  is usually observed.<sup>25</sup> One possible explanation for the  $T_g$  data of DMCOD-POSS copolymers is that copolymers with a  $-66^{\circ}\text{C}$   $T_g$  have blocky-like structures, where the others are random copolymers. The DSC traces show only a  $T_g$  on

second heating, as there are no POSS melting peaks. POSS homopolymers or block copolymers rarely show melting temperatures or glass transition temperatures in literature reports. The DMCOD-POSS  $T_g$  data could be attributed to the extent of cross metathesis reactions in the copolymers.

Decomposition temperatures and char yield of the copolymers were determined by TGA studies. The general trend in literature reports shows an increase in decomposition temperature by the incorporation of POSS into polymers. In DMCOD-POSS copolymers, the DMCOD homopolymer shows a 2% decomposition temperature of 203°C. The IbuPOSS copolymers show a significant increase in 2% decomposition temperature, with values over 300°C with all samples except Ibu48. The Ibu48 sample has a low molecular weight component, which may decompose before the high molecular weight polymer. The PhPOSS copolymers show similar results, with 2% decomposition temperatures near 290°C, except for Ph35, which has a lower value of 228°C. All CpPOSS copolymers have relatively low 2% decomposition temperatures, and only one EtPOSS copolymer shows a high 2% decomposition temperature. This trend is due to the nature of the copolymer, as all the samples with relatively low 2% decomposition temperatures have a low molecular weight peak. This part of the sample should decompose before the rest of the sample. Also, EtPOSS copolymers are expected to have low decomposition temperatures, as EtPOSSnorbornene has a 2% decomposition temperature of 193°C.

When POSS decomposes under air, it undergoes an oxidative transformation from  $\text{SiO}_{1.5}$  to  $\text{SiO}_2$  (silica). When this occurs, significant char yields are seen in TGA. Char yields of DMCOD-POSS copolymers are expected to show char resulting only from

silica formation, as the DMCOD completely decomposes. Also, a theoretical char yield can be calculated which assumes a complete conversion of POSS to silica. The DMCOD-POSS copolymers generally show a lower char yield than expected, indicating an incomplete conversion to silica. The PhPOSS copolymers, however, show a higher char yield than expected. This is due to the formation of carbonaceous char from the phenyl periphery.

#### 4.4.3. Wide angle X-ray studies

Wide angle X-ray diffraction is a common method to determine aggregation of POSS in copolymers. Diffraction patterns of the copolymers are shown in Figures 4.2-4.5.

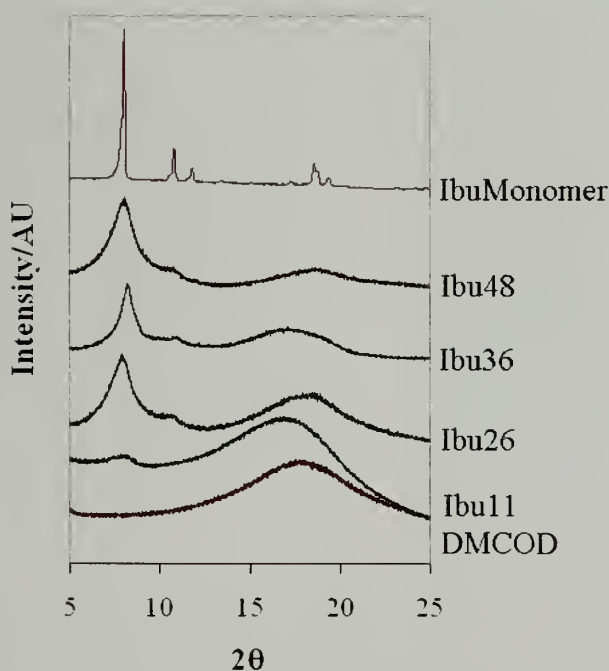


**Figure 4.2.** WAXD patterns for DMCOD-IbuPOSS copolymers.



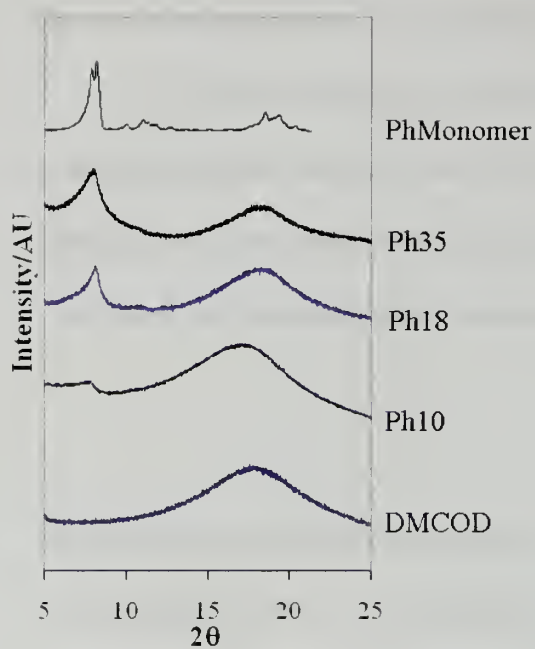


**Figure 4.3.** WAXD patterns for DMCOD-PhPOSS copolymers.

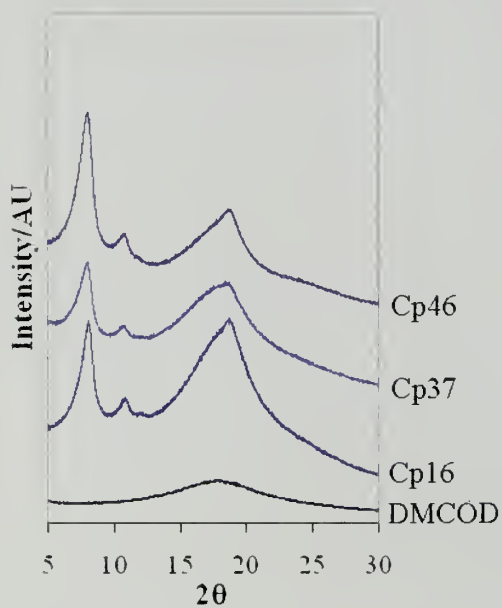


**Figure 4.4.** WAXD patterns for DMCOD-CpPOSS copolymers.

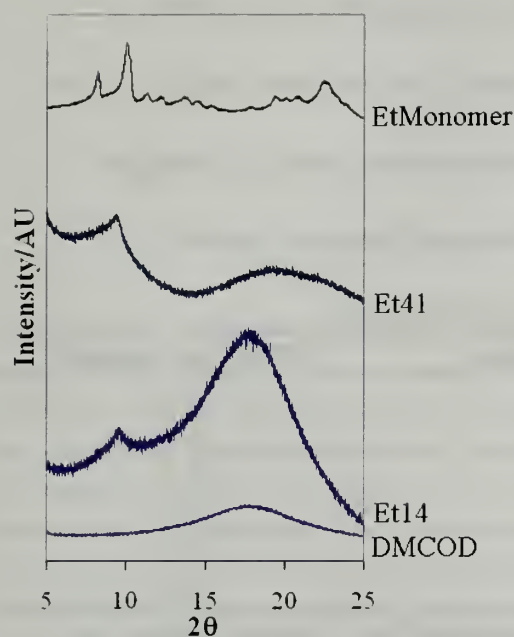


**Figure 4.5.** WAXD patterns for DMCOD-EtPOSS copolymers.

The DMCOD homopolymer is completely amorphous, with an amorphous halo centered at a  $2\theta$  value of 18. POSS monomers show a sharp diffraction peak at a  $2\theta$  value around 8. With the isobutyl, phenyl, and cyclopentyl peripheries, sharp diffraction peaks are seen, which increase in intensity with an increase in POSS incorporation. This was expected with the cyclic peripheries, as they have less favorable interactions with a linear hydrocarbon polymer. The aggregation of the isobutyl peripheries were unexpected, as IbuPOSS was shown to disperse in EPPOSS polymers. The EtPOSS copolymers also show strong aggregation peaks. The diffraction peaks, however, lack the strong intensity seen with the other peripheries. These WAXD studies show POSS aggregates with each periphery. This differs from the EPPOSS polymers, as POSS disperses in the EP matrix with the ethyl and isobutyl peripheries. This is due to the different chemical nature of the polymeric backbone, as the DMCOD backbone contains main chain unsaturation.

The domain sizes of the POSS aggregates were estimated using Scherer's equation. In Scherer's equation,  $L=0.9\lambda/\beta\cos\theta$ , where  $L$  is the domain length,  $\lambda$  is the wavelength of the X-ray,  $\beta$  is the peak width at half maximum, and  $\theta$  is the angle. It is assumed that POSS has a 1.5nm diameter. The results are shown in Table 4.3.

**Table 4.3.** POSS domain sizes in DMCOD-POSS Copolymers

Sample	Domain Size(nm)	~POSS per domain <sup>a</sup>
Ph35	5.4	3-4
Ph18	8.3	5-6
Ibu48	5.0	3-4
Ibu26	6.9	4-5
Cp37	5.2	4-5
Cp13	7.7	5-6

<sup>a</sup> Number of POSS per domain was estimated by dividing the estimated domain size by 1.5, the approximate diameter of POSS.

This method simply estimates the longest domain size, with the number of POSS molecules it takes to fill a domain size this long. POSS aggregates could also form in another direction, with the third dimension having either one or two POSS cubes. Therefore, the number of POSS molecules per domains is probably larger than this estimated value. These POSS domain sizes are on the same length as in the ethylene-propylene-POSS and poly(octafluoropentyl acrylate)-POSS polymers. The POSS domain sizes are slightly larger with small POSS loadings. This could be due to the decreased mobility of POSS copolymers at higher loadings, making it more difficult for POSS domains to form.

#### 4.5. Conclusions

The effect of the POSS peripheral group on the aggregation of POSS in a model isoprene-like copolymer was studied. Copolymers were synthesized through the ring-opening metathesis polymerization of dimethylcyclooctadiene and POSSnorbornene

using Grubbs second generation catalyst, altering the POSS periphery to include isobutyl, cyclopentyl, phenyl, and ethyl groups. The synthesized copolymers had high molecular weights and moderate polydispersities. Differential scanning calorimetry studies suggest some of the polymers were random and some of the copolymers were blocky, as the  $T_g$  of the random copolymers were higher than the homopolymer and the same with blocky copolymers. Wide angle X-ray diffraction studies of these copolymer show relatively sharp POSS diffraction peaks with all POSS peripheries, indicating POSS aggregation with each periphery. Thermal studies of the copolymers show a significant increase in the 2% decomposition temperature of copolymers as compared to the DMCOD copolymer, except for the samples containing a small, low molecular weight peak.

#### 4.6. References

- (1) Iacono, S.; Ligon Jr., S.; Mabry, J.; Vij, A.; Smith Jr. D.; *Polymer Preprints* **2005**, *46*, 639-640.
- (2) Fu, B., Lee, A., Haddad, T. *Macromolecules* **2004**, *37*, 5211-5218.
- (3) Drazkowski, D., Lee, A., Haddad, T., and Cookson, D. *Macromolecules* **2006**, *39*, 1854-1863.
- (4) Drazkowski, D., Lee, A., Haddad, T. *Macromolecules* **2007**, *40*, 2798-2805.
- (5) Waddon, A., Zheng, L., Farris, R., and Coughlin, E.B. *Nano Letters* **2002**, *2*, 1149-1155.
- (6) Zheng, L., Hong, S., Cardoen, G., Burgaz, E., Gido, S., and Coughlin, E.B. *Macromolecules* **2004**, *37*, 8606-8611.
- (7) Bielawski, C. and Grubbs, R. *Angewandte Chemie, International Edition* **2000**, *39*, 2903-2906.

## CHAPTER 5

### SUMMARY AND FUTURE WORK

#### 5.1. Dissertation summary

The addition of POSS into polymers has previously been shown to impart the unique properties of POSS, such as oxidative resistance, thermal stability, insulation properties, high gas permeabilities, and mechanical strength, into novel hybrid copolymers.<sup>1-17</sup> One important consequence of these unique properties is the propensity of POSS to aggregate in copolymers. The POSS-POSS interactions are akin to secondary interactions, such as hydrogen bonding and metal-ion interactions that are important to the physical structure of polymers, copolymers and composites and provide excellent material properties to various polymer systems.<sup>18</sup> Thermoplastic elastomers are one specific type of material that takes advantages of secondary forces to provide physical crosslinks, which give elastomers their strong, elastic properties. Prior to the research conducted in this thesis, there had been no studies on POSS aggregates acting as physical crosslinks for thermoplastic elastomers. Section 5.3 summarizes these studies and conclusions of this research.

The physical properties of POSS is effected by the periphery groups, as shown by the change in the melting points and the decomposition temperatures by altering the POSS periphery.<sup>19</sup> Also, most studies of POSS copolymers have utilized only one or two different peripheries. Therefore, an extended study of the physical changes that occur in copolymers containing POSS while varying the periphery will provide useful insight into the design of novel POSS-polymer systems in the future. Along with an expanded understanding of POSS, this study will be useful for choosing a specific periphery for a



targeted application. These studies are outlined in Section 5.2. It is important to note, also, that these studies were performed primarily on random (perhaps not the DMCOD-POSS copolymers) copolymers. These polymerizations are much less arduous than those involved in the synthesis of diblock or triblock copolymers, which are typically utilized as thermoplastic elastomers.

## **5.2. POSS peripheral effect on aggregation in copolymers**

The aggregation of POSS is shown to be dependent not only on the POSS periphery, but also on the nature of the polymer matrix. In the ethylene-propylene-POSS terpolymers, the saturated hydrocarbon ethylene-propylene chain interacts positively with both the IbuPOSS periphery and the EtPOSS periphery, and either disperse in the polymer matrix or forms very small aggregates. When changing the POSS periphery to a phenyl group, POSS was observed to aggregate in the EP polymer matrix. The length of these aggregates, as determined by Scherer's equation, ranged from 5.3-9.5 nm. The domain sizes could be increased by thermally annealing the polymer films.

The effect of altering the polymer chain on the aggregation of POSS was studied next. The polymer was changed to a fluorinated chain. Fluoropolymers have repulsive chains due to their chemical nature. These polymers were expected to drive POSS aggregation, as the hydrocarbon peripheries are repelled by the fluorinated chains. In these octafluoropentyl acrylate-POSS copolymers, POSS was shown to aggregate with the phenyl and isobutyl peripheries, but not with the isooctyl periphery. The isooctyl periphery did not aggregate due the long isooctyl chains, which do not allow the POSS cubes to form crystal structures with the monomer. Therefore, it was not expected to observe aggregation with these copolymers. The length of the POSS aggregates were

similar to those of the EPPOSS polymers, except for POFPA-Ibu36, which had a 15 nm domain length. These studies show the polymer chain can be altered to drive POSS aggregation.

The third polymer chain used in this study was a copolymer of POSS with DMCOD, akin to 1,4-polyisoprene. This chain varies from the ethylene-propylene chain, as it has unsaturation along the backbone. This unsaturation had an impact on POSS aggregation, as studies showed POSS aggregation with the isobutyl, phenyl, ethyl, and cyclopentyl peripheries. The size of these aggregates was also on the same scale as the EPPOSS polymers. Overall, these studies show the aggregation of POSS in various polymers is dependent both on the POSS periphery and the nature of the polymer backbone.

### **5.3. Mechanical studies**

In order to study the applicability of POSS aggregates as a physical crosslink for thermoplastic elastomers, a strong polymeric system is needed, such as the EP backbone. The only EPPOSS polymers with sufficient strength for mechanical studies were those with the phenyl periphery, as this was the only periphery to show POSS aggregates. These materials were studied by DMA, rheology, and tensile studies. Studies of the EPhPOSS polymers by DMA show an increase in the rubbery plateau modulus by addition of POSS, as compared to the EP parent polymer, which has a limited rubbery plateau region. Also, the modulus increases with increasing POSS incorporation. This shows that the POSS particles pendent to the polymer chain interact in a manner to create physical crosslinks, which are sufficiently strong to create an extended rubbery plateau region.

Rheological studies were performed to compare the EPhPOSS polymers to the EPIbuPOSS and EPetPOSS copolymer, which did not have sufficient mechanical strength for DMA studies. Frequency sweeps were also performed to probe the frequency dependence of the materials. Comparing the EPhPOSS samples (POSS aggregation) to the EPIbuPOSS samples (POSS dispersion), the EPhPOSS samples have a much higher modulus, especially at increased temperatures. Looking specifically at the frequency sweeps of EPh30 and EPIbu30 at 100°C (Figures 2.11 and 2.12), it is apparent that EPh30 remains a solid at low frequencies (long times), and EPIbu30 acts as a liquid. These studies display the importance of POSS aggregation to obtain strong mechanical properties in elastomers.

Tensile tests were also performed on EPhPOSS polymers. These polymers display an elongation at break between 450 and 720 %, which is on the order to typical elastomers.<sup>20</sup> The EP parent polymer had a value of 170%, which is much less than the EPhPOSS polymers. The elastic modulus of the polymers increased with increasing POSS loading, with a maximum value of 19.4 MPa for EPh36, which is on the order of thermoplastic elastomers and some thermosets.<sup>20</sup> The elastic modulus of the EP parent polymer lies between Ph21 and Ph36, as it is a semi-crystalline material, which gives the polymer its relatively high strength. These elastomers also show a Payne effect, in which the low amplitude modulus is higher than the high amplitude modulus. This is commonly found in elastomers containing fillers. Physically, this effect could be due to the breaking of a few POSS particles from POSS aggregates, thus decreasing either the size or quantity of crosslinking sites. This results in a decrease of the modulus.

Cyclic tensile tests on the EPPOSS elastomers further show the unique properties of the material. Each material shows the Mullins effect, where upon relaxation of an initial stress, the material deforms. Next, upon stretching of the sample to the same elongation, followed by a relaxation cycle, the material shows little deformation from the previous cycle. This is commonly found in elastomers with positively enhancing fillers.<sup>19</sup> These materials show how POSS aggregates act as physical crosslinks, and can be utilized as thermoplastic elastomers.

#### **5.4. Future work**

The current work displays the applicability of POSS to act as a physical crosslink for thermoplastic elastomers. There are several follow-up studies that could be done to further explore properties of these polymers, and to study new POSS containing polymers based on the current findings.

##### **5.4.1. WAXD studies**

There are several WAXD studies that could be performed to further study the ethylene-propylene-POSS and octafluoropentyl acrylate-POSS polymers. Diffraction patterns of each polymer should be obtained at various temperatures in order to study the domain size changes at increased temperatures and to observe the temperature range in which POSS aggregates disperse. This temperature can be determined by observing the broadening of the POSS diffraction peaks as the temperature is increased.

Another WAXD study would ascertain the increase in modulus seen in the EPPH36 DMA studies. This can be done by observing WAXD patterns of thin films samples when they are stretched. Patterns should also be obtained at varying temperatures while heating the samples. By comparing the two, the increase and



modulus can be determined to be thermal or strain based, or the combination of both.

This study will also show if the POSS domain sizes increase when stretch the sample, heating the sample, or heating and stretching the sample.

#### **5.4.2. Mechanical properties**

The mechanical properties can be further studied by tensile studies with the EPPOSS polymers. The elastic modulus and the elongation of break of EPIbuPOSS, EPETPOSS, and an amorphous ethylene-propylene polymer would provide more information about reinforcement effects of aggregated POSS elastomers versus polymers with POSS dispersion. Also, performing these tensile tests on annealed EPhPOSS films would allow for the study of the tensile properties of polymers with slightly larger POSS domain sizes. Further cyclic tests with the EPhPOSS elastomers would provide more information about the elasticity of these materials. These cycles could be expanded to 400%, 500%, 600%, and 700% elongations, or until the samples break. Performing these tests on annealed samples would also provide more information on these polymers with larger POSS domain sizes.

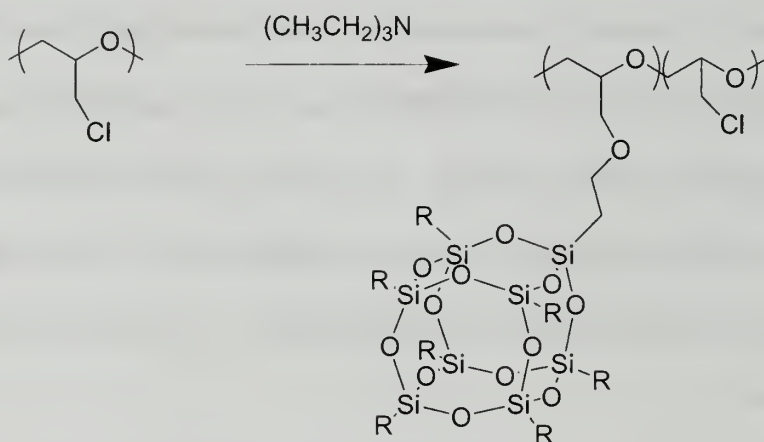
The rheological tests on the poly(octafluoropentylacrylate)-POSS copolymers can be continued to include copolymers with higher POSS incorporation. The POFPA-Ibu10 sample behaves more as a liquid than a solid. By studying the material at higher POSS incorporation, the minimum IbuPOSS loading required for elastomers can be determined. Also, rheological tests on IbuPOSS and PhPOSS copolymers can be used to study the shear modulus at increasing POSS loadings.



### 5.4.3. Synthesis of novel POSS containing polymers

Although the EPPOSS polymers show strong mechanical properties, the applicability of POSS to act as a physical crosslink for thermoplastic elastomers should be studied in different polymer systems. In an ideal polymer system, POSS should be grafted to a polymer, as this allows the only change in polymer system to be the POSS incorporation. This is advantageous over ethylene-propylene-POSS elastomers, as the ethylene to propylene ratio varies in these polymers. Different POSS peripheries can also be studied in such polymer systems.

One such polymer system is poly(epichlorohydrin) elastomers.



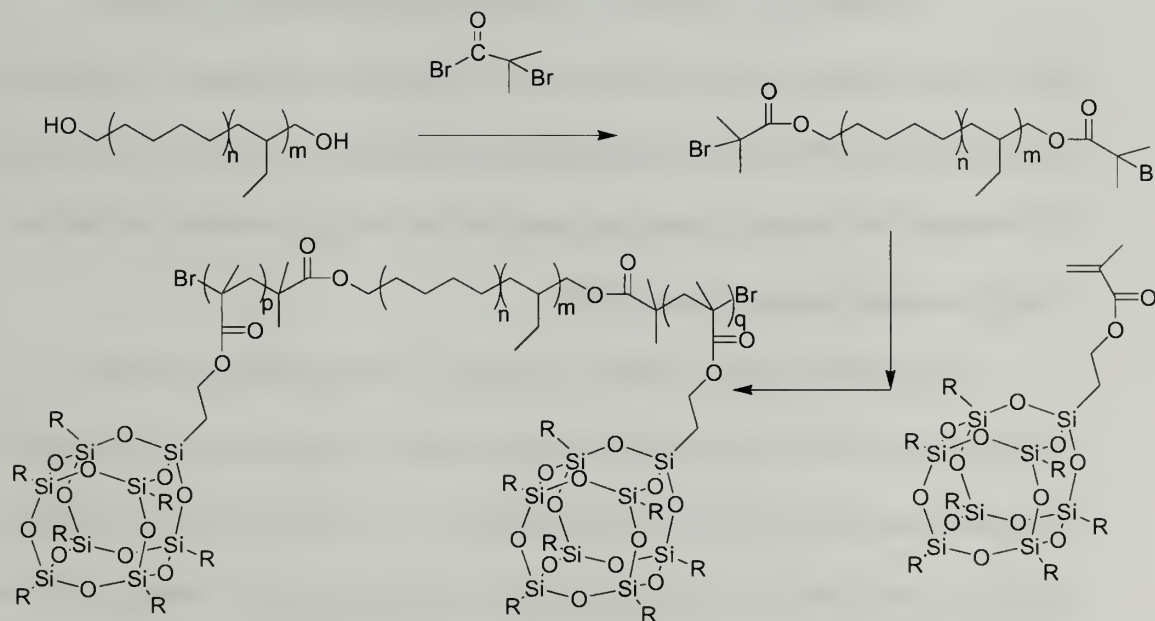
**Scheme 5.1.** Synthesis of poly(epichlorohydrin)-POSS elastomers

Poly(epichlorohydrin) elastomers can be synthesized in large quantities, and can be chemically altered through reaction with an alcohol or an amine. A proposed reaction scheme is shown in scheme 5.1, in which POSS, with an alcohol functional group, is grafted onto the polymer. The POSS periphery can be altered to include cyclic and straight or branched chained hydrocarbon peripheries. Copolymer studies could follow the same format as with the EPPOSS elastomers, determining both the effect of the POSS

periphery on aggregation and the applicability of POSS as a crosslink for thermoplastic elastomers..

#### 5.4.4. POSS triblock copolymers

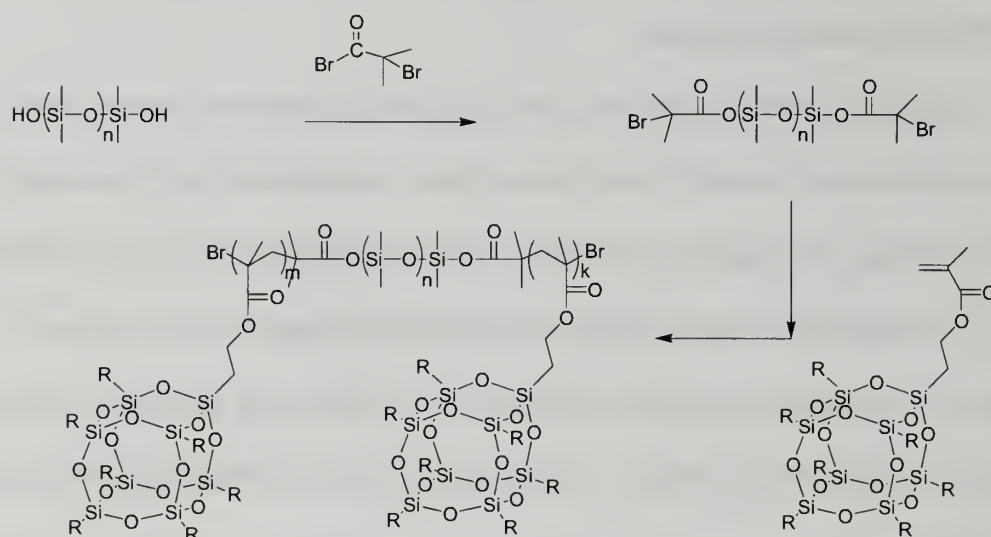
During the current studies, POSS was randomly incorporated into polymers. These polymers show relatively small domain sizes, with domain lengths generally on the order of 5-10 nm. By lengthening POSS domain sizes, the polymer properties should change. One method to study the effect of larger POSS domain sizes on polymer properties is to synthesize triblock copolymers, with POSS as the hard block, and an elastomeric block as the soft block. Two potential reaction schemes are shown in scheme 5.2 and 5.3 below.



**Scheme 5.2.** Synthesis of POSS-hBD-POSS triblock copolymers

In scheme 5.2, POSSmethacrylate is attached to a polymer chain by atom transfer radical polymerization. The polymer choice is dihydroxy terminated polybutadiene with a high enough amount of 1,2-butadiene to afford an amorphous material. This polymer is then hydrogenated (hBD) to give better material properties. Another polymer soft block

to use is dihydroxy terminated polydimethylsiloxane (PDMS), which is commercially available, or can be synthesized by living anionic polymerization techniques.<sup>18</sup>



**Scheme 5.3.** Synthesis of POSS-PDMS-POSS block copolymers

Both of these reaction schemes offer novel POSS triblock copolymers. The PDMS reaction scheme offers a more straightforward synthesis of the soft block. However, the POSS-hBD-POSS triblock copolymer should offer a stronger material, as hBD has stronger material properties than PDMS.

The synthesis of these triblock copolymers would permit several future investigations. First, the study of the change in POSS domain sizes with different POSS incorporations and peripheries can be performed. In the POSS-hBD-POSS triblocks, isobutyl and ethyl POSS peripheries would be expected to interact with the hBD block. On the other hand, any cyclic periphery would be expected to show strong POSS aggregation, due to unfavorable interactions between the POSS periphery and the hBD block. With the PDMS midblock, it is expected that POSS will aggregate with all the peripheries, due to unfavorable interactions between component blocks.

The change in the volume fraction of POSS will allow for the formation of lamellae, cylindrical, and spherical morphologies, which will have an impact on material properties. These materials could be studied and compared to the random copolymers studied during the current thesis research, comparing these relative ease of synthesis of the random copolymer versus potentially stronger material properties of the triblock copolymers.

## 5.5. References

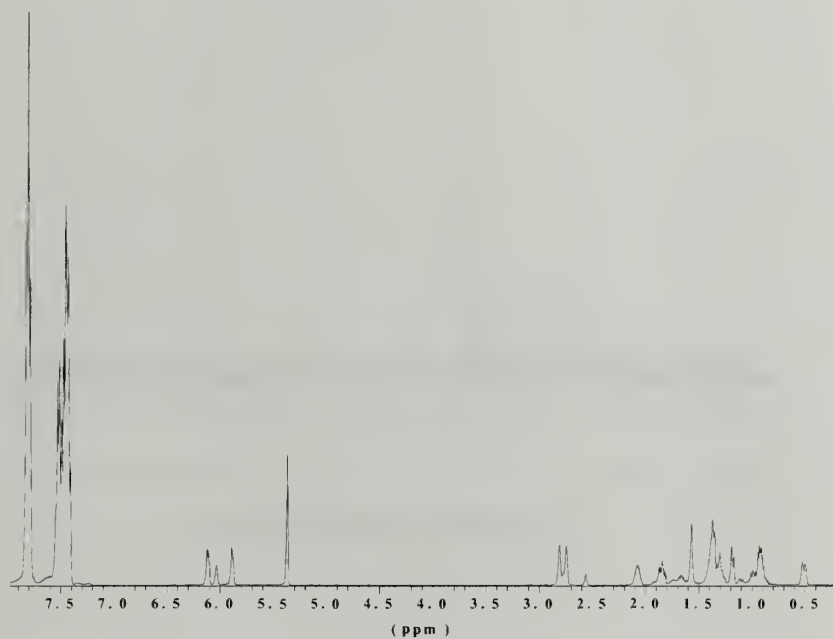
- (1) Joshi, M. and Butola, B. *Journal of Macromolecular Science Part C-Polymer Reviews* **2004**, 44, 389-410.
- (2) Li, G., Wang, L., Ni, H., and Pittman Jr., C. *Journal of Inorganic and Organometallic Polymers* **2001**, 11, 123-154.
- (3) Phillips, S., Haddad, T., and Tomczak, S. *Current Opinion in Solid State and Materials Science* **2004**, 8, 21-29.
- (4) Haddad, T., Viers, B., and Phillips, S. *Journal of Inorganic and Organometallic Polymers* **2001**, 11, 155-164.
- (5) Zheng, L., Kasi, R., Farris, R., and Coughlin, E.B. *Journal of Polymer Science Part A: Polymer Chemistry* **2002**, 40, 885-891.
- (6) Lichtenhan, Y., Otonari, Y., and Carr, M. *Macromolecules* **1995**, 28, 8435-8437.
- (7) Kopesky, E., Haddad, T., Cohen, R., and McKinley, G. *Macromolecules* **2004**, 37, 8993-9004.
- (8) Zheng, L., Farris, R., and Coughlin, E.B. *Macromolecules* **2001**, 34, 8034-8039.
- (9) Zheng, L., Farris, R., and Coughlin, E.B. *Journal of Polymer Science Part A: Polymer Chemistry* **2001**, 39, 2920-2928.
- (10) Waddon, A., Zheng, L., Farris, R., and Coughlin, E.B. *Nano Letters* **2002**, 2, 1149-1155.
- (11) Tsuchida, A., Bolln, C., Sernetz, F., Frey, H., and Mülhaupt R. *Macromolecules*, **1997**, 30, 2818-2831.



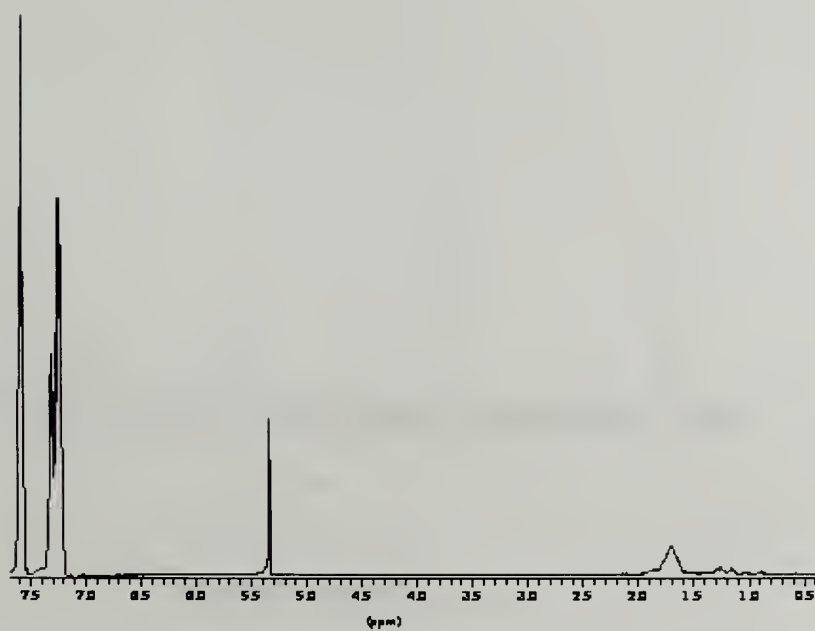
- (12) Leu, C., Reddy, G., Wei, K., and Shu, C. *Chemistry of Materials* **2003**, *15*, 2261-2265.
- (13) Joen, H., Mather, P., and Haddad, T. *Polymer International* **2000**, *49*, 453-457.
- (14) Fu, B., Lee, A., and Haddad, T. *Macromolecules* **2004**, *37*, 5211-5218.
- (15) Drzakowski, D., Lee, A., Haddad, T., and Cookson, D. *Macromolecules* **2006**, *39*, 1854-1863.
- (16) Drzakowski, D., Lee, A., Haddad, T. *Macromolecules* **2007**, *40*, 2798-2805.
- (17) Constable, G., Lesser, A., and Coughlin, E.B. *Macromolecules* **2004**, *37*, 1276-1782.
- (18) Odian, G. *Principles of Polymerization*, 3<sup>rd</sup> Ed. Wiley Interscience & Sons, Inc. New York, 1991.
- (19) Bolln, C.; Tsuchida, A.; Frey, H.; and Mülhaupt, R. *Chemistry of Materials* **1997**, *2*, 1475-1479.
- (20) Web of Materials <http://www.webmat.com>
- (21) Zheng, L., Hong, S., Cardoen, G., Burgaz, E., Gido, S., Coughlin, E.B. *Macromolecules* **2004**, *37*, 8606-8611.

## Appendices

### Appendix A

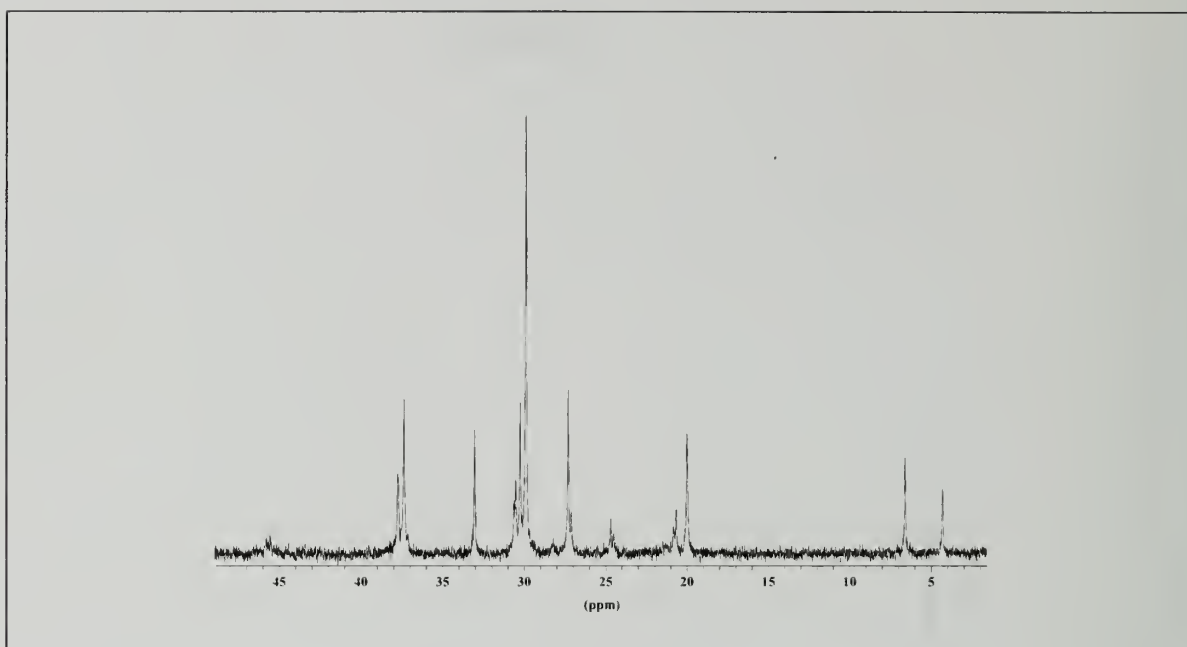


$^1\text{H}$  NMR of PhPOSSnorbornene monomer

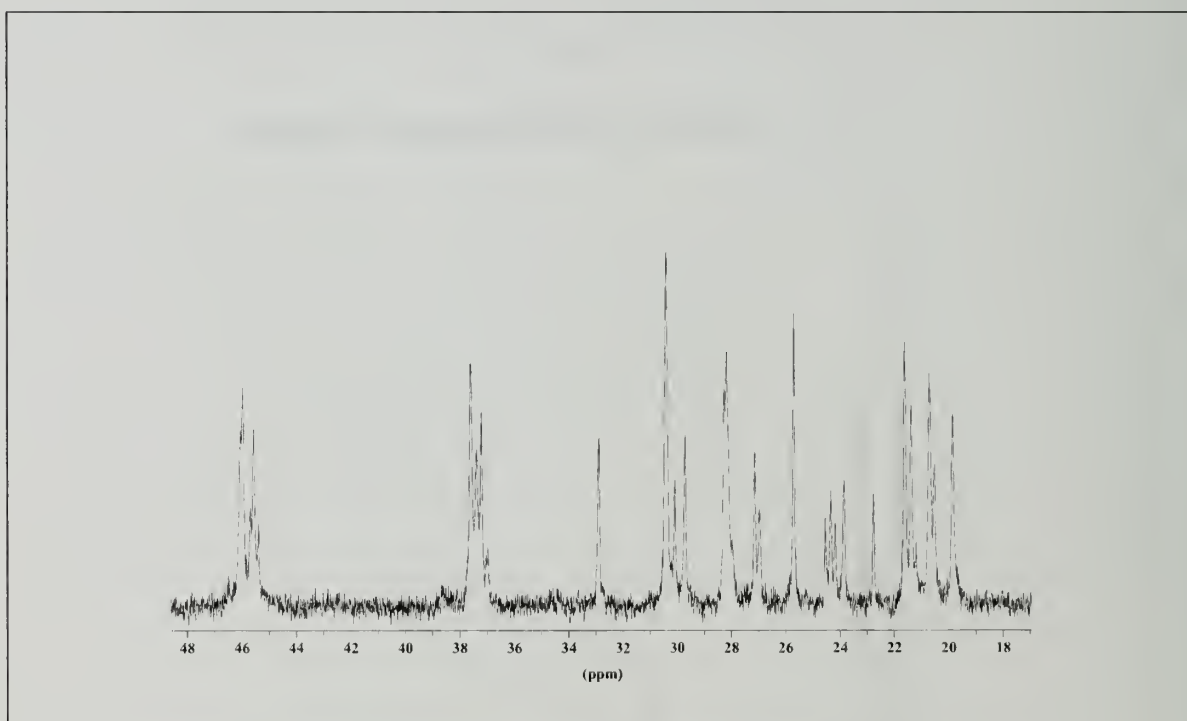


$^1\text{H}$  NMR of T<sub>7</sub> PhPOSStrisilanol

## Appendix B

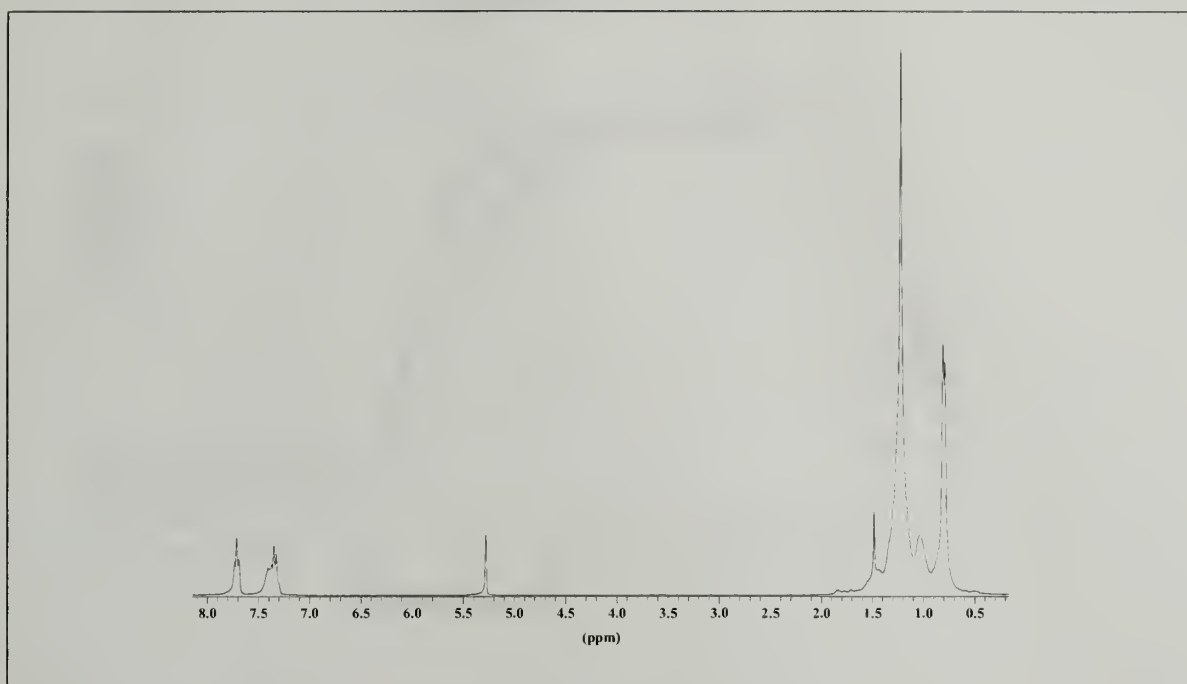


$^{13}\text{C}$  NMR of EPet30 Polymer

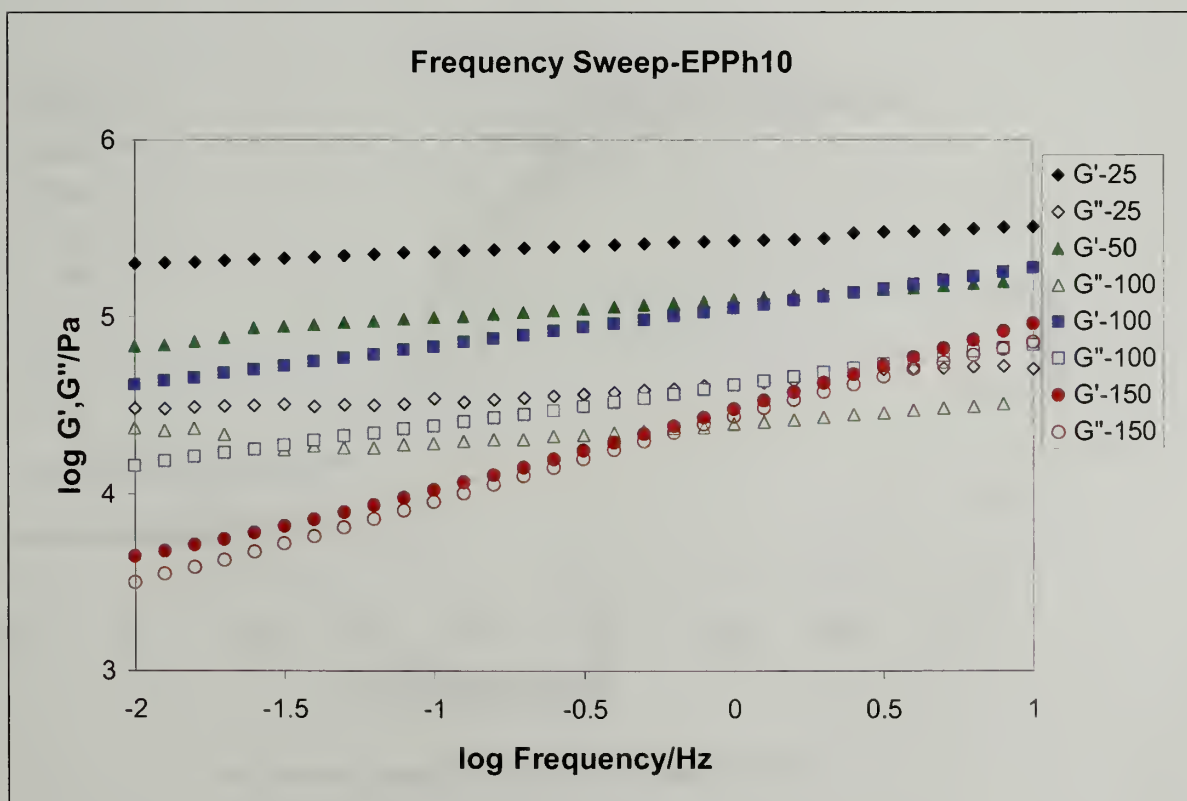


$^{13}\text{C}$  NMR of EPibu16

## Appendix C



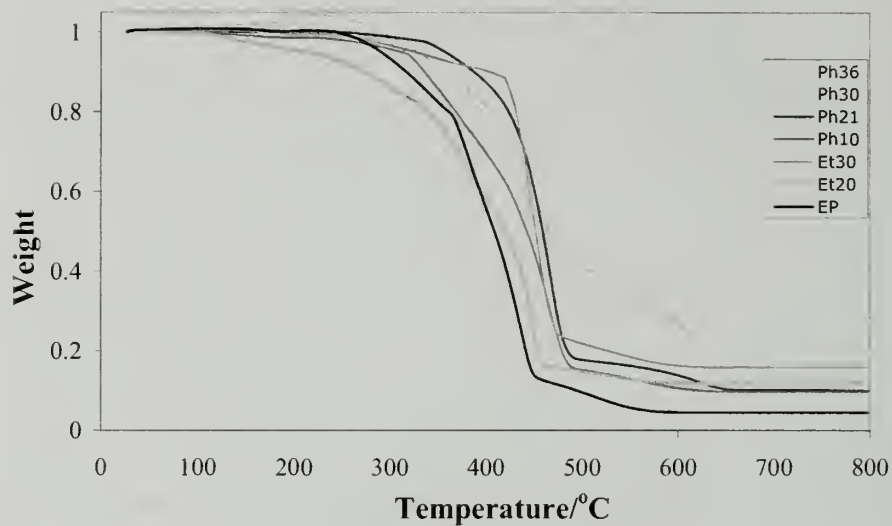
$^1\text{H}$  NMR of EPh36 Polymer



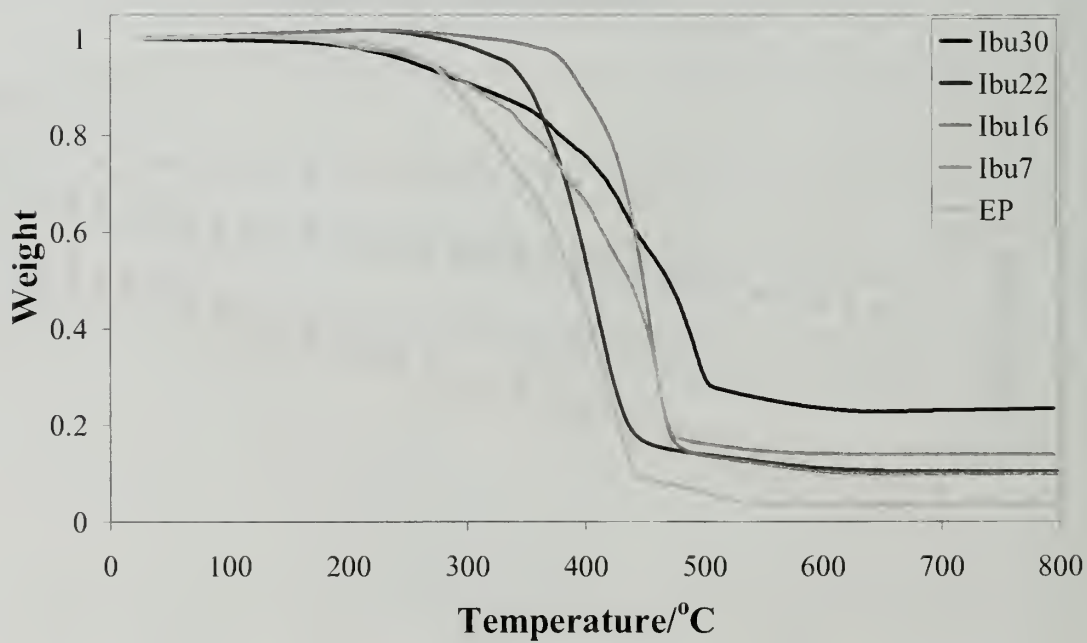
Frequency sweeps of EPh10 at varying temperatures, from 25°C to 250°C



## Appendix D

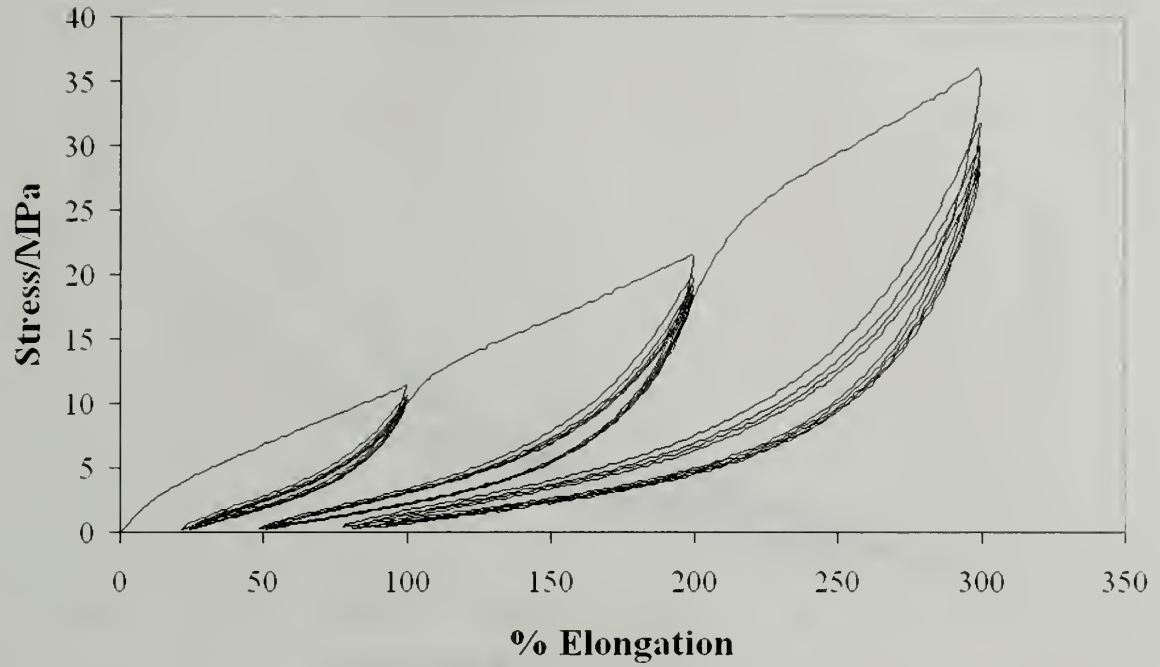


TGA Plot of EPPhPOSS and EtPOSS Copolymers in Air.

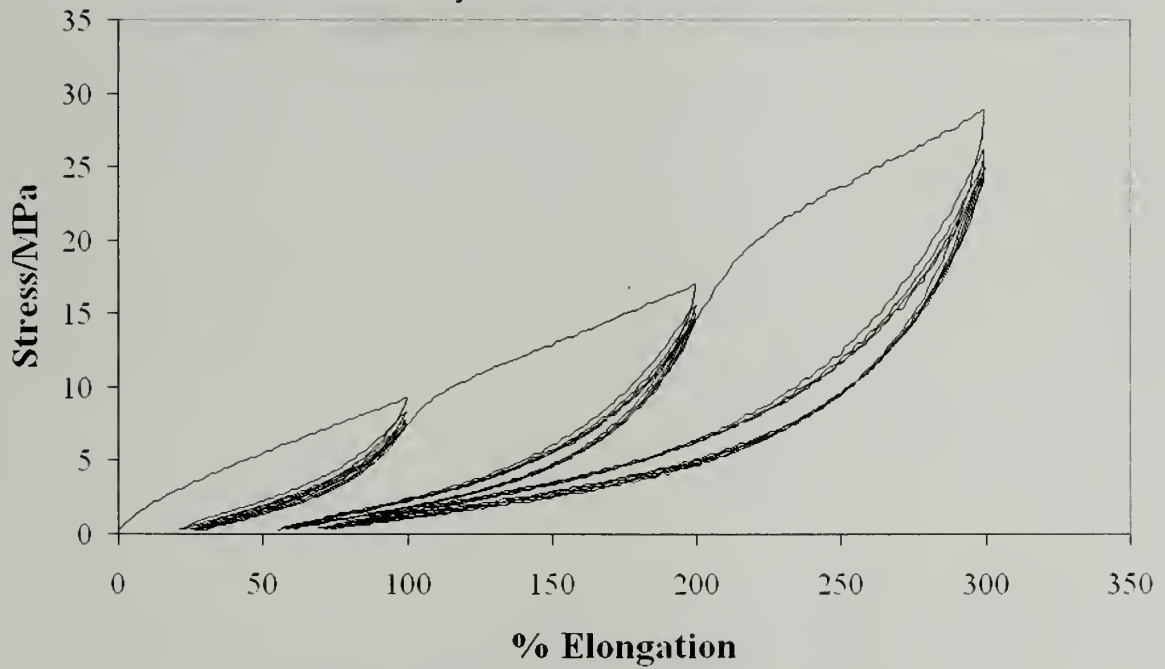


TGA Plot of EPIbuPOSS Copolymers in Air.

# Appendix E

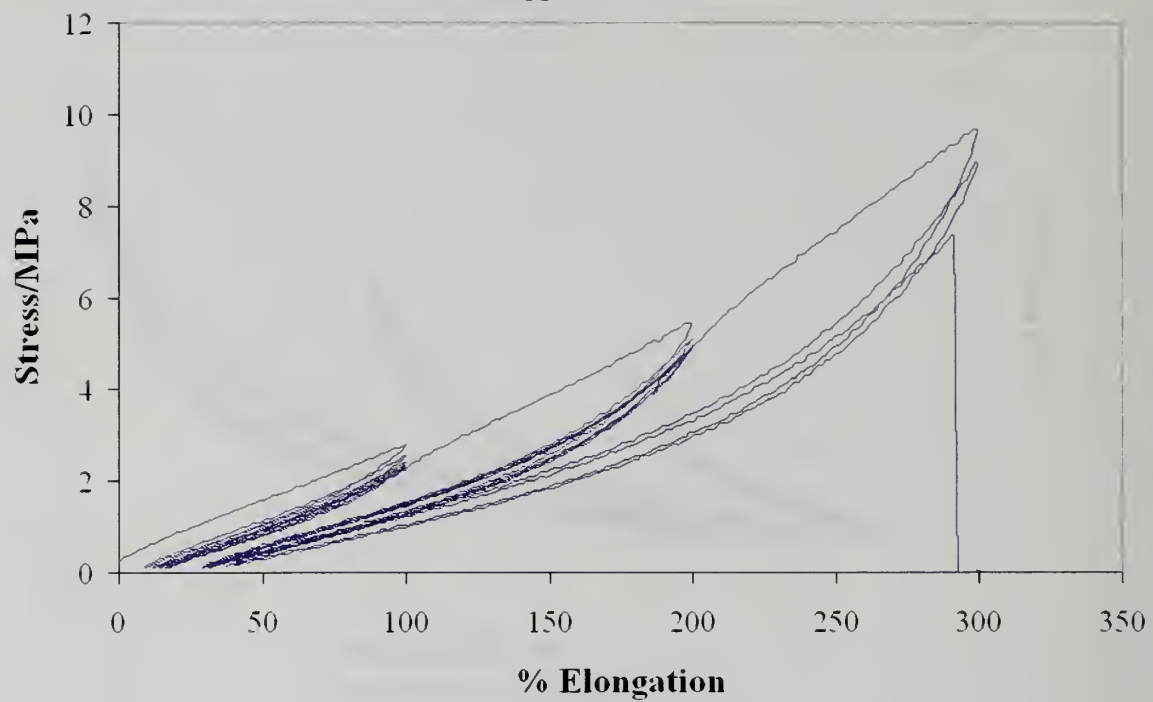


Cyclic test for EPPH36



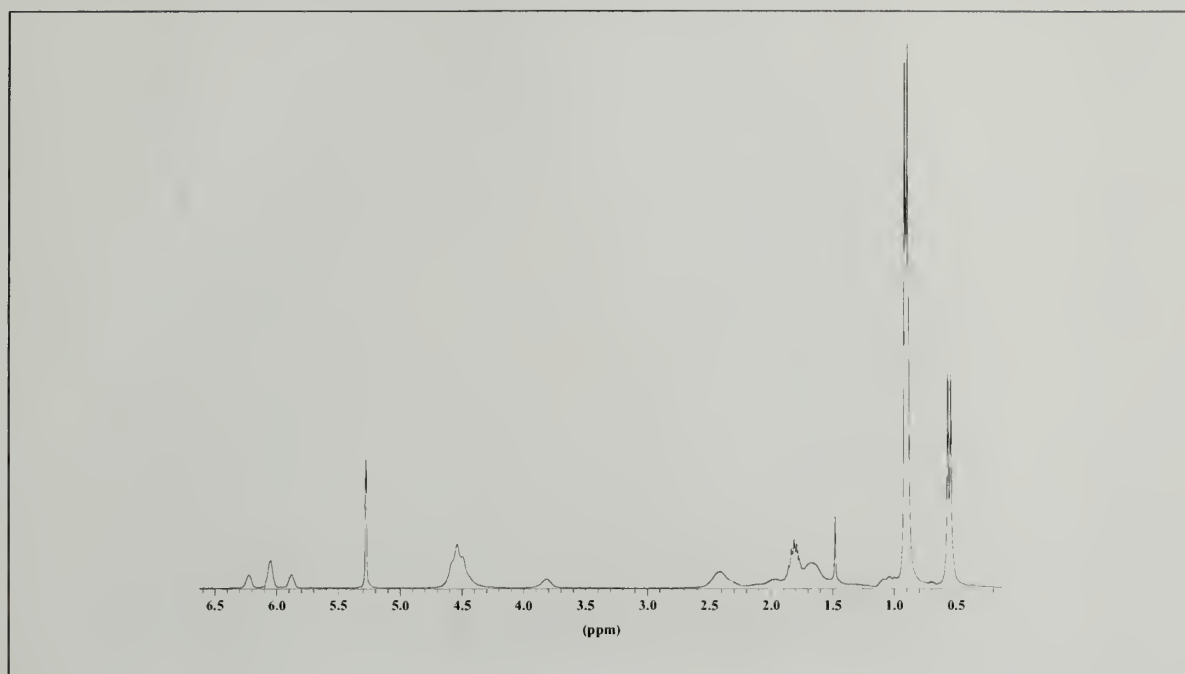
Cyclic test for EPPH30

# Appendix F

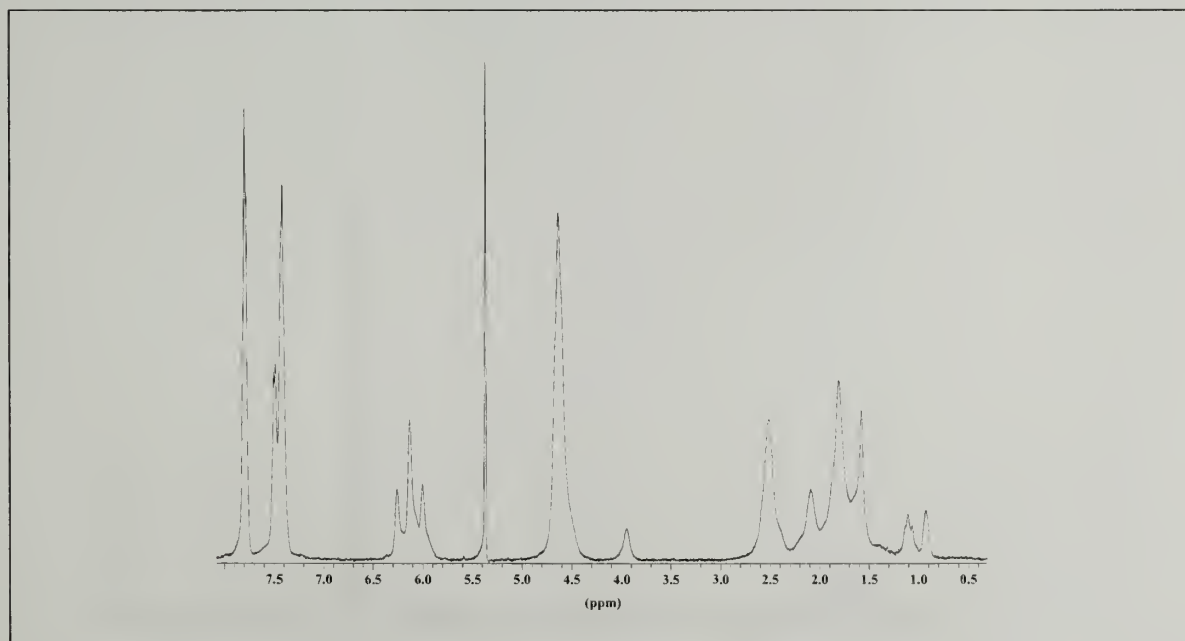


Cyclic test for EPPH10

## Appendix G

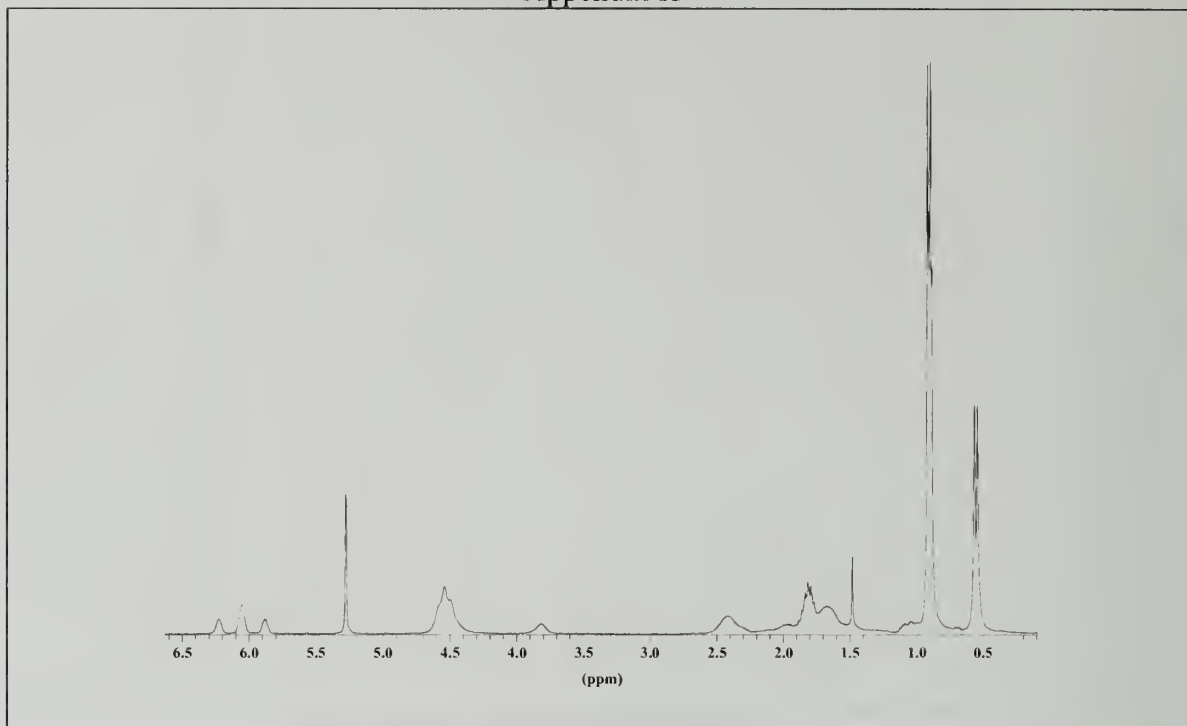


$^1\text{H}$  NMR of POFPA-Ibu36 Copolymer

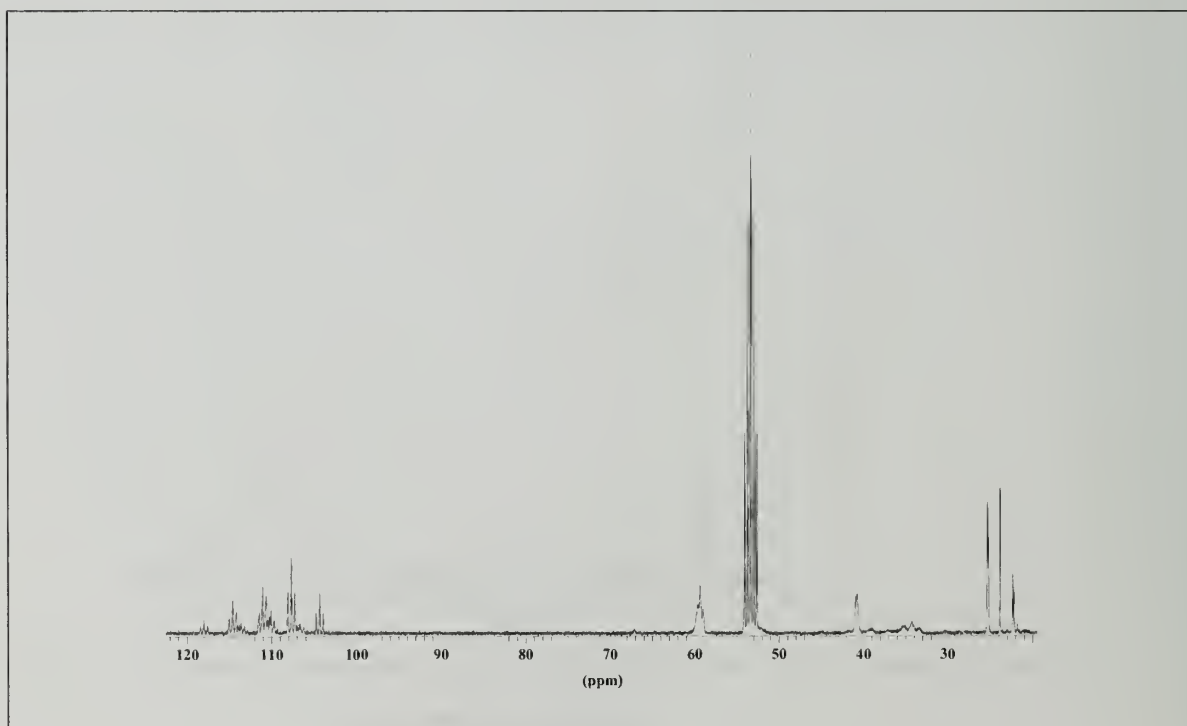


$^1\text{H}$  NMR of POFPA-Ph32

## Appendix H



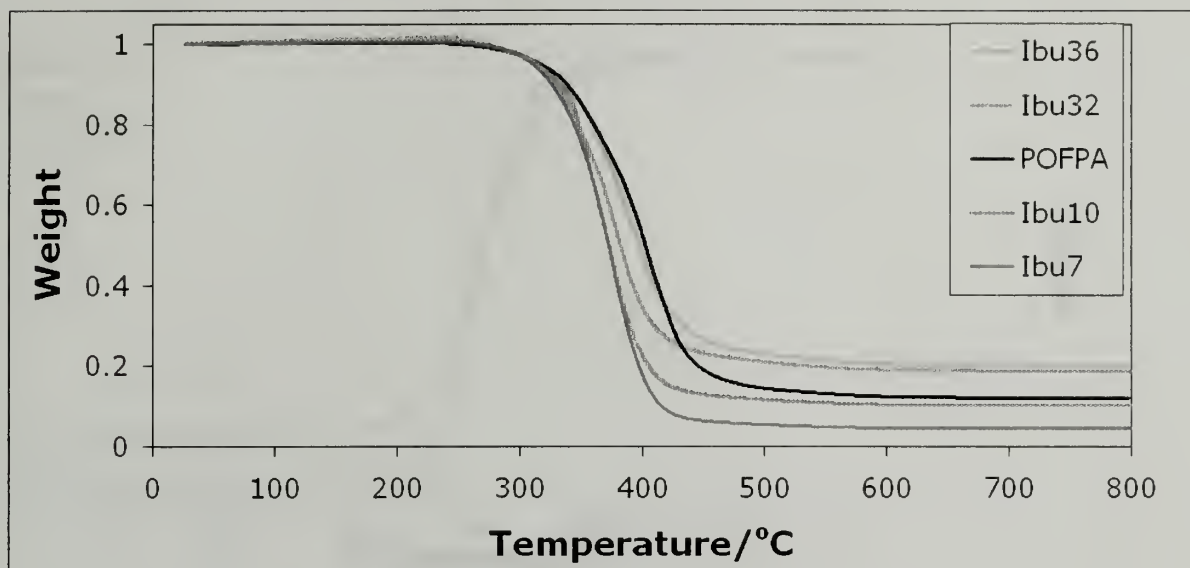
$^1\text{H}$  NMR of POFPA-Io13 Copolymer



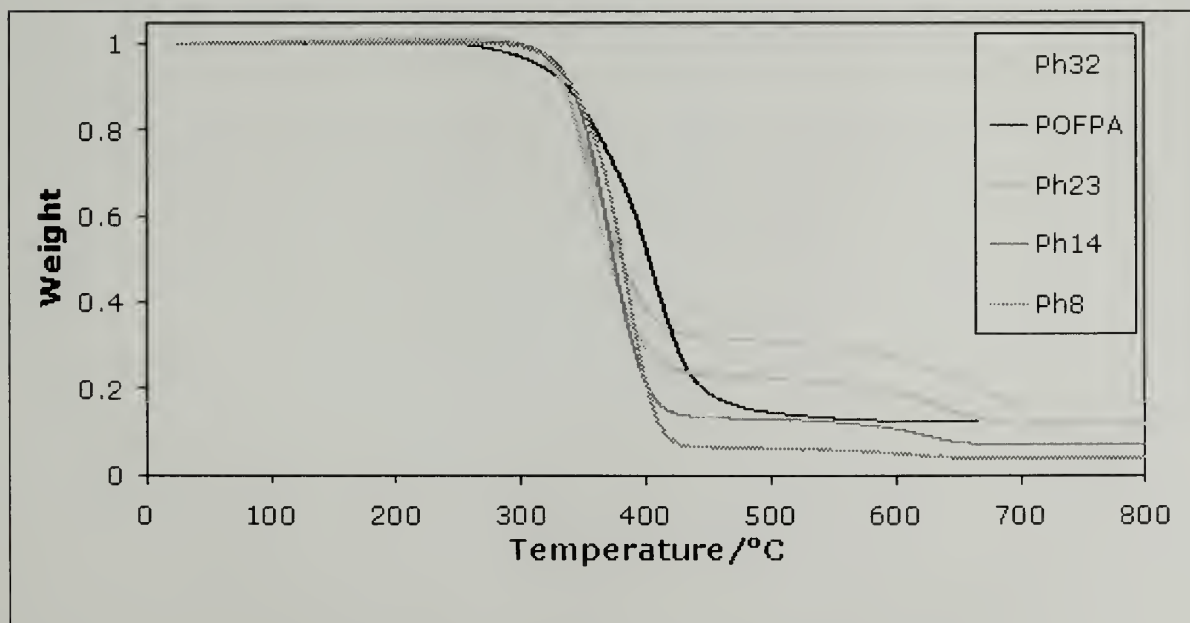
$^{13}\text{C}$  NMR of POFPAIbu250 Copolymer



# Appendix I

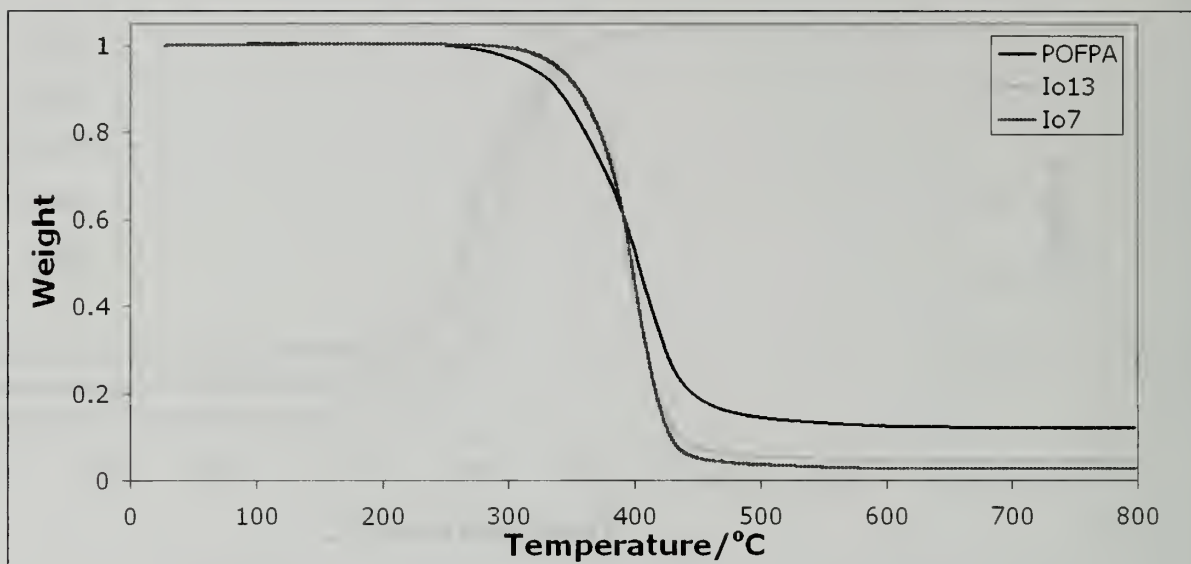


TGA Plot of POFPA-IbuPOSS Copolymers in Air.



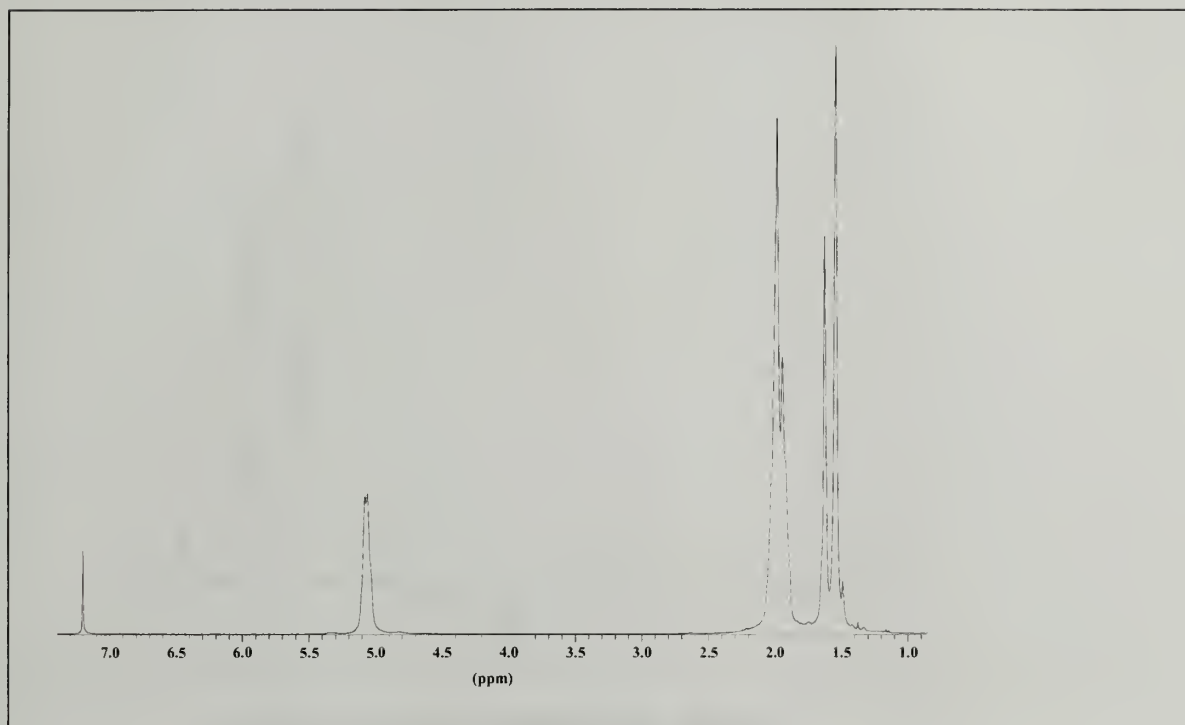
TGA Plot of POFPA-PhPOSS Copolymers in Air.

## Appendix J

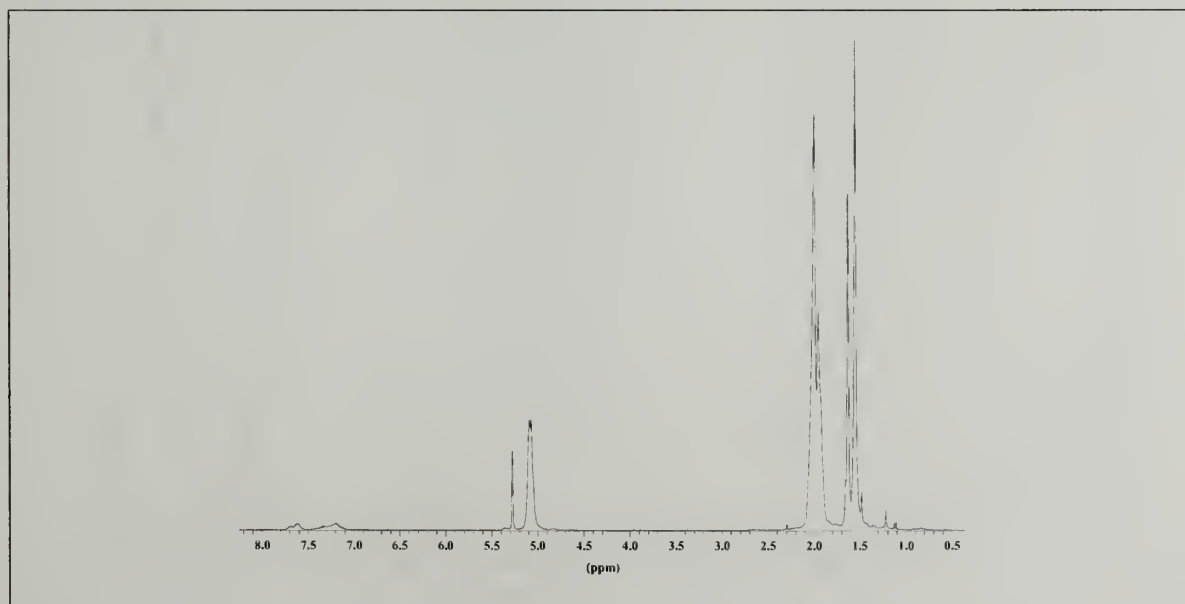


TGA Plot of POFPA-IoPOSS Copolymers in Air.

## Appendix K

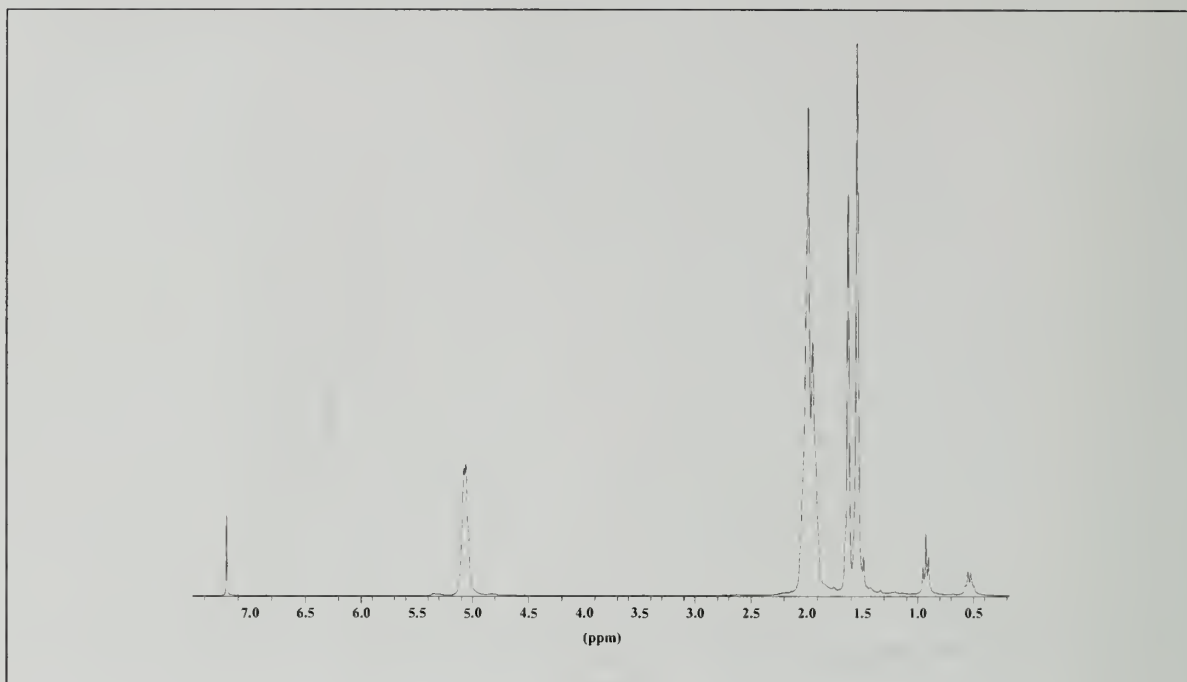


$^1\text{H}$  NMR of PolyDMCOD Homopolymer

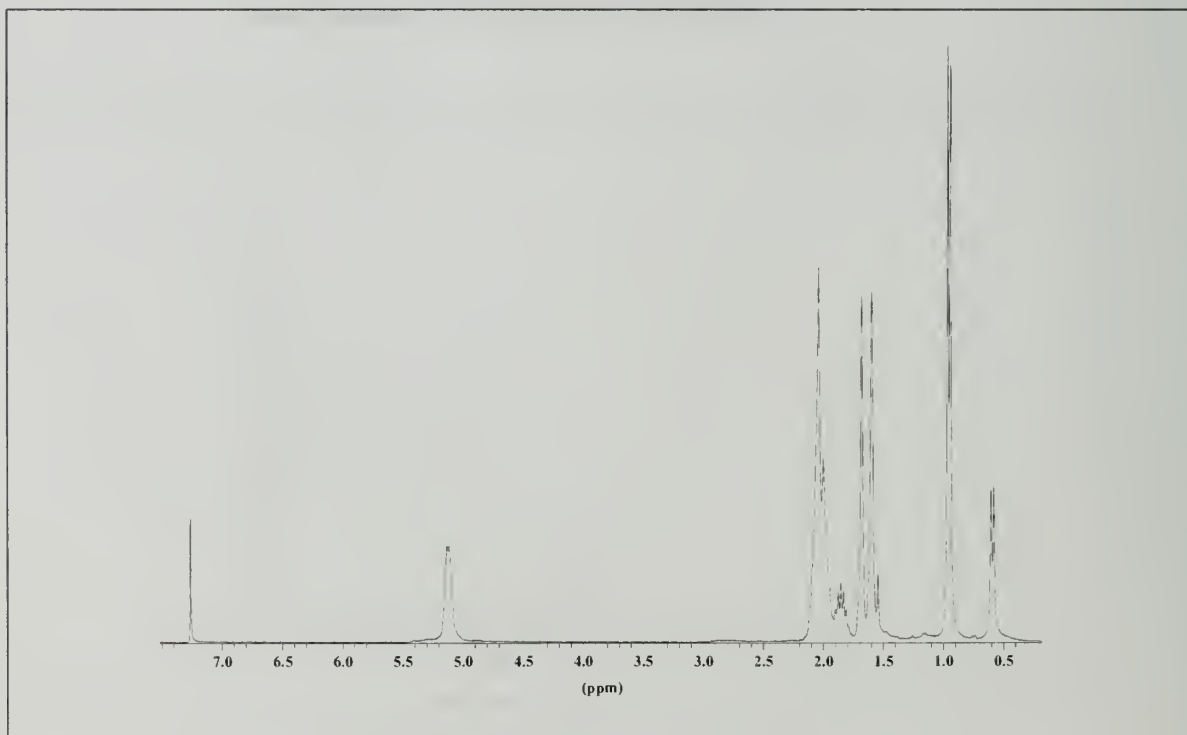


$^1\text{H}$  NMR of PolyDMCOD-Ph10 Copolymer

## Appendix L

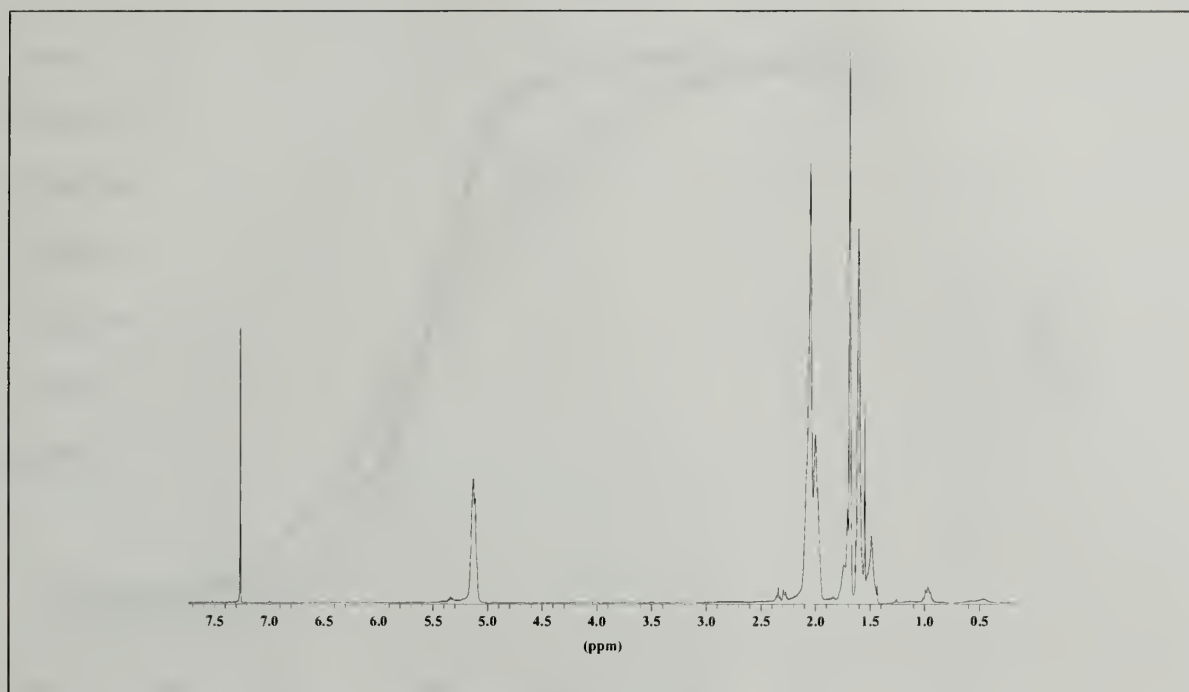


$^1\text{H}$  NMR of PolyDMCOD-Et13 Copolymer

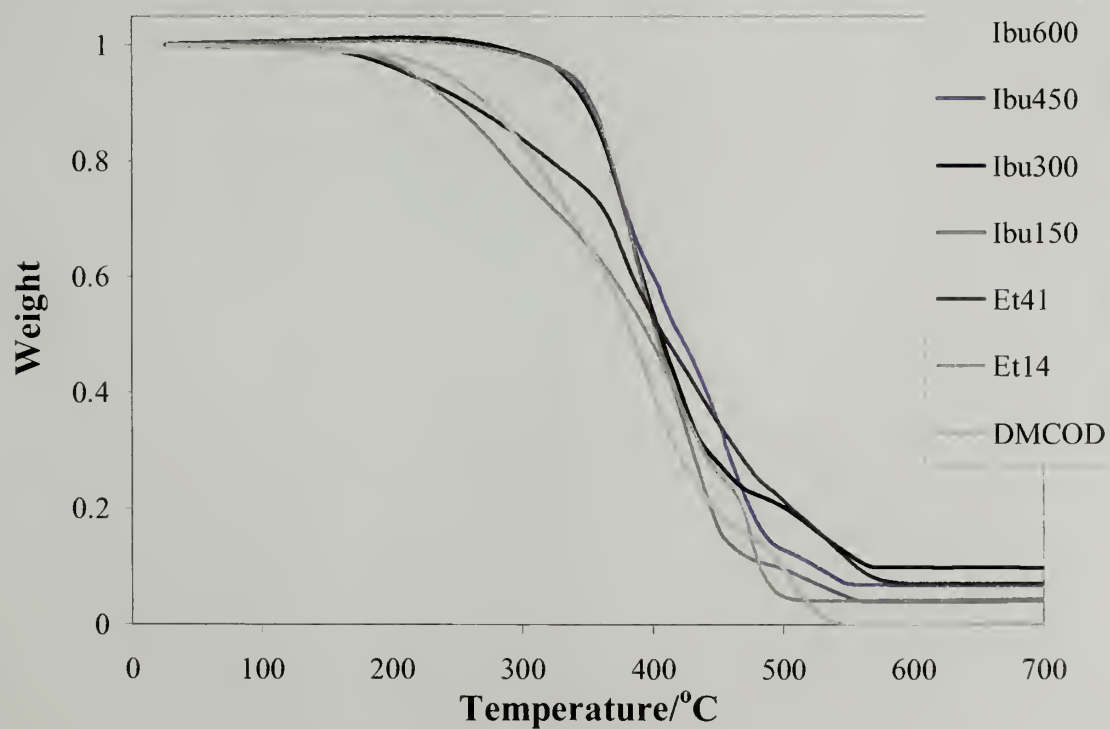


$^1\text{H}$  NMR of PolyDMCOD-Ibu48 Copolymer

## Appendix M



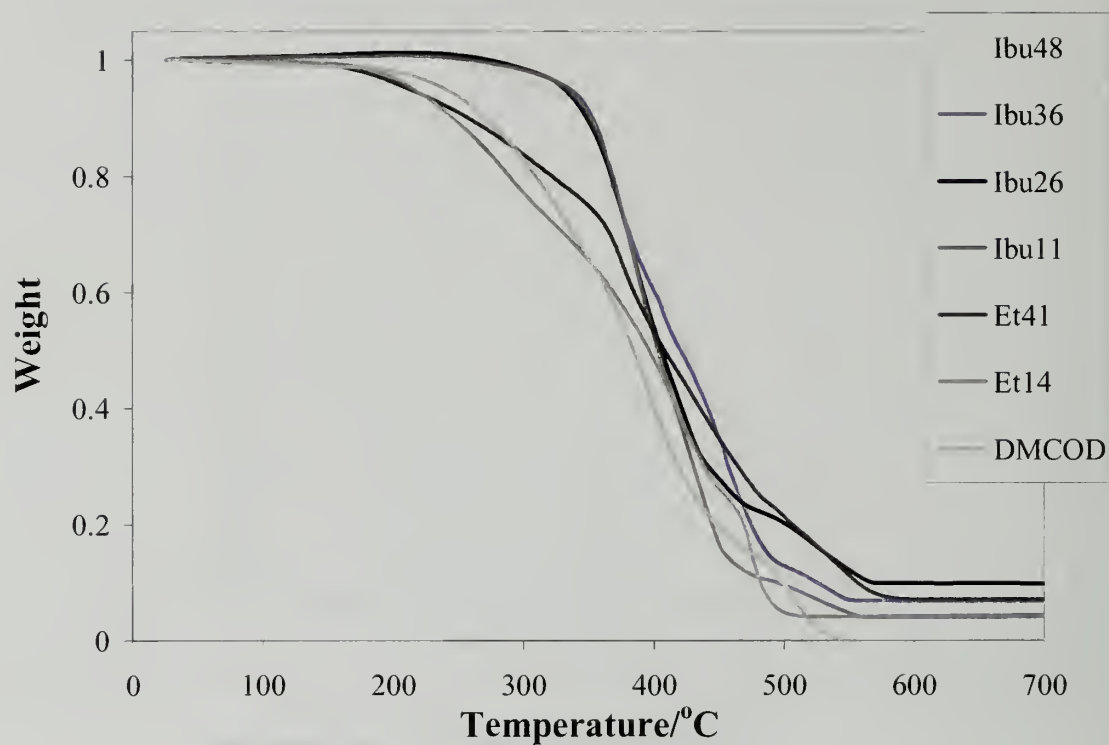
$^1\text{H}$  NMR of PolyDMCOD-Cp6 Copolymer



TGA of DMCOD-IbuPOSS, EtPOSS Copolymers.



## Appendix N



TGA of DMCOD-PhPOSS,CpPOSS Copolymers.

## Bibliography

- Abad, M.; Barral, L.; Fasce, D.; and Williams, J. *Macromolecules* **2003**, *36*, 3128-3135.
- Aklonis, J., and MacKnight, W. *Introduction to Polymer Viscoelasticity*, 2<sup>nd</sup> Ed. Wiley Interscience & Sons, Inc. New York, 1983.
- Ameduri, B.; Boutevin, B.; and Kostov, G. *Progress in Polymer Science* **2001**, *26*, 105-187.
- Arrowsmith, D.; Kaminsky, W.; Schauwienold, A.; Weingarten, U. *Journal of Molecular Catalysis A: Chemical* **2000**, *160*, 97-105.
- The Automobile Trimmings Co. <http://www.automobiletrim.com/door-seal-rubber.html>
- Bavarian, N., Baird, M., and Parent, S. *Macromolecular Chemistry and Physics* **2001**, *202*, 3248-3252.
- Bhowmick, A. and Stephens, H. *Handbook of Elastomers*, 2<sup>nd</sup> Ed. Marcel Dekker, Inc., New York, 2001.
- Bielawski, C. and Grubbs, R. *Angewandte Chemie, International Edition* **2000**, *39*, 2903-2906.
- Brintzinger, H., Fischer, D., Mülhaupt, Rieger, B., and Waymouth, R. *Angewandte Chemie, International Edition* **1995**, *34*, 1143-1170.
- Britovsek, G., Givson, V., and Wass, D. *Angewandte Chemie, International Edition* **1999**, *38*, 428-447.
- Bolln, C.; Tsuchida, A.; Frey, H.; and Mülhaupt, R. *Chemistry of Materials* **1997**, *2*, 1475-1479.
- Cardoen, G. and Coughlin, E.B. *Macromolecules* **2004**, *37*, 5123-5126.
- Chemical and Engineering News  
<http://pubs.acs.org/cen/coverstory/83/8342elastomers.html>
- Chou C.; Hsu S. ; Dinakaran K.; Chiu M.; and Wei K. *Macromolecules* **2005**, *38*, 745-751.
- Waddon, A., Zheng, L., Farris, R., and Coughlin, E.B. *Nano Letters* **2002**, *2*, 1149-1155.
- David, G., Boyer, C., Tonner, J., Améduri, B., Lacroix-Desmazes, P., and Boutevin, B. *Chemistry Reviews* **2006**, *106*, 3936-3962.

- Drazkowski, D.; Lee, A.; Haddad, T.; and Cookson, D. *Macromolecules* **2006**, *39*, 1854-1863.
- Dvornic, P.; Hartmann-Thompson, C.; Keinath, S.; and Hill, E. *Macromolecules*, **2004**, *37*, 7818-7831.
- Fan, W., Leclerc, M., and Waymouth, R. *Journal of the American Chemical Society* **2001**, *123*, 9555-9563.
- Firestone [http://www.firestonebpe.com/roofing/rubbergard/\\_en/index.shtm](http://www.firestonebpe.com/roofing/rubbergard/_en/index.shtm)
- Fu, B.; Hsiao, B.; Pagola, S.; Stephens, P.; White, H.; Rafailovich, M.; Sokolov, J.; Mather, P.; Jeon, H.; Phillips, S.; Lichtenhan, J.; and Schwab, J. *Polymer*, **2001**, *42*, 599-611.
- Fu, B.; Lee, A.; and Haddad, T. *Macromolecules* **2004**, *37*, 5211-5218.
- Galimberti, M., Mascellani, N., Piemontesi, F., and Camurati, I. *Macromolecular Rapid Communications* **1999**, *20*, 214-218.
- Galimberti, M., Piemontesi, F., Mascellani, N., Camurati, I., Fusco, O., and Destro, M. *Macromolecules* **1999**, *32*, 7968-7976.
- Gillis, D. and Karpeles, R. **US Pat 6,060,572** May 9, 2000
- Gonzalez-Ruiz, R., Quevedo-Sanchez, B., Laurence, R., Coughlin, E.B., Henson, M. *AIChE Journal* **2006**, *52*, 1824-1835.
- Haddad, T. and Lichtenhan, J. *Macromolecules*, **1996**, *29*, 7302-7304.
- Haddad, T.; Viers, B.; and Phillips, S. *Journal of Inorganic and Organometallic Polymers* **2001**, *11*, 155-164.
- Harper, Charles. *Handbook of Plastics, Elastomers, and Composites*, 3<sup>rd</sup> Ed. McGraw-Hill, New York, 1996.
- Hongyao, X.; Kuo, S.; and Chang, F. *Polymer Bulletin* **2002**, *48*, 469-474.
- Hybrid Plastics <http://www.hybridplastics.com>
- Iacono, S.; Ligon Jr., S.; Mabry, J.; Vij, A.; Smith Jr. D.; *Polymer Preprints* **2005**, *46*, 639-640.
- Ishii, S., Saito, J., Matsuura, S., Suzuki, Y., Furuyama, R., Mitani, M., Nakano, T., Kashiwa, N., and Fujita, T. *Macromolecular Rapid Communications* **2002**, *23*, 693-697.

- Jeon, H.; Mather, P.; and Haddad, T. *Polymer International* **2000**, *49*, 453-457.
- Joshi, M. and Butola, B. *Journal of Macromolecular Science Part C-Polymer Reviews* **2004**, *44*, 389-410.
- Kaminsky, W. and Miri, M. *Journal of Polymer Science Part A: Polymer Chemistry* **1985**, *23*, 2151-2164.
- Kolbert, A. and Didier, J. *Journal of Applied Polymer Science* **1999**, *71*, 523-530.
- Kopesky, E.; Haddad, T.; Cohen, R.; and McKinley, G. *Macromolecules* **2004**, *37*, 8993-9004.
- Kravchenko, R., and Waymouth R. *Macromolecules* **1998**, *31*, 1-6.
- Laine, R.; Choi, J.; and Lee, I. *Advanced Materials* **2001**, *13*, 800.
- Leclerc, M., and Waymouth, R. *Angewandte Chemie, International Edition* **1998**, *23*, 922-925.
- Lee, A. and Lichtenhan, J. *Macromolecules* **1998**, *31*, 4970-4974.
- Lee, J.; Cho, H.; Jung, B.; Cho, N.; and Shim, H.; *Macromolecules* **2004**, *37*, 8523-8529.
- Lee, Y.; Kuo, S.; Su, Y.; Chen, J.; Tu, C.; and Chang, F. *Polymer* **2004**, *45*, 6321-6331.
- Li, G.; Wang, L.; Ni, H.; and Pittman Jr., C. *Journal of Inorganic and Organometallic Polymers* **2001**, *11*, 123-154.
- Li, G. Wang, L. Toghiani, H. Daulton, T. Koyama, K. Pittman Jr., C. *Macromolecules* **2001**, *34*, 8686-8693.
- Li, G. Wang, L. Toghiani, H. Daulton, T. and Pittman Jr., C. *Polymer* **2002**, *43*, 4167-4176.
- Lide, David. *CRC Handbook of Chemistry and Physics*, 81<sup>st</sup> Ed. CRC Press, New York, 2001.
- Liu, Y.; Zheng, S.; and Nie, K. *Polymer*, **2005**, *46*, 12016-12025.
- Lichtenhan, Y.; Otonari, Y.; and Carr, M. *Macromolecules* **1995**, *28*, 8435-8437.
- Longo, P., Siani, E., Pragliola, S., and Monaco, G. *Journal of Polymer Science Part A: Polymer Chemistry* **2002**, *40*, 3249-3255.
- Malmberg, A. and Löfgren, B. *Journal of Applied Polymer Science* **1997**, *66*, 35-44.



- Matejka, L.; Strachota, A.; Plestil, J.; Whelan, P.; Steihhart, M.; and Slaof, M. *Macromolecules* **2004**, *37*, 9449-9456.
- Mather, P.; Jeon, H.; Romo-Uribe, A.; Haddad, T.; and Lichtenhan, J. *Macromolecules* **1999**, *32*, 1194-1203.
- McKnight, A., and Waymouth R. *Chemistry Reviews* **1998**, *98*, 2587-2598.
- Möhring P., and Coville, N. *Journal of Organometallic Chemistry* **1994**, *479*, 1-29.
- Odian, G. *Principles of Polymerization*, 3<sup>rd</sup> Ed. Wiley Interscience & Sons, Inc. New York, 1991.
- Park, S., Wang, W., and Zhu, S. *Macromolecular Chemistry and Physics* **2000**, *201*, 2203-2209.
- Phillips, S.; Haddad, T.; and Tomczak, S. *Current Opinion in Solid State and Materials Science* **2004**, *8*, 21-29.
- Pyun, J.; Matyjaszewski, K.; Wu, J.; Kim, G.; Chun, S.; and Mather, P. *Polymer*, **2003**, *44*, 2739-2750.
- Quevedo-Sanchez B., J. F. Nimmons, E. B. Coughlin, M. A. Henson *Macromolecules* **2006**, *13*, 4306-4316.
- Ricco L.; Russo S.; Monticelli O.; Bordo A.; and Bellucci F. *Polymer* **2005**, *46*, 6810-6819.
- Romo-Uribe, A.; Mather, P.; Haddad, T.; and Lichtenhan, J. *Journal of Polymer Science Part B: Polymer Physics* **1998**, *36*, 1857-1872.
- Ropartz L.; Morris R.; Foster D.; Cole-Hamilton D. *Chemistry Communications* **2001**, *4*, 361-362.
- Ropartz L.; Morris R.; Schwartz G.; Foster D.; Cole-Hamilton, D.; *Inorganic Chemistry Communications* **2000**, *3*, 714-717.
- Salamore, J. *Polymer Materials Encyclopedia* 1996, 2264-2271.
- Sanchez, C.; Julián, B.; Belleville, P.; and Popall, M. *Journal of Materials Chemistry* **2005**, *15*, 3559-3592.
- Sanchez, C.; Soler-Illia, G.; Ribot, F.; Lalot, T.; Mayer, C.; and Cabuil V. *Chemistry of Materials* **2001**, *13*, 3061-3083.



- Sperling, L. *Physical Polymer Science*, 3<sup>rd</sup> Ed. Wiley Interscience & Sons, Inc. New York, 2001.
- Strachota, A.; Kroutilova, I.; Kovarova, J.; and Matejka, L. *Macromolecules* **2004**, *37*, 9457-9464.
- Tatemoto, M. European Patent 399543, 1990.
- Tegou, E.; Bellas, V.; Gogolides, E.; Argitis, P.; Eon, D.; Cartry, G.; and Cardinaud, C. *Chemistry of Materials* **2004**, *16*, 2567-2577.
- Tsuchida, A.; Bolln, C.; Sernetz, F.; Frey, H.; and Mülhaupt, R.; *Macromolecules* **1997**, *30*, 2818-2824.
- Vasile, C. *Handbook of Polyolefins*, 2<sup>nd</sup> Ed. Marcel Dekker, Inc., New York, 2001.
- Waddon, A.; Zheng, L.; Farris, R.; and Coughlin, E.B. *Nano Letters* **2002**, *2*, 1149-1155.
- Web of Materials <http://www.webmat.com>
- Zheng, L.; Farris, R.; and Coughlin, E.B. *Journal of Polymer Science Part A: Polymer Chemistry* **2001**, *39*, 2920.
- Zheng, L.; Farris, R.; and Coughlin, E.B. *Macromolecules* **2001**, *34*, 8034-8039.
- Zheng, L.; Kasi, R.; Farris, R.; and Coughlin, E.B. *Journal of Polymer Science Part A: Polymer Chemistry* **2002**, *40*, 885-891.
- Zheng, L., Hong, S., Cardoen, G., Burgaz, E., Gido, S., Coughlin, E.B. *Macromolecules* **2004**, *37*, 8606-8611.
- Zhengtian, Y.; Marques, M.; Rausch, M.; and Chien, J. *Journal of Polymer Science Part A: Polymer Chemistry* **1995**, *33*, 2795-2801.

